

**ANALYSIS ON STOCHASTIC
CHARACTERISTICS OF BREAKDOWN
PHENOMENA ON INTERCITY
EXPRESSWAY SECTIONS**

MA, Danpeng

July, 2013

**ANALYSIS ON STOCHASTIC CHARACTERISTICS
OF BREAKDOWN PHENOMENA ON INTERCITY
EXPRESSWAY SECTIONS**

Doctoral Dissertation

Submitted in Partial Fulfillment of the
Requirements for the Degree of
Doctor of Engineering

by

MA, Danpeng

Academic Adviser:

Prof. Hideki Nakamura

Department of Civil Engineering
Nagoya University
July, 2013

Acknowledgements

This dissertation is the result of several years of hard work which is memorable experience in my life. It would not have been made possible without the support of many people. It is a pleasure to express my gratitude to them in my humble acknowledgment.

In the first place, I am deeply indebted to my academic adviser, Prof. Hideki Nakamura for his supervision, advice, and guidance as well as providing me with an invaluable opportunity to study at Nagoya University in Japan. He has supplied me with supports in various ways and offered me the chance to be involved the interesting research topic. His truly scientific manner has been inspiring and enriching my growth, and I am indebted to him deeply.

I gratefully acknowledge Prof. Takayuki Morikawa, Prof. Toshiyuki Yamamoto and Prof. Yukimasa Matsumoto for their advice and comments as the members of doctoral examination committee. Their significant recommendations, and sensible insights helped me a lot to enrich this dissertation.

I would like to express my gratitude to Central Nippon Expressway Company Limited for their invaluable assistance for this research. Many thanks go in particular to Mr. Hideo Yonekawa and Mr. Hiroyuki Konda for their great supports.

My grateful thanks also go to Assistant Professor Miho Asano for her help, support, as well as valuable advices and discussion for the research. Many thanks go to Mr. Masato Kobayashi and Ms. Xi Wang for their contributions to this dissertation. It is a pleasure to express my thanks to all members of our laboratory for their kindness and supports to me. It has been my nice experience with them full of happiness and great memories.

I would also like to express my deep thanks to Prof. Keping Li at Tongji University in China for his deep care for me and encouragement for my study during these years.

I am very grateful to the Japanese Ministry of Education, Culture, Sports, Science and Technology for granting me a scholarship.

Finally, I would like to express my deepest thanks to my family whose great dedication, deep love and persistent confidence in me, have offer me the courage to face the future. I owe them deeply for being supportive and affectionate for my lifetime.

Abstract

Analysis on breakdown phenomena is the base for various practical issues on intercity expressways at both the operational and the planning stages.

With respect to the operational stage, a macroscopic simulation platform is currently under construction which covers intercity expressway network of central Japan. It will enable evaluation of intercity expressway performance in response to traffic flow characteristics at the operational stage. As for development of this simulation platform, analysis on breakdown phenomena is a critical issue in light of their significant impacts on intercity expressway performance.

Furthermore, with respect to the planning stage, there exist the requirements for control on traffic condition characteristics, improvement on geometric configurations to alleviate breakdown phenomena. Again analysis on breakdown phenomena is desirable to quantify impacts of traffic condition and geometric characteristics.

To analyze breakdown phenomena, capacity of recurrent bottleneck will be focused on which includes two distinct aspects, namely breakdown flow rate and discharge flow rate. They impact on breakdown occurrence and its duration respectively. Both breakdown flow rate and discharge flow rate are characterized of stochastic natures which are influenced by traffic condition and geometric characteristics.

The objective of this study is to model breakdown flow rate and discharge flow rate by considering impacts of traffic condition characteristics and geometries on intercity expressways.

Chapter 1 describes significance of analyzing breakdown phenomena at recurrent bottlenecks for both the operational stage and the planning stages in practice. Then problem statement and objective of the study are presented. Finally, the research outline is generally reviewed.

Chapter 2 discusses the preparation for modeling breakdown and discharge flow rates. Intercity expressway network of central Japan is focused on where breakdown phenomena

exist at diverge, merge and sag bottleneck locations which are identified based on flow rate-speed diagram of each detector. In light of its influence on breakdown occurrence, lane utilization rate (*LUR*) is modeled as a function of traffic condition and geometric characteristics.

In **Chapter 3**, a lane based method is proposed to identify breakdown occurrence. The existing cross-section based method oversimplifies breakdown identification for bottlenecks at expressway facilities where lane usage preferences on each lane significantly differ like nearby diverge and merge sections. Therefore, a lane based method is proposed to identify breakdown on each lane. And timing of breakdown occurrence is determined by a critical speed which is optimized through obtaining the most significant speed drops accompanying with breakdown occurrences.

The proposed lane based method is applied to diverge and merge bottlenecks. Superiorities of lane based method are highlighted as follows. Firstly, it can identify and exclude semi-congested cases where some lanes are congested and others are not. Secondly, timing of breakdown occurrence can be appropriately determined through this lane based method. These superiorities significantly improve the accuracy of extracting breakdown flow rates which are underestimated by the existing cross-section based method.

In **Chapter 4**, breakdown probability models are developed. At diverge and merge bottlenecks, modeling is based on the identification results by using lane based method as described in chapter 3. Besides lane utilization rate, diverge rate and merge rate are also found to have significant impacts on breakdown probability at diverge and merge bottlenecks respectively. With respect to sag bottlenecks, the general breakdown probability model is established by considering impacts of site-specific geometries of negative and positive slopes.

As for practical application in simulation, the models enable estimation of breakdown occurrence at the operational stage. Estimation accuracy can be improved by taking traffic condition characteristics into account. In addition, consideration of geometric characteristics enables the estimation of potential bottleneck.

Chapter 5 introduces modeling on discharge flow rate in a stochastic way. Breakdown flow rate and the elapsed time of breakdown duration are found to have significant impacts

on discharge flow rate which are taken into consideration when modeling. In addition, the general discharge flow rate models are established respectively for each bottleneck type. At diverge and merge bottlenecks, site-specific deceleration and acceleration lane lengths are taken into account when generalizing *DCF* model respectively. With respect to sag bottleneck, site-specific geometries of negative and positive slopes are considered.

With respect to practical application in simulation, the developed stochastic *DCF* models enable the performance evaluation for breakdown duration in a stochastic way. Advantages of the developed models are highlighted as follows which improve evaluation accuracy. The relationship between breakdown and discharge flow rates is taken into account. Furthermore, a descending tendency of discharge flow rate is modeled with increase of elapsed time of breakdown duration.

Chapter 6 discusses simulation of breakdown phenomena by using the developed breakdown probability and discharge flow rate models. Simulation is performed through Monte Carlo method in the way as follows: 1) breakdown flow rates are stochastically generated by using breakdown probability models, and then 2) discharge flow rate distributions are reproduced based on input of breakdown flow rate values. The simulated number of breakdown occurrence, time-dependent frequency and breakdown duration are adopted as performance measure to evaluate simulation. The investigation in this chapter verifies the effectiveness of the developed models for simulation in practice.

Chapter 7 introduces the case study by applying the developed stochastic models. The selected test bed is located on Tomei Expressway of westbound direction from Okazaki IC to Toyota JCT. With respect to test bed, the map of breakdown probability distributions is developed considering impacts of traffic flow characteristics. This kind of map enables the estimation on the risk of breakdown occurrence due to change of traffic condition characteristics.

Finally, **Chapter 8** summarizes research conclusions and provides some recommendations for future research. Most of all, the breakdown and discharge flow rates are modeled which enables simulation of breakdown phenomena at the operational stage. Also these models offer the base for improvement on geometric configurations to alleviate breakdown phenomena at the planning stage.

Furthermore, it is concluded that lane based method is superior over the conventional cross-section based method for breakdown identification at diverge and merge bottlenecks. For example, it significantly improve accuracy of extracting breakdown flow rates by 2.6% which are underestimated by the existing cross-section based method at Toyota diverge bottleneck.

Meanwhile traffic condition characteristics have been taken into consideration when modeling which improves estimation accuracy of breakdown probability. At Toyota diverge bottleneck, estimation accuracy can be improved by 20.5% when reproducing breakdown phenomena there. In addition, map of breakdown probability distribution enables evaluation of breakdown occurrence at the operational stage for users.

Table of Contents

Acknowledgements	V
Abstract	VII
Table of Contents.....	XI
List of Tables.....	XVI
List of Figures	XIX
Chapter 1 Introduction	1
1.1 Background.....	1
1.1.1 Significance of analyzing breakdown phenomena at both the operational and the planning stages	2
1.1.2 Two aspects of bottleneck capacity to represent breakdown phenomena	3
1.1.3 Insights of lane based analysis	4
1.1.4 Impacts of traffic condition and geometric characteristics.....	4
1.1.5 Simulation by incorporating breakdown probability and discharge flow rate models.....	5
1.1.6 Assessment of potential bottlenecks.....	5
1.2 Problem statement	6
1.3 Objectives	7
1.4 Research outline	8
Chapter 2 Test bed and data descriptions.....	11
2.1 Introduction	11
2.2 Test bed: intercity expressway network of central Japan	12
2.3 Identification of bottleneck location.....	13
2.4 Descriptions of the bottleneck locations.....	15
2.4.1 Diverge bottlenecks	16
2.4.2 Merge bottlenecks	19
2.4.3 Sag bottlenecks	21
2.5 Descriptions of traffic flow data	22

2.6 Lane utilization rate (<i>LUR</i>) modeling to describe lane-specific driving behaviors...	23
2.6.1 Data description for <i>LUR</i> modeling	24
2.6.2 Influencing factors on <i>LUR</i>	25
2.6.3 Parameter estimation of <i>LUR</i> model	25
2.6.4 Validation of <i>LUR</i> model	28
2.7 Summary.....	28
Chapter 3 Identification of breakdown occurrence	30
3.1 Introduction	30
3.2 Literature review.....	31
3.3 Breakdown Identification through the lane based method	33
3.3.1 Data descriptions for lane based method.....	33
3.3.2 Introduction of lane based identification method.....	34
3.3.3 Procedure of lane based method.....	34
3.3.4 Comparison of the identified breakdown events between cross-section and lane based methods	37
3.4 The extracted <i>BDF</i> distributions at diverge bottlenecks	43
3.5 The extracted <i>BDF</i> distributions at merge bottlenecks	44
3.6 The extracted <i>BDF</i> distributions at sag bottlenecks	45
3.7 Summary.....	48
Chapter 4 Modeling on breakdown probability	50
4.1 Introduction	50
4.2 Literature review.....	51
4.3 Modeling on breakdown probability	53
4.3.1 Breakdown probability models at diverge bottlenecks	54
4.3.2 Breakdown probability models at merge bottlenecks	55
4.3.3 Breakdown probability models at sag bottlenecks	57
4.3.4 Summary of breakdown probability models	59
4.4 Impact of traffic flow characteristics.....	60
4.4.1 Diverge bottleneck.....	60
4.4.1.1 Diverge rate (<i>DR</i>).....	62
4.4.1.2 Lane utilization rate (<i>LUR</i>)	63

4.4.1.3 Modeling considering impacts of DR and LUR	65
4.4.2 Merge bottleneck	66
4.4.2.1 Merge rate (MR).....	66
4.4.2.2 Lane utilization rate (LUR)	67
4.4.2.3 Modeling considering impacts of MR and LUR	67
4.5 Impact of geometric characteristics	68
4.6 Summary.....	69
Chapter 5 Modeling on discharge flow rate.....	71
5.1 Introduction	71
5.2 Literature review.....	73
5.3 Statistic analysis of discharge flow rate distributions at bottlenecks	75
5.3.1 Diverge bottlenecks	75
5.3.2 Merge bottlenecks	76
5.3.3 Sag bottlenecks	77
5.4 Stochastic modeling on discharge flow rate	78
5.4.1 Hypothesis of modeling.....	78
5.4.2 Procedure of modeling	79
5.4.3 Impact of breakdown flow rate (BDF)	80
5.4.4 Impact of the elapsed time of breakdown duration (t)	82
5.4.5 Development of DCF model	83
5.4.6 Validation of discharge flow rate (DCF) model.....	84
5.5 Generalizing DCF model.....	85
5.5.1 Diverge bottlenecks	86
5.5.2 Merge bottlenecks	88
5.5.3 Sag bottlenecks	89
5.6 Summary.....	90
Chapter 6 Simulation of breakdown phenomena by applying the developed models	92
6.1 Introduction	92
6.2 Simulation of breakdown phenomena at the bottlenecks	93
6.3 Simulation at diverge bottleneck	94
6.3.1 Bottleneck location for simulation	94

6.3.2 Input of simulation procedure	95
6.3.2.1 <i>Traffic demand</i>	95
6.3.2.2 <i>Lane utilization rate</i>	96
6.3.2.3 <i>Diverge rate</i>	98
6.3.3 Breakdown occurrence	99
6.3.3.1 <i>Stochastic model</i>	99
6.3.3.2 <i>The simulated number of breakdown occurrence</i>	100
6.3.3.3 <i>Time-dependent breakdown frequency</i>	101
6.3.3.4 <i>The simulated BDF distribution</i>	104
6.3.4 Breakdown duration	105
6.3.4.1 <i>Determining method of breakdown duration</i>	105
6.3.4.2 <i>The determined result</i>	106
6.4 Simulation at merge bottleneck	107
6.4.1 Input of simulation procedure	107
6.4.2 Output of simulation procedure.....	109
6.5 Simulation at sag bottleneck.....	110
6.5.1 Input of simulation procedure	110
6.5.2 Output of simulation procedure.....	111
6.6 Summary.....	112
Chapter 7 Case study by applying the developed models.....	113
7.1 Introduction	113
7.2 Descriptions of test bed	114
7.3 Distribution of breakdown probability at the test bed.....	116
7.3.1 Output of simulation procedure.....	118
7.3.2 Impact of heavy vehicle percentage	121
7.4 Summary.....	123
Chapter 8 Conclusions and recommendations	125
8.1 Conclusions	125
8.1.1 Modeling lane utilization rate (<i>LUR</i>) by considering impacts of traffic condition and geometric characteristics	126
8.1.2 Proposing lane based breakdown identification method.....	126
8.1.3 Breakdown probability modeling by considering traffic condition and geometric characteristics	127

8.1.4 Modeling discharge flow rate in a stochastic way.....	128
8.1.5 Simulating breakdown phenomena by applying the developed models	129
8.2 Recommendations for future work.....	130
8.2.1 Application to three-lane sections	130
8.2.2 Estimation on change of geometric configuration.....	130
References.....	132

List of Tables

Table 2.1 Basic information on each intercity expressway	13
Table 2.2 Descriptions of diverge bottlenecks	16
Table 2.3 Descriptions of merge bottlenecks	20
Table 2.4 Descriptions of sag bottlenecks	21
Table 2.5 Influencing factors on <i>LUR</i>	25
Table 2.6 Estimation of <i>LUR</i> model parameters	27
Table 2.7 Goodness of fit for each developed model	28
Table 3.1 Optimal critical speeds (km/h) at diverge bottlenecks	40
Table 3.2 Identification results at Toyota, Toki and Komaki diverge bottlenecks	40
Table 3.3 Impact of <i>DR</i> on time lag of breakdown occurrence on each lane.....	41
Table 3.4 Identification results at Nagoya diverge bottleneck	41
Table 3.5 A comparison between <i>BDF</i> values of type <i>S</i> and <i>SAM</i> at Toyota diverge bottleneck	42
Table 3.6 A comparison between <i>BDF</i> values of type <i>STM</i> by using two methods	42
Table 3.7 Statistic analysis of <i>BDF</i> distribution at diverge bottlenecks.....	43
Table 3.8 Statistic analysis of <i>BDF</i> distributions at merge bottleneck.....	45
Table 3.9 Statistic analysis of <i>BDF</i> distributions at sag bottlenecks on Tomei Expressway of eastbound direction	46
Table 3.10 Statistic analysis of <i>BDF</i> distributions at sag bottlenecks on Tomei Expressway of westbound direction	46
Table 3.11 Statistic analysis of <i>BDF</i> distributions at sag bottlenecks on Higashi-Meihan Expressway.....	47
Table 3.12 Statistic analysis of <i>BDF</i> distributions at sag bottlenecks on Chuo Expressway	48
Table 4.1 Breakdown probability models at diverge bottlenecks	54
Table 4.2 Breakdown probability models at merge bottlenecks	56
Table 4.3 Breakdown probability models at sag bottlenecks	57
Table 4.4 Impact of <i>DR</i> and <i>LUR</i> at Toyota diverge bottleneck	65
Table 5.1 Statistic analysis of <i>DCF</i> distributions at diverge bottlenecks	76

Table 5.2	Statistic analysis of <i>DCF</i> distributions at merge bottlenecks	77
Table 5.3	Statistic analysis of <i>DCF</i> distributions at sag bottlenecks.....	77
Table 5.4	Regression result for the first 5 minute	81
Table 5.5	The estimated parameters for <i>DCF</i> models at diverge bottlenecks.....	83
Table 5.6	The estimated parameters for <i>DCF</i> models at merge bottlenecks.....	84
Table 5.7	The estimated parameters for <i>DCF</i> models at sag bottlenecks	84
Table 6.1	Number of breakdown occurrences.....	100
Table 8.1	Influencing factor in <i>LUR</i> model.....	126
Table 8.2	Proposal of lane based method at diverge and merge bottlenecks	127
Table 8.3	Summary of breakdown probability models	128
Table 8.4	Summary of discharge flow rate models	129

List of Figures

Figure 1.1 Flowchart for simulating breakdown phenomena.....	7
Figure 1.2 General research outline.....	9
Figure 2.1 The intercity expressway network of central Japan	12
Figure 2.2 Illustration of detector locations nearby bottleneck	14
Figure 2.3 Flow rate-speed diagram at bottleneck upstream (299.5KP on Tomei Expressway of westbound direction).....	14
Figure 2.4 Flow rate-speed diagram at bottleneck location (302.15KP on Tomei Expressway of westbound direction).....	15
Figure 2.5 Flow rate-speed diagram at bottleneck downstream (304.2KP on Tomei Expressway of westbound direction).....	15
Figure 2.6 The aerial view of Toyota diverge bottleneck.....	17
Figure 2.7 Illustration of Toyota diverge bottleneck.....	17
Figure 2.8 Video images of Toyota diverge bottleneck	18
Figure 2.9 Illustration of Toki diverge bottleneck	18
Figure 2.10 Illustration of Komaki diverge bottleneck.....	18
Figure 2.11 Illustration of Nagoya diverge bottleneck	18
Figure 2.12 Illustration of Toyota merge bottleneck.....	20
Figure 2.13 Illustration of Toki merge bottleneck.....	20
Figure 2.14 Illustration of Komaki merge bottleneck	21
Figure 2.15 Flow rate and speed on shoulder lane at Toyota diverge bottleneck (302.15KP on Tomei Expressway of westbound direction)	22
Figure 2.16 Flow rate and speed on median lane at Toyota diverge bottleneck (302.15KP on Tomei Expressway of westbound direction)	22
Figure 2.17 Aggregated flow rate and speed of cross-section at Toyota diverge bottleneck (302.15KP on Tomei Expressway of westbound direction).....	23
Figure 2.18 Relationship between <i>LUR</i> and traffic flow rate of cross-section at Toyota diverge bottleneck (302.15KP).....	24
Figure 2.19 <i>LUR</i> model parameters.....	26

Figure 2.20 Validation results on 4-lane expressway.....	28
Figure 3.1 Flow rate-speed diagrams of 302.15KP at Toyota diverge bottleneck	33
Figure 3.2 Illustration of a breakdown occurrence.....	35
Figure 3.3 Critical speeds on shoulder lane and median Lane	36
Figure 3.4 Classification of breakdown types at two-lane diverge and merge bottlenecks	37
Figure 3.5 Flowchart for applying the lane based identification method.....	38
Figure 3.6 Representative examples of breakdown types.....	39
Figure 3.7 A representative example at Nagoya diverge bottleneck.....	39
Figure 3.8 The extracted <i>BDF</i> dataset by using two methods.....	42
Figure 3.9 The extracted <i>BDF</i> distributions at diverge bottlenecks	44
Figure 3.10 The extracted <i>BDF</i> distributions at merge bottlenecks	45
Figure 3.11 The extracted <i>BDF</i> distributions at sag bottlenecks on Tomei Expressway of eastbound direction.....	46
Figure 3.12 The extracted <i>BDF</i> distributions at sag bottlenecks on Tomei Expressway of westbound direction.....	47
Figure 3.13 The extracted <i>BDF</i> distributions at sag bottlenecks on Higashi-meihan Expressway.....	47
Figure 3.14 The extracted <i>BDF</i> distributions at sag bottlenecks on Chuo Expressway.....	48
Figure 4.1 Impacts of parameters on breakdown probability distributions.....	53
Figure 4.2 Breakdown probability distributions at diverge bottlenecks.....	54
Figure 4.3 Breakdown probability distributions at merge bottlenecks.....	56
Figure 4.4 Breakdown probability distributions at sag bottlenecks	58
Figure 4.5 Breakdown probability distributions at bottlenecks of different expressway bottleneck types	59
Figure 4.6 Vicinity of Toyota diverge bottleneck	60
Figure 4.7 Flow rates on each lane and diverge at detector 302.15KP for location of Toyota diverge bottleneck.....	61
Figure 4.8 Change tendency for flow rates on each lane from upstream to location of Toyota diverge bottleneck	61
Figure 4.9 Flow rate on shoulder lane and diverge	62
Figure 4.10 <i>LUR</i> distribution on shoulder lane at detector 299.5KP for upstream of Toyota diverge bottleneck.....	64

Figure 4.11 <i>LUR</i> distribution on shoulder lane at detector 302.15KP for location of Toyota diverge bottleneck.....	64
Figure 4.12 A comparison between the measured and the estimated values	66
Figure 4.13 Vicinity of Toyota merge bottleneck	66
Figure 4.14 Illustration of vertical slope change	68
Figure 5.1 Empirical <i>DCF</i> distribution at Toyota diverge bottleneck.....	78
Figure 5.2 Empirical <i>BDF</i> and <i>DCF</i> distributions at Toyota diverge bottleneck	79
Figure 5.3 Flowchart of stochastic modeling on <i>DCF</i>	80
Figure 5.4 Classification of <i>BDF</i> distribution	80
Figure 5.5 Impact of <i>BDF</i> value on <i>DCF</i> distribution	81
Figure 5.6 Impact of <i>t</i> on mean values of <i>DCF</i> distribution	82
Figure 5.7 Impact of <i>t</i> on standard deviations of <i>DCF</i> distribution	82
Figure 5.8 Flowchart of <i>DCF</i> model validation	85
Figure 5.9 Validation of <i>DCF</i> model at Toyota diverge bottleneck.....	85
Figure 5.10 Impact of deceleration lane length on a_1 and a_2	87
Figure 5.11 Impact of deceleration lane length on b_1 and b_2	87
Figure 5.12 Impact of deceleration lane length on c_1 and c_2	88
Figure 6.1 Simulation framework.....	93
Figure 6.2 Test bed location and position of detectors in vicinity of Toyota diverge bottleneck	94
Figure 6.3 Traffic demand distribution at Toyota diverge bottleneck.....	95
Figure 6.4 Heavy vehicle distribution at Toyota diverge bottleneck	96
Figure 6.5 The simulated <i>LUR</i> on shoulder lane at Toyota diverge bottleneck	97
Figure 6.6 The measured <i>DR</i> at Toyota diverge bottleneck	98
Figure 6.7 Capacity and demand distributions at Toyota diverge bottleneck	100
Figure 6.8 The measured frequency distribution of breakdown occurrence	101
Figure 6.9 The simulated frequency distribution of breakdown occurrence	101
Figure 6.10 Time-dependent distribution	102
Figure 6.11 Breakdown frequency on weekdays/non-holidays.....	103
Figure 6.12 Breakdown frequency on weekends/holidays	103
Figure 6.13 Comparison between the measured and simulated <i>BDF</i> distributions.....	104
Figure 6.14 Estimation method of breakdown duration	105
Figure 6.15 Comparison between the measured and simulated breakdown duration	106

Figure 6.16 Test bed location and position of detectors in vicinity of Toyota merge bottleneck	107
Figure 6.17 Traffic demand distribution at Toyota merge bottleneck.....	107
Figure 6.18 The simulated <i>LUR</i> on shoulder lane at Toyota merge bottleneck	108
Figure 6.19 The measured <i>MR</i> at Toyota merge bottleneck	108
Figure 6.20 Time-dependent breakdown frequency at Toyota merge bottleneck.....	109
Figure 6.21 Sag bottleneck between Toyota JCT and Okazaki IC on Tomei Expressway of eastbound direction.....	110
Figure 6.22 Traffic demand distribution at sag bottleneck.....	111
Figure 6.23 Time-dependent breakdown frequency at sag bottleneck.....	111
Figure 7.1 Location of test bed for case study.....	114
Figure 7.2 Views nearby Okazaki IC	115
Figure 7.3 Views between Okazaki IC and Toyota JCT	115
Figure 7.4 Views nearby Toyota JCT.....	116
Figure 7.5 Configuration of test bed.....	116
Figure 7.6 Procedure to develop breakdown probability distribution.....	117
Figure 7.7 Breakdown probability distributions regarding traffic demand (heavy vehicle percentage=15%).....	118
Figure 7.8 Breakdown probability distributions regarding traffic demand (heavy vehicle percentage=5%).....	120
Figure 7.9 Breakdown probability distributions regarding traffic demand (heavy vehicle percentage=25%).....	120
Figure 7.10 Breakdown probability distributions regarding heavy vehicle percentage (traffic demand=3500 veh/h).....	121
Figure 7.11 Breakdown probability distributions regarding heavy vehicle percentage (traffic demand=3300 veh/h).....	122
Figure 7.12 Breakdown probability distributions regarding heavy vehicle percentage (traffic demand=3700 veh/h).....	123

Chapter 1

INTRODUCTION

1.1 Background

Intercity expressway network in Japan plays an important role in Japanese economic activities as it provides prime service to intercity expressway users. However, various sections of Japanese intercity expressways experience the extended periods of congestion due to breakdown phenomena, especially near large metropolitan areas.

Once breakdown occurs on a segment, intercity expressway performance will be significantly influenced such as deterioration of travel time reliability, increase of accident occurrence probability, etc. Therefore, analysis on breakdown phenomena is the base for various practical issues on intercity expressways at both the operational and the planning stages.

With respect to the operational stage, a macroscopic simulation platform is currently under construction which covers intercity expressway network of central Japan. It will enable evaluation of intercity expressway performance in response to traffic flow characteristics at the operational stage. As for development of this simulation platform, analysis on breakdown phenomena is a critical issue in light of their significant impacts on intercity expressway performance.

Furthermore, with respect to the planning stage, there exist the requirements for control on traffic condition characteristics, improvement on geometric configurations to alleviate breakdown phenomena. Again analysis on breakdown phenomena is desirable to quantify impacts of traffic condition and geometric characteristics.

Recurrent bottlenecks are the critical points in intercity expressway network and are consequently the major source of congestion. According to the report from JSTE (Japan society of traffic engineers) in 2006, 82.9% congestions are attributed to breakdown phenomena at recurrent bottlenecks due to the overloaded traffic demand.

To analyze breakdown phenomena, capacity of recurrent bottleneck will be focused on. It includes two distinct aspects which are commonly called "two-capacity phenomenon". One aspect is regarding the traffic flow rate which causes breakdown occurrence, and this flow rate is defined as breakdown flow rate (*BDF*) in this study. The other aspect is on the traffic flow rate for breakdown duration which is defined as discharge flow rate (*DCF*) in this study. They are characterized of stochastic natures which are influenced by traffic condition and geometric characteristics.

1.1.1 Significance of analyzing breakdown phenomena at both the operational and the planning stages

In practice at the operational stage, intercity expressway performance needs to be evaluated in response to change of traffic condition characteristics. Intercity expressway performance is greatly impacted by breakdown phenomena at recurrent bottlenecks. Once breakdown occurs, it will be significantly influenced such as deterioration of travel time reliability, increase of accident occurrence probability, etc.

Therefore, it is very significant to simulate breakdown phenomena at recurrent bottleneck. In response to change of traffic condition characteristics, simulation of breakdown occurrence is a critical step which depends on quantification of breakdown flow rate. After breakdown occurs, its duration relies on discharge flow rate which determines the ability to dissipate queue.

As for the planning stage, there exist the requirements for control on traffic condition characteristics, improvement on geometric configurations to alleviate breakdown phenomena. Again analysis on breakdown phenomena is desirable to quantify impacts of traffic condition and geometric characteristics.

1.1.2 Two aspects of bottleneck capacity to represent breakdown phenomena

With respect to breakdown flow rate, it has become evident that breakdown does not necessarily occur at the constant flow rate values based on the empirical observations. More and more researches have suggested that breakdown occurrence is a stochastic event. With respect to a certain bottleneck location, breakdown flow rate values are distributed in a wide range. In this sense, breakdown flow rate is better represented as a random variable rather than a deterministic value.

Considerable number of studies have adopted breakdown probability model to describe and quantify breakdown flow rate in light of its stochastic characteristic. Furthermore, with respect to the stochastic nature of breakdown occurrence and the resulted breakdown flow rate distribution, impacts of traffic flow characteristics and geometries are speculated. However, to date, analyses supporting this kind of claim are limited.

With respect to discharge flow rate, it is typically characterized in a deterministic manner by the existing studies. In other words, after breakdown occurs, it is assumed that the queue will discharge at a deterministic flow rate. Recently it has been becoming more and more obvious that the conventional deterministic measurement of discharge flow rate is not sufficient for intercity expressway traffic performance assessment without considering its stochastic nature. Based on field data, some researches have already indicated that discharge flow rate is also stochastic in nature. However, there are rare studies on the stochastic modeling on discharge flow rate up to now.

Furthermore, what is more noteworthy is the relationship between breakdown flow rate and discharge flow rate as it significantly impacts on intercity expressway performance accompanied with breakdown occurrence. As aforementioned, breakdown and discharge flow rates represent two distinct aspects of expressway capacity. Typical investigation of their relationship is to estimate "capacity drop" accompanied with breakdown occurrence. According to the above discussion, due to limited knowledge, especially on stochastic nature of discharge flow rate, such traditional investigations are mainly from deterministic viewpoints. To date, analyses on relationship between breakdown and discharge flow rates considering their stochastic natures are quite limited.

1.1.3 Insights of lane based analysis

The insights of lane based analysis also need particular concern. On multilane expressways, lane utilization rate (*LUR*) is an important parameter, which is defined as the proportion of traffic flow rate on individual lanes out of the cross-section flow rate during a certain time interval. Past studies have indicated that the *LUR* is closely related to breakdown probability and further more impacts on breakdown phenomena.

Furthermore, identification of breakdown occurrence is a decisive issue for modeling breakdown flow rate and discharge flow rate. To date, most of the existing identification methods have treated all lanes of mainline as one unit for an intercity expressway facility, and are conducted mainly through a check of the aggregated data of cross-section. However, this cross-section based method oversimplifies breakdown occurrence for bottlenecks at intercity expressway facilities where lane usage preferences on each lane significantly differ like nearby diverge and merge sections.

Traffic flows are assigned at these sections which make that mainline traffic flows are generally interrupted by diverge and merge traffic flow there. Hence, lane usage preference by drivers apparently varies due to the influence of diverge and merge traffic flow. Impacted by off-ramp diverge or on-ramp merge traffic flow, possibly breakdown occurrences on each lane would be more significantly different. Furthermore existence of semi-congested state has been observed at diverge sections, where some lanes are congested and others are not. To sum it up, necessarily, a lane based identification method is required to identify breakdown occurrence particularly at diverge and merge sections which are located at the interrupted intercity expressway facilities.

1.1.4 Impacts of traffic condition and geometric characteristics

With respect to the stochastic natures of breakdown occurrence and the resulted breakdown flow rate distribution, impact of traffic flow characteristics and geometries are speculated. To date, analyses supporting this kind of claim are limited. For example, at diverge sections, diverge flow apparently has certain impact on mainline flow, and is likely to influence breakdown occurrence. In addition, as aforementioned, lane specific breakdown characteristics have significant impacts on breakdown occurrence. Therefore diverge rate

(*DR*) and lane utilization rate (*LUR*) can be chosen as candidates of the representative influencing factors.

In addition, with respect to different intercity expressway facility types, parameters of breakdown probability and discharge flow rate models for each bottleneck are possibly impacted by its site-specific geometries. In this sense, the general breakdown probability model can be developed by considering site-specific geometries for each facility type. This kind of general model enables evaluation of possible breakdown occurrence at potential bottlenecks which is likely to be triggered by change of traffic demand in future. In this study, there exist several bottlenecks for each facility type in intercity expressway network which has different geometric configurations. This enables the generalization of breakdown probability and discharge flow rate models.

1.1.5 Simulation by incorporating breakdown probability and discharge flow rate models

By applying the developed breakdown probability and discharge flow rate models, breakdown phenomena can be simulated. Such a simulation tool would help plan countermeasures to alleviate breakdown occurrence like traffic demand management, lane usage recommendation.

With respect to the existing bottleneck locations, reproduction of breakdown phenomena can serve as the base for planning breakdown relief schemes. This kind of reproduction can be realized by incorporating the developed stochastic models. Based on the arriving traffic demand, the breakdown occurrence can be generated in a stochastic way by using the developed breakdown probability model. As for breakdown duration, it can be estimated through discharge flow rate model.

1.1.6 Assessment of potential bottlenecks

With respect to the potential bottleneck locations, there exist certain locations in the intercity expressway network where no significant breakdown occurrence phenomena have been observed under the current traffic condition. However, in future, there are possible changes of traffic flow condition accompanying with change of network, adjustment of traffic policies. It is likely that breakdown can also occur at these locations due to such

changes in future. These kinds of locations are regarded as potential bottlenecks. Evaluation of potential bottleneck performances at the operational stage is significant issues for roadway authorities.

1.2 Problem statement

According to the discussions above, several problems can be highlighted as follows.

Firstly, with respect to recurrent bottleneck capacity, both breakdown flow rate and discharge flow rate need to be modeled in a stochastic way in light of their stochastic characteristics. With respect to breakdown flow rate, breakdown probability model is a preferable measure to describe and quantify breakdown flow rate in light of its stochastic nature. However for discharge flow rate, stochastic modeling is also needed. Furthermore, the relationship between breakdown flow rate and discharge flow rate needs to be taken into consideration when modeling.

Secondly, with respect to the stochastic natures of breakdown occurrence and the resulted breakdown flow rate distribution, impact of traffic flow characteristics and geometries are speculated. To date, analyses supporting this kind of claim are limited which need to be further investigated. Thirdly, insights of lane based analysis need to be paid attention to considering the lane usage preference at bottleneck locations especially at diverge and merge bottleneck locations.

Finally, the developed breakdown probability and discharge flow rate models need to be incorporated for simulating breakdown phenomena at the existing bottleneck locations. Moreover, evaluation of potential bottleneck performances also needs to be conducted by applying the developed models.

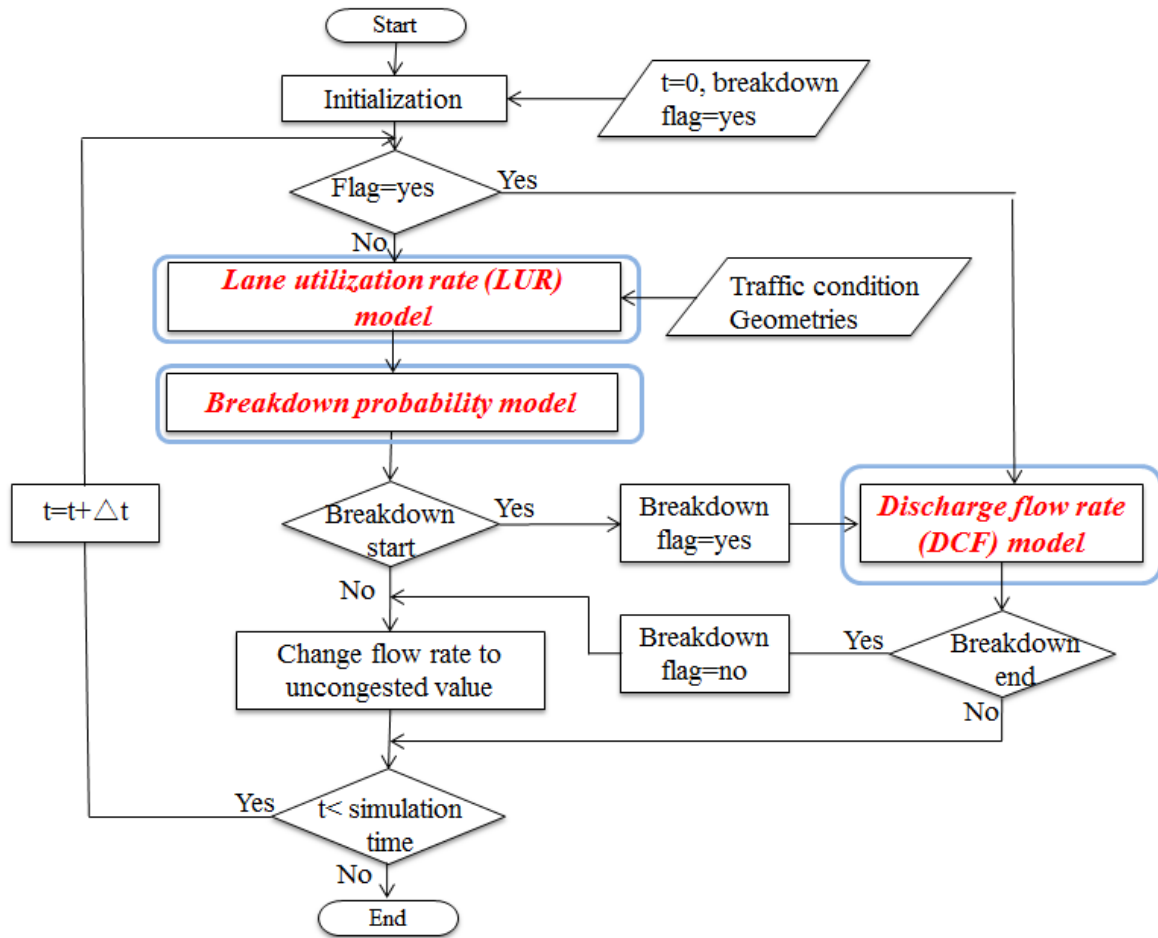


Figure 1.1 Flowchart for simulating breakdown phenomena

In summary, Figure 1.1 presents the flowchart for simulating breakdown phenomena. Three types of models are necessary, namely lane utilization rate (*LUR*) model, breakdown probability model and discharge flow rate model.

1.3 Objectives

The objective of this study is to model breakdown flow rate and discharge flow rate by considering traffic condition characteristics and geometries on intercity expressways.

This objective is achieved through taking the following steps:

- Modeling lane utilization rate (*LUR*) as a function of traffic condition characteristics and geometries.
- Selecting appropriate breakdown identification methods in order to determine breakdown occurrence at diverge, merge and sag bottlenecks.

- Identifying the main influencing factors on breakdown and discharge flow rates.
- Modeling breakdown and discharge flow rates by considering traffic condition and geometric characteristics.
- Simulating breakdown phenomena by applying the developed breakdown probability and discharge flow rate models.
- Developing maps of breakdown probability distribution on intercity expressway.

1.4 Research outline

This study will be carried out by following the general research outline as presented in Figure 1.2. Firstly, after defining research objective, preparation is made for modeling breakdown and discharge flow rates on intercity expressway sections. Intercity expressway network of central Japan is focused on where breakdown phenomena exist at facility types such as diverge, merge and sag sections. Secondly a lane a lane based method is proposed to identify breakdown occurrence. The most significant step in this study is probably to model breakdown flow rate and discharge flow rate in a stochastic way. Then the developed stochastic models are incorporated for simulating breakdown phenomena at the existing bottleneck locations. Moreover, evaluation of potential bottleneck performances need also be conducted by applying the developed models. Finally conclusions and some recommendations for future research are provided.

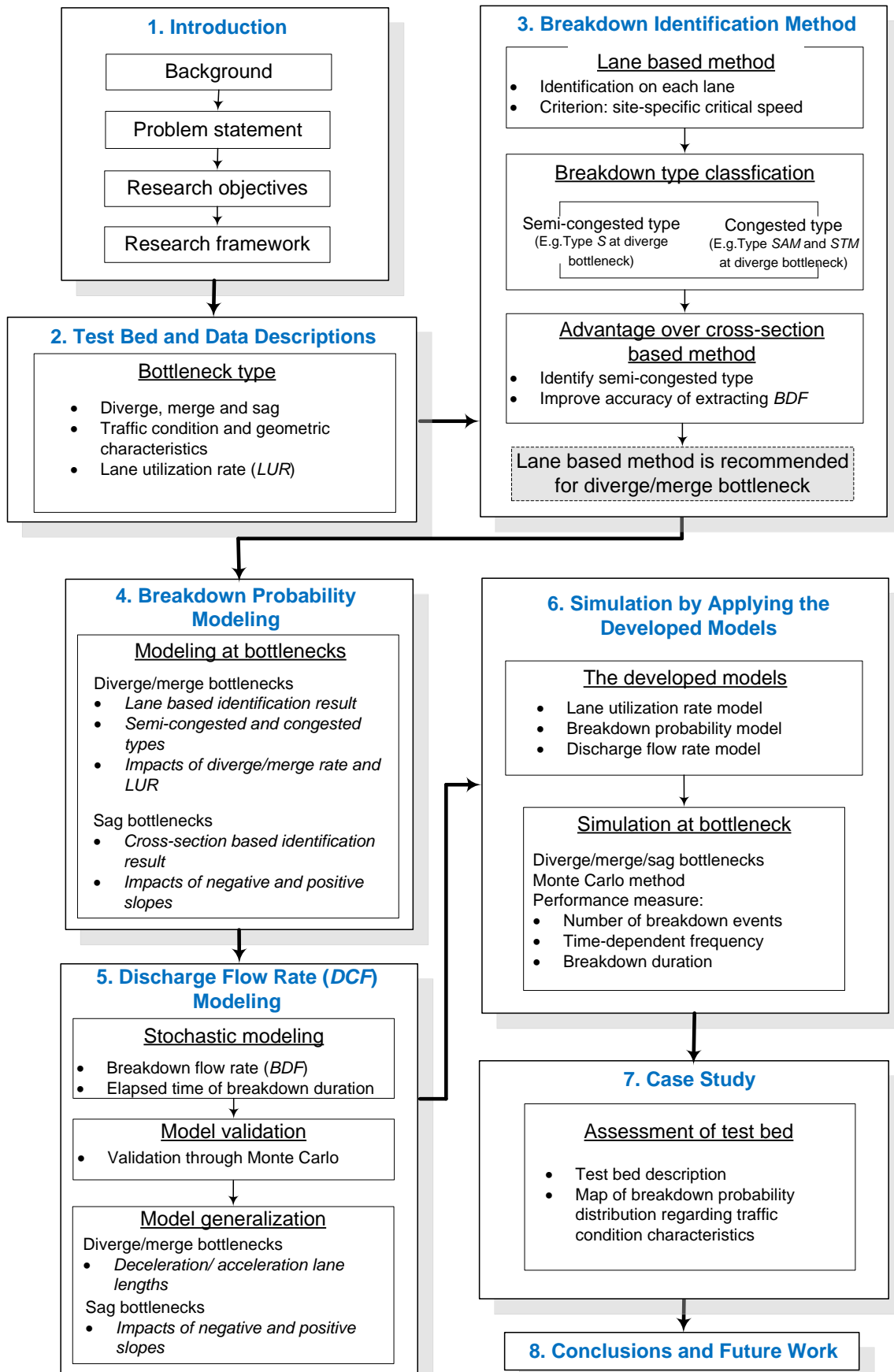


Figure 1.2 General research outline

Chapter 2

TEST BED AND DATA DESCRIPTIONS

2.1 Introduction

This chapter introduces the preparation for modeling breakdown flow rate and discharge flow rate in this study. Intercity expressway network of central Japan is focused on where breakdown phenomena exist at facility types such as diverge, merge and sag sections.

Two groups can be categorized among these types of bottlenecks. One group includes bottlenecks at the interrupted expressway sections like diverge and merge sections. Traffic flows are assigned at these sections which make that mainline traffic flows are generally interrupted by diverge and merge traffic flow there. Hence, lane usage preference by drivers apparently varies due to the influence of diverge and merge traffic flow. Diverge and merge traffic flow and the resulted lane usage preference are regarded as main cause of breakdown occurrence. Change of traffic demand distributions in intercity expressway network is closely related to possible breakdown occurrence. A representative example is that after operation of Shin-Meishin Expressway in March, 2008, frequent breakdown events have been observed at diverge section of Toyota JCT (Junction) in the westbound direction of Tomei Expressway, where higher diverge rate acts as a key influencing factor.

The other uninterrupted group refers to bottleneck at sag section which is the typical bottleneck type in Japanese intercity expressway network due to characteristics of mountainous terrain in Japan.

Along the mainlines, off-ramps and on-ramps of intercity expressways, double-loop detectors are installed approximately every two kilometers. Thanks to Central Nippon Expressway Company Limited (NEXCO), traffic flow data records at each detector are

available. This study investigates recurrent breakdown phenomena during the period from 3/1/2008 to 12/31/2009.

Traffic flow rates and average speeds on each lane were measured and aggregated at a 5-minute interval. Breakdown events due to other non-recurrent causes such as roadway maintenance works and accidents were excluded. Some preliminary studies have been conducted on constructing the flow-speed diagrams at each detector, which help identify bottleneck locations.

At the identified bottleneck locations, traffic conditions and geometric characteristics are discussed. Lane utilization rate (*LUR*) has been found to play a significant role in analyzing bottleneck capacity. Therefore, it is modeled as a function of traffic condition and geometries based on traffic flow data.

2.2 Test bed: intercity expressway network of central Japan

Figure 2.1 illustrates the scope for intercity expressway network of central Japan. Basic information on each expressway is listed in Table 2.1.

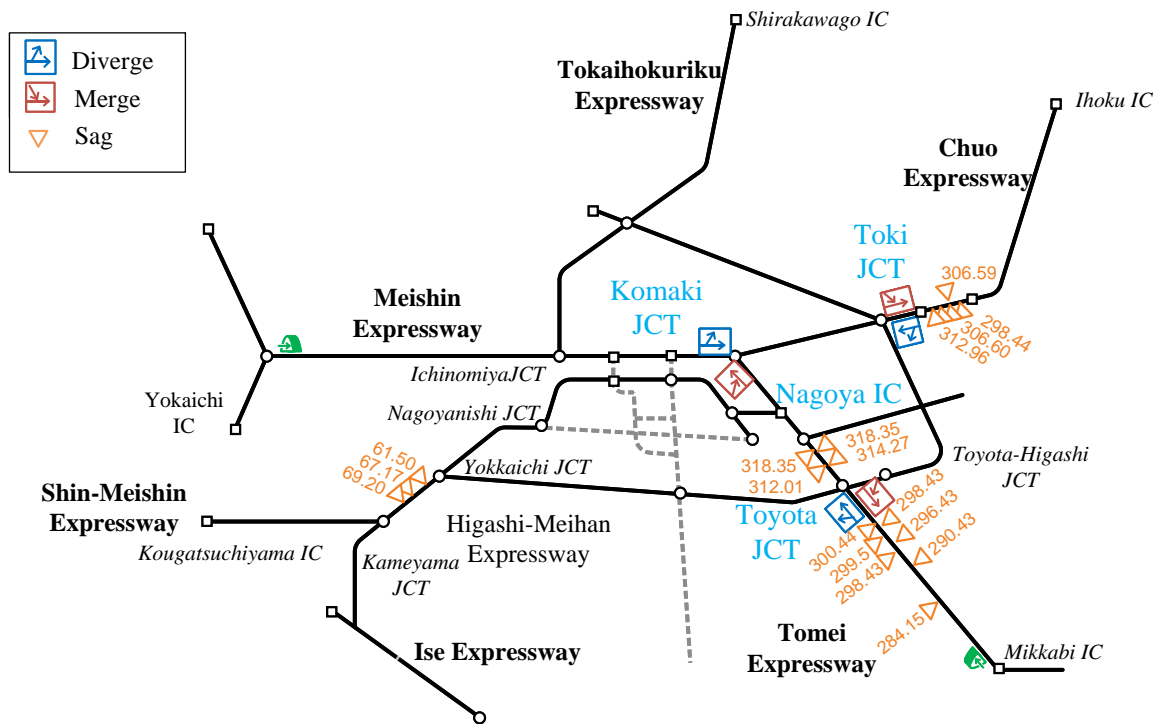


Figure 2.1 The intercity expressway network of central Japan

Table 2.1 Basic information on each intercity expressway

Expressway	Sections	KP (km)	Extension (km)
Tomei	Mikkabi IC- Komaki IC	251.0-346.7	95.7
Meishin	Komaki IC-Yokkaichi IC	346.7-434.6	87.9
Shin-meishin	Kameyama JCT- Kougatuchiyama IC	22.5-41.3	18.8
Higashi-meihan	Nagoyanishi JCT- kameyama IC	29.05-81.06	52.01
Tokaihokuriku	Ichinomiya JCT-Shirotori IC	-0.2-59.7	59.9
Chuo	Ihoku IC- Komaki JCT	195.9-343.9	148
Isewangan	Toyotahigashi JCT-Yokkaichi JCT	0-56.5	56.5

Note: JCT stands for Junction and IC stands for Interchange. KP stands for Kilometer Post.

Tomei and Meishin Expressways are corridor expressways in Japan which connects metropolis like Tokyo, Nagoya and Kobe. They are characterized of high traffic demands and high heavy vehicle percentages. Shin-Meishin Expressway has been opened from 3/1/2008 which results in shorter distance and better driving perception for drivers compared to Meixin Expressway. This causes the shift of traffic flow onto this route. Tokaihokuriku, Higashi-Meihan and Chuo Expressways have tight curves and steep slopes.

2.3 Identification of bottleneck location

The existing bottleneck locations are identified by using the fundamental traffic flow-speed diagrams as introduced in the following parts. At each detector location, traffic flow-speed diagram is constructed based on historical traffic data. In fact, recurrent bottleneck location is the weakness point of the intercity expressway network from the viewpoint of capacity. In other words, recurrent breakdown phenomena always occur at bottleneck locations rather than other locations. Once breakdown occurs at a certain bottleneck location, its adjacent upstream location will be impacted by the location of the built queue. Also at its adjacent downstream location, only the uncongested traffic flow can be observed due to the filter effect of bottleneck location. Such conditions can be reflected by using the illustrations of traffic flow-flow rate diagrams.

Figure 2.2 illustrates configuration of detector locations nearby bottleneck. Figures 2.3 to 2.5 present the representative examples of traffic flow-speed diagrams nearby an existing bottleneck which is located at 302.15KP on Tomei Expressway of westbound direction.

At bottleneck observation location 302.15KP and its adjacent upstream detector location 299.5KP, distributions of traffic flow-speed include both the congested and the uncongested traffic flows as shown in Figures 2.3 and 2.4 respectively. Accordingly, at its adjacent downstream detector location 304.2KP, only the uncongested traffic flow can be found as illustrated in Figure 2.5. Thus, this detector location 302.15KP can be identified as the bottleneck location.

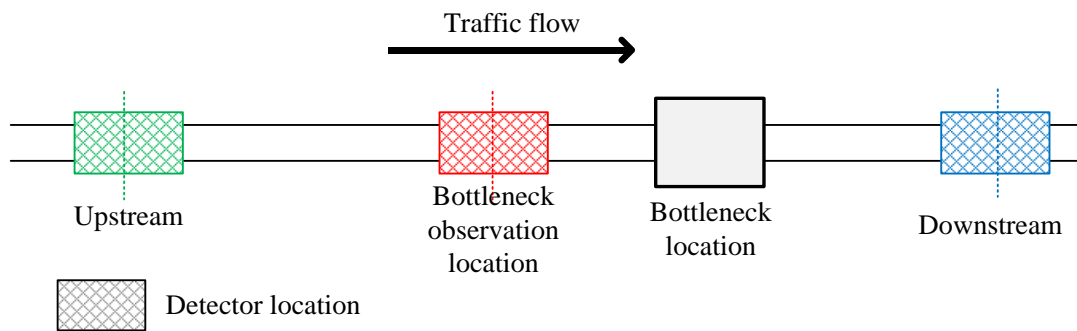


Figure 2.2 Illustration of detector locations nearby bottleneck

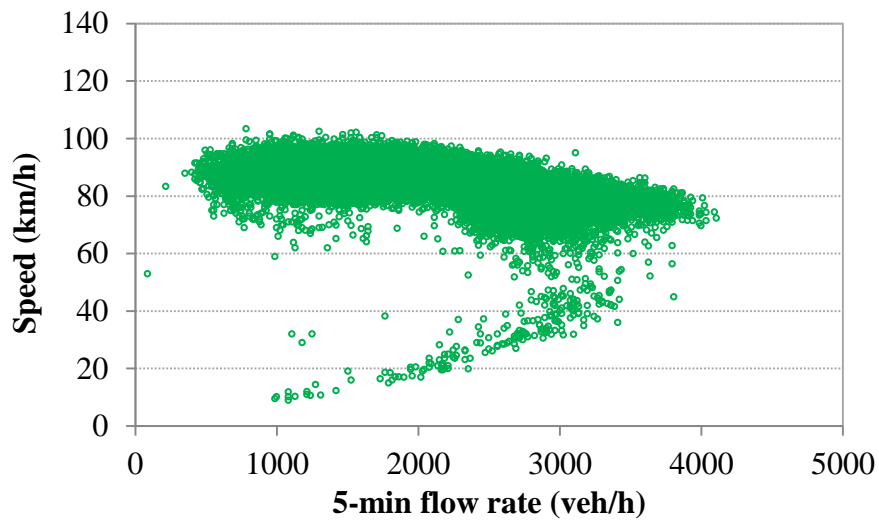


Figure 2.3 Flow rate-speed diagram at bottleneck upstream (299.5KP on Tomei Expressway of westbound direction)

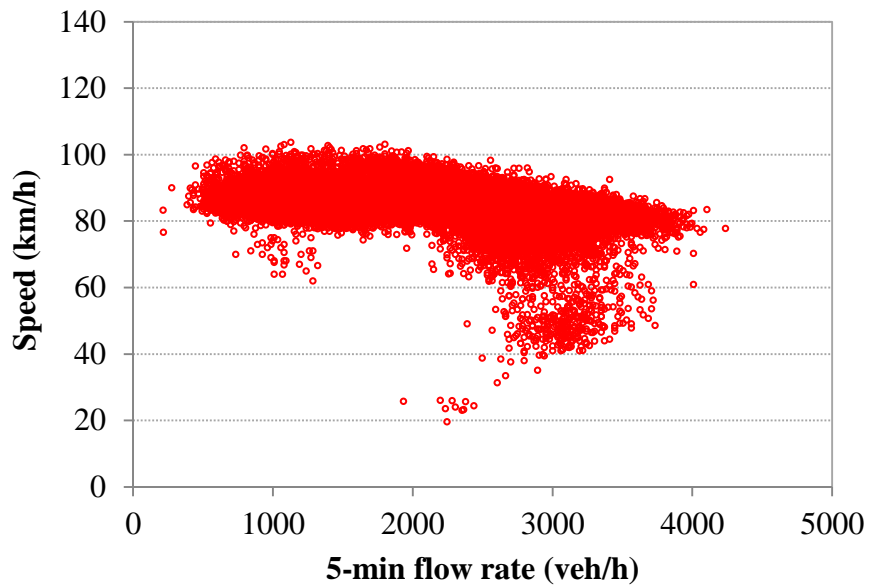


Figure 2.4 Flow rate-speed diagram at bottleneck location (302.15KP on Tomei Expressway of westbound direction)

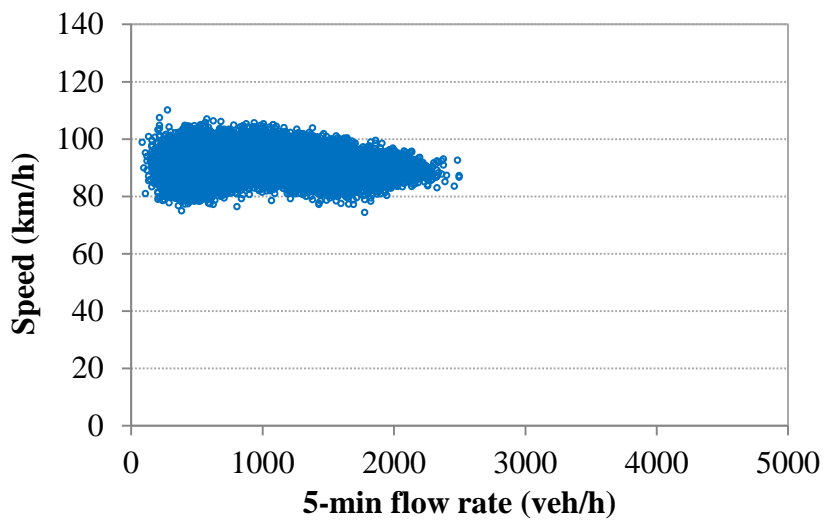


Figure 2.5 Flow rate-speed diagram at bottleneck downstream (304.2KP on Tomei Expressway of westbound direction)

2.4 Descriptions of the bottleneck locations

The preliminary analyses have been conducted to identify the recurrent bottleneck locations in the way as discussed above. The findings on the identified bottlenecks are introduced in this section. Three types of bottlenecks are focused on in this study, namely bottlenecks at diverge, merge and sag sections.

With respect to diverge and merge bottlenecks, they are located at the interrupted expressway sections. Their mainline traffic flows are generally interrupted by diverge or merge traffic flow. Hence, lane usage preference by drivers apparently varies due to the influence of diverge and merge traffic flow. Diverge or merge traffic flow and the resulted lane usage preference are regarded as main cause of breakdown occurrence there. Change of traffic demand distributions in intercity expressway network is closely related to possible breakdown occurrence there. To sum it up, diverge and merge bottlenecks can be attributed to the bottleneck group at the interrupted expressway sections.

With respect to sag bottleneck, it is located at the uninterrupted intercity expressway sections. Sag bottleneck is the typical bottleneck type in Japanese intercity expressway network due to characteristics of mountainous terrain in Japan. Sag bottleneck belongs to bottleneck group at the uninterrupted expressway sections.

2.4.1 Diverge bottlenecks

As listed in Table 2.2, there are four bottlenecks which have been identified at diverge sections in the intercity expressway network of central Japan.

Table 2.2 Descriptions of diverge bottlenecks

Name	Expressway	Direction	Location	Number of lanes	KP (km)
Toyota diverge bottleneck	Tomei	Westbound	Toyota JCT	2	302.15
Toki diverge bottleneck	Chuo	Southbound	Toki JCT	2	321.06
Komaki diverge bottleneck	Tomei	Eastbound	Komaki JCT	2	341.49
Nagoya diverge bottleneck	Tomei	Westbound	Nagoya IC	3	324.40

It needs to be noted that in conventional concept, diverge sections are not regarded as source of breakdown phenomena. However, the findings in this study indicate that breakdown phenomena can also exist at diverge sections if high diverge flows are available there. For example, at Toyota diverge bottleneck, high diverge flow onto Shin-Meishin Expressway can be regarded as the cause of breakdown occurrence. The findings on breakdown phenomena at diverge bottlenecks locations need particular concerns which may be ignored in conventional investigations.

Four bottlenecks at diverge sections are analyzed as listed in Table 2.2. Their geometries, lane configurations and detector locations are presented in Figures 2.6 to 2.11. In this study, these four diverge bottlenecks are denoted as Toyota, Toki, Komaki and Nagoya diverge bottlenecks respectively.



Figure 2.6 The aerial view of Toyota diverge bottleneck

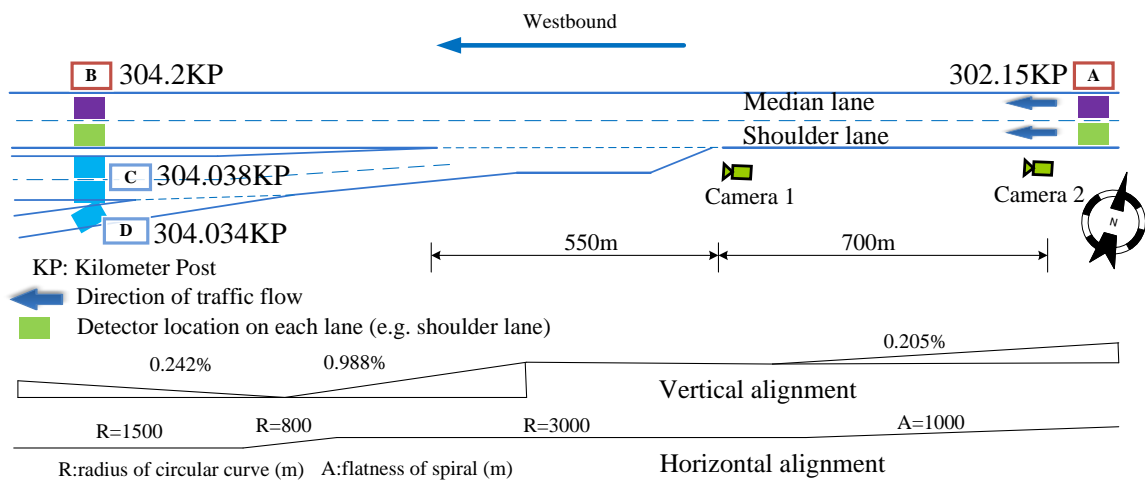


Figure 2.7 Illustration of Toyota diverge bottleneck



(a) View from Camera 1

(b) View from Camera 2

Figure 2.8 Video images of Toyota diverge bottleneck

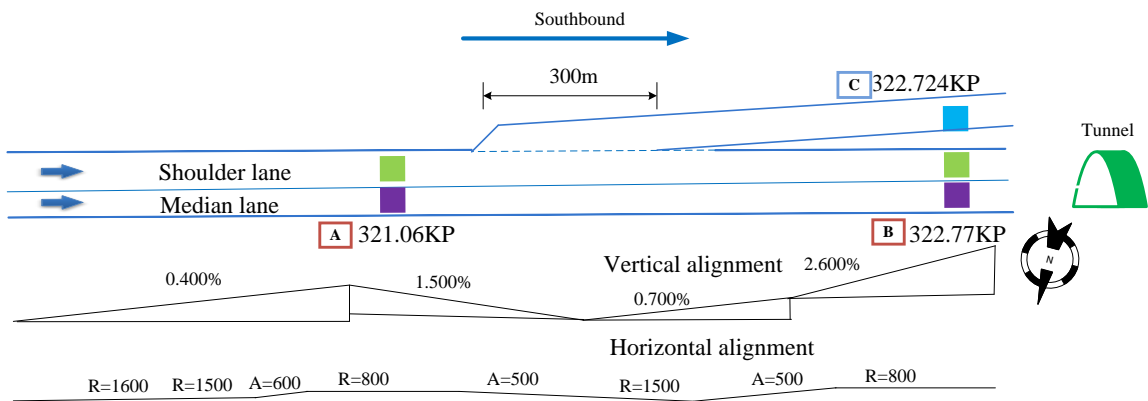


Figure 2.9 Illustration of Toki diverge bottleneck

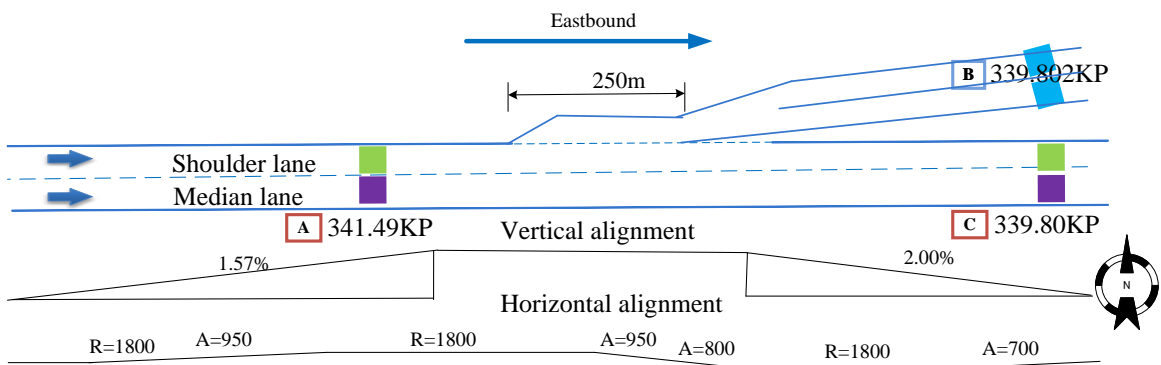


Figure 2.10 Illustration of Komaki diverge bottleneck

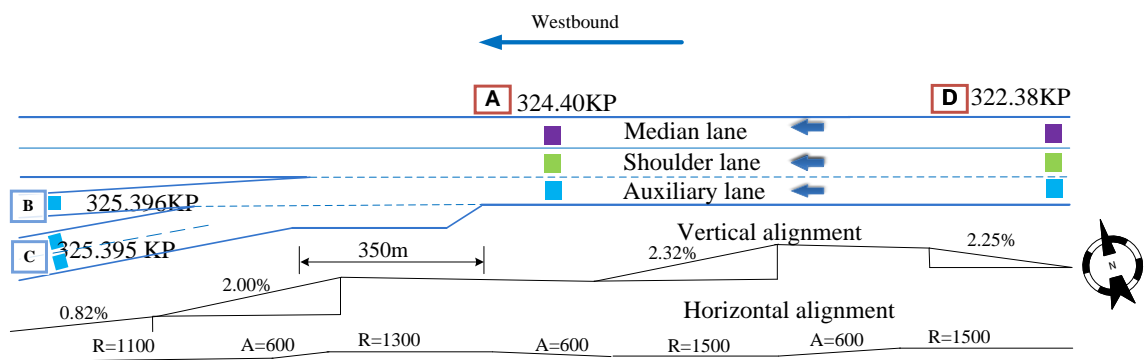


Figure 2.11 Illustration of Nagoya diverge bottleneck

As illustrated in Figures 2.6 to 2.11, layout of diverge section in Japan is similar to the off-ramp area described in HCM 2010. All of four diverge sections have left-side off-ramps. Figure 2.8 (a) and Figure 2.8 (b) present more distinct and direct overlooks of such a layout at Toyota diverge bottleneck.

With respect to Toyota diverge bottleneck, as shown in Figure 2.7, its mainline has two lanes, namely shoulder lane and median lane (at this diverge bottleneck, its mainline has been broadened to three lanes by fully utilizing shoulder from 10/21/2011). Toyota Junction that connects Tomei and Isewangan Expressways was opened in 2005, before the opening of the EXPO 2005 in Nagoya. Consequently, at its diverge section on Tomei Expressway of westbound direction, frequent breakdown events have been observed. Breakdown phenomena there are attributed to high diverge traffic flows which aim at using Shin-Meishin Expressway due to its better driving perception and shorter distance after its operation in March, 2008. Westbound directional AADT (Average Annual Daily Traffic Volume) on Tomei Expressway stays about 48,200 (veh/day) in 2009. AADT of diverge flow reaches about 28,200 (veh/day) which is approximately 45% of mainline flow. This high diverge flow level is regarded as the main cause of breakdown occurrence at this diverge section. Analysis in this study covers period from 3/1/2008 to 12/31/2009.

With respect to Toki and Komaki diverge bottlenecks, as for lane configuration, their mainlines also have two lanes, namely shoulder lane and median lane as shown in Figures 2.9 and 2.10 respectively. As for Nagoya diverge bottleneck, an auxiliary lane is configured besides shoulder lane and median lane as illustrated in Figure 2.11. A tunnel exists at the downstream of Toki diverge bottleneck.

2.4.2 Merge bottlenecks

As listed in Table 2.3, there are three bottlenecks which have been identified at merge sections in the intercity expressway network of central Japan.

Their geometries, lane configurations and detector locations are presented in Figures 2.12 to 2.14. In this study, these three merge bottlenecks are denoted as Toyota, Toki and Komaki merge bottlenecks respectively. As illustrated in Figures 2.12 to 2.14, layout of merge section in Japan is similar to the on-ramp area described in HCM 2010. All of three merge bottlenecks have left-side on-ramps.

With respect to lane configuration, for Toyota, Toki and Komaki merge bottlenecks, all of their mainlines have two lanes, namely shoulder lane and median lane (for Toyota merge section on Tomei Expressway, its mainline has been broadened to three lanes by fully utilizing shoulder from 10/21/2011).

Table 2.3 Descriptions of merge bottlenecks

Name	Expressway	Direction	Location	Number of lanes	KP (km)
Toyota merge bottleneck	Tomei	Eastbound	Toyota JCT	2	302.15
Toki merge bottleneck	Chuo	Northbound	Toki JCT	2	321.06
Komaki merge bottleneck	Tomei	Westbound	Komaki JCT	2	341.49

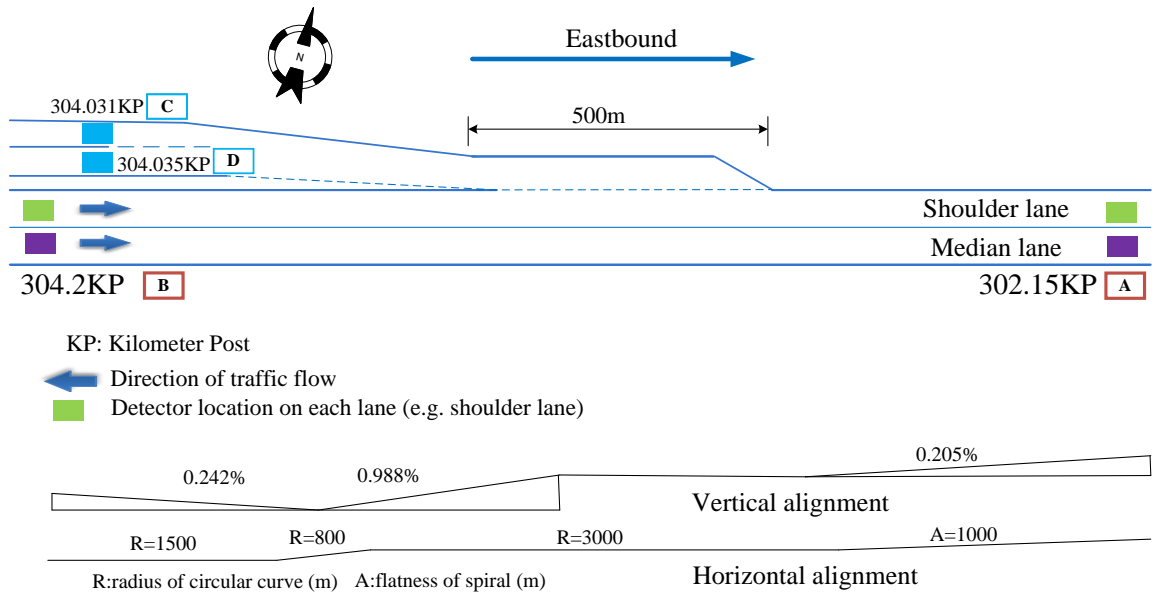


Figure 2.12 Illustration of Toyota merge bottleneck

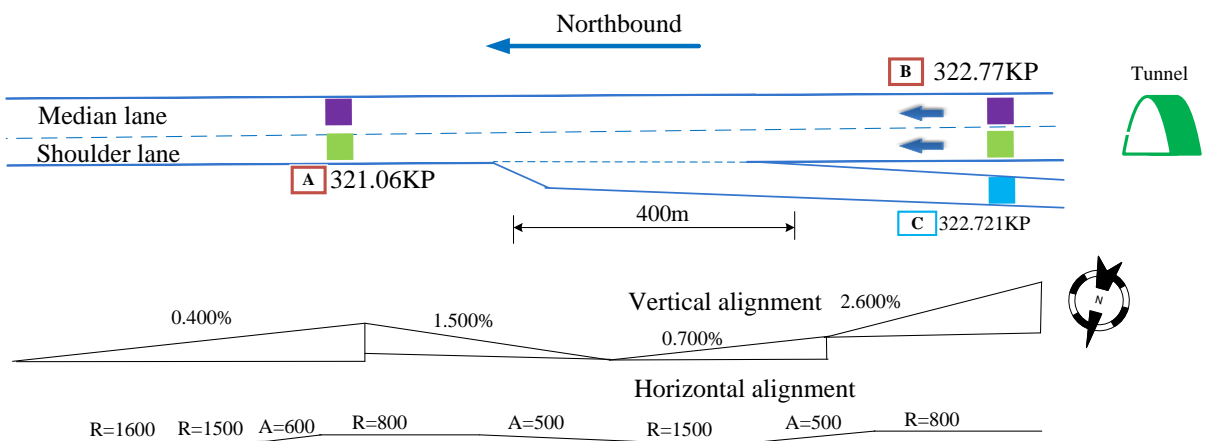


Figure 2.13 Illustration of Toki merge bottleneck

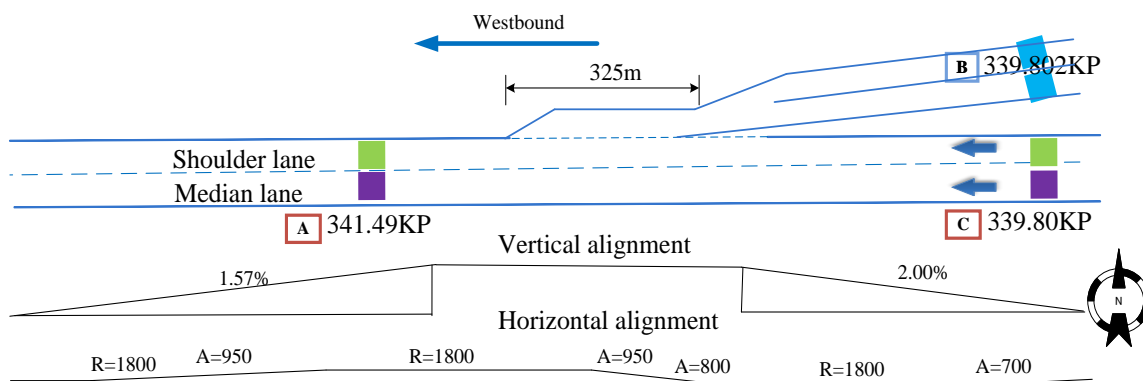


Figure 2.14 Illustration of Komaki merge bottleneck

2.4.3 Sag bottlenecks

As listed in Table 2.4, there are sixteen bottlenecks which have been identified at sag locations in the intercity expressway network of central Japan. They are located on Tomei, Meishin, Higashi-Meihan and Chuo Expressways respectively. With respect to lane configuration, all of their mainlines have two lanes, namely shoulder lane and median lane. Their locations and KP positions are listed in Table 2.4.

Table 2.4 Descriptions of sag bottlenecks

Number	Expressway	Direction	Location	KP (km)
1	Tomei	Eastbound	Toyota JCT-Okazaki IC	296.43
2	Tomei	Eastbound	Toyota JCT-Okazaki IC	298.43
3	Tomei	Eastbound	Okazaki IC- Otowa Gamagori IC	290.43
4	Tomei	Eastbound	Tomei Miyoshi IC-Toyota IC	314.27
5	Tomei	Westbound	Okazaki IC-Toyota JCT	294.43
6	Tomei	Westbound	Okazaki IC-Toyota JCT	298.43
7	Tomei	Westbound	Okazaki IC-Toyota JCT	299.50
8	Tomei	Westbound	Toyota IC-Tomei Miyoshi IC	312.01
9	Higashi-Meihan	Eastbound	Suzuka IC-Yokkaichi IC	61.5
10	Higashi-Meihan	Eastbound	Suzuka IC-Yokkaichi IC	67.17
11	Higashi-Meihan	Eastbound	Yokkaichi Higashi IC -Yokkaichi IC	58.54
12	Chuo	Westbound	Mizunami IC-Ena IC	306.59
13	Chuo	Northbound	Ena IC- Mizunami IC	298.44
14	Chuo	Southbound	Ena IC- Mizunami IC	306.6
15	Chuo	Southbound	Ena IC- Mizunami IC	312.96
16	Chuo	Southbound	Ena IC- Mizunami IC	317.49

2.5 Descriptions of traffic flow data

This section introduces the traffic flow data which serves as the base for investigation of this study.

Along the mainlines, off-ramps and on-ramps of intercity expressway, double-loop detectors are installed approximately every two kilometers. Thanks to Central Nippon Expressway Company Limited (NEXCO), traffic flow data records at each detector are available. This study investigates recurrent breakdown phenomena during the period from 3/1/2008 to 12/31/2009. Breakdown events due to other non-recurrent causes such as roadway maintenance work and accidents have been excluded.

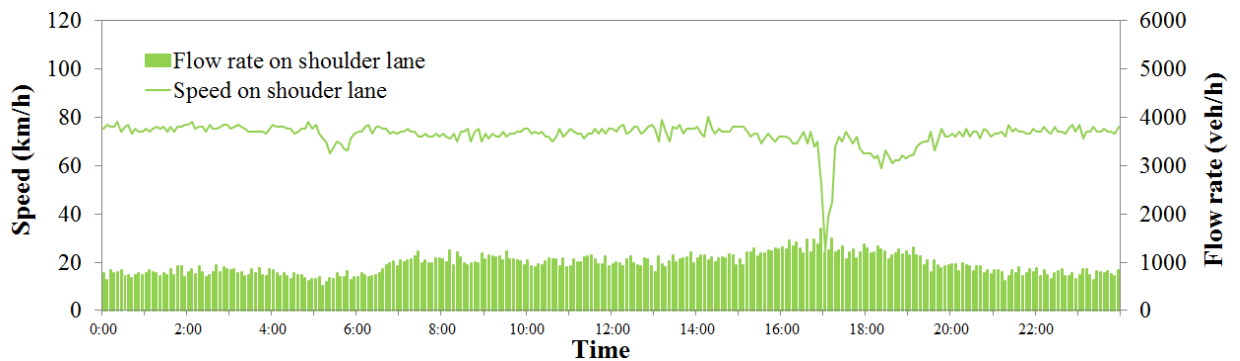


Figure 2.15 Flow rate and speed on shoulder lane at Toyota diverge bottleneck (302.15KP on Tomei Expressway of westbound direction)

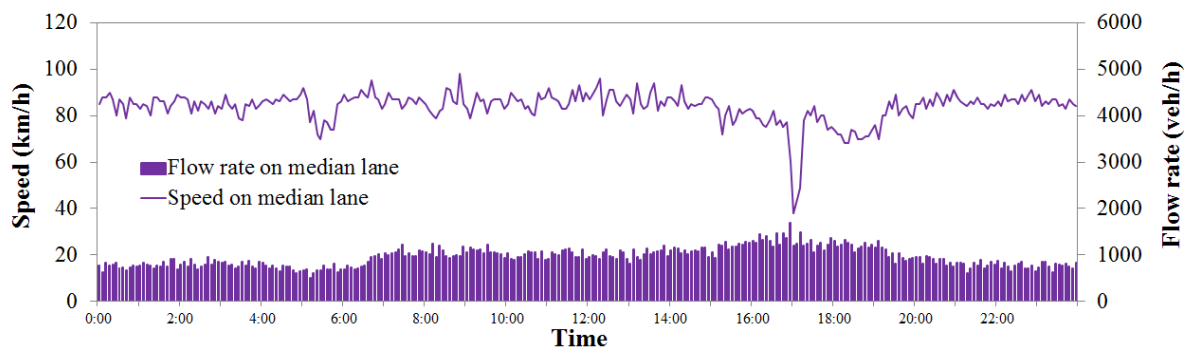


Figure 2.16 Flow rate and speed on median lane at Toyota diverge bottleneck (302.15KP on Tomei Expressway of westbound direction)

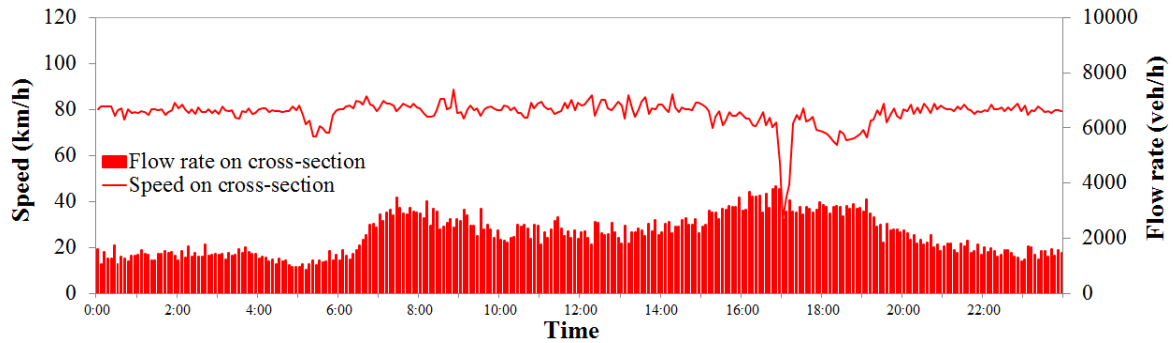


Figure 2.17 Aggregated flow rate and speed of cross-section at Toyota diverge bottleneck (302.15KP on Tomei Expressway of westbound direction)

Traffic flow rates and average speeds on each lane were measured and aggregated at a 5-minute interval. For example, such kinds of data are illustrated by the traffic data distribution at the location of Toyota diverge bottleneck on 3/4/2008. Figures 2.15 and 2.16 present the flow rate and speed distributions on shoulder lane and median lane respectively. By comparing distributions of them, it can be found that flow rate and speed distributions on each lane apparently differ. This kind of issue will be further investigated in the following sections.

On this day (Monday), peak traffic flow rates on both lanes concentrate during the time period about 17:00. Significant speed drops occurred during that period on both shoulder and median lanes which indicate the breakdown occurrences. Figure 2.17 shows the flow rate and speed of cross-section by aggregating them on shoulder lane and median lane.

In addition, traffic flow rate of heavy vehicles are also recorded on each lane at each detector location.

2.6 Lane utilization rate (*LUR*) modeling to describe lane-specific driving behaviors

As discussed above, traffic flow rate on each lane apparently differs. This difference actually plays a significant role in determining intercity expressway performance. The existing studies have found that breakdown occurrence can be influenced by it.

Therefore, in this study, lane utilization rate (*LUR*) is used as a macroscopic variable to describe the lane-specific characteristics on the multilane expressway. Wang *et al.* (2013) have modeled lane utilization rate by considering traffic condition characteristics and geometries on intercity expressways of central Japan. The modeling result will be quoted

in this study. LUR on a certain lane is defined as rate of the flow rate on this lane by the flow rate of cross-section as expressed in Equation (2.1).

$$LUR = \frac{FR}{FR_{total}} \quad (2.1)$$

Where FR is traffic flow rate on a certain lane and FR_{total} is total traffic flow rate of cross-section.

Figure 2.18 presents the relationship between traffic flow rate of cross-section and LUR on shoulder lane at Toyota diverge bottleneck. It can be found that LUR on shoulder lane decreases with the increase of traffic flow rate of cross-section.

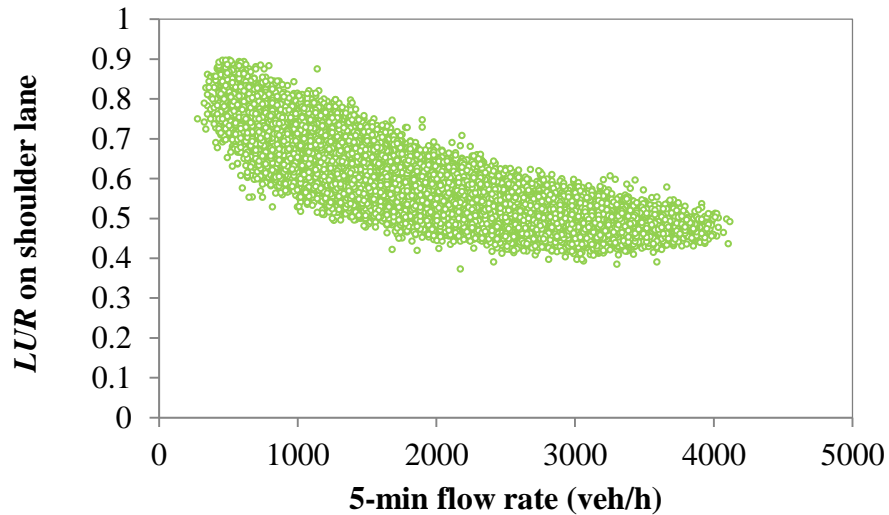


Figure 2.18 Relationship between LUR and traffic flow rate of cross-section at Toyota diverge bottleneck (302.15KP)

In the following sections, LUR model will be developed which enables estimation of LUR distribution in the intercity expressway network of central Japan in this study.

2.6.1 Data description for LUR modeling

With respect to intercity expressway network of central Japan, eight intercity expressways are used for LUR modeling. The 5-min aggregated detector data in 2009 are utilized for this analysis. Altogether, the data are from 373 detectors installed on 4-lane expressways.

As for data processing, the first step in handling the data is to remove the missing and erroneous values due to traffic accidents, road maintenance or other abnormal conditions from detector records. Ma *et al.* (2011) has proposed a methodology to analyze traffic flow characteristics due to accidents which is adopted in this analysis. Then traffic flow data at the uncongested flow conditions are distinguished from those at congested flow conditions by adopting a critical speed threshold based on the flow rate-speed diagram which is constructed at each detector location.

Total uncongested flow data at each detector are further categorized into several groups by cross-section flow rate (i.e. every 300 veh/h) and heavy vehicle percentage (i.e. every 10%). The groups which have sample size over 20 will be used for analysis. On the 4-lane expressways, *LUR* for shoulder lane will be used for modeling as the mainline owns two lanes, namely shoulder lane and median lane.

2.6.2 Influencing factors on *LUR*

LUR is affected by various factors, such as cross-section traffic flow rate, heavy vehicle percentage, geometric characteristics and etc. They are summarized into several categories as shown in Table 2.5. Due to lack of data record at some off-ramps locations, impacts from diverge flow rate has not been taken into consideration in this study.

Table 2.5 Influencing factors on *LUR*

Items	Influencing factors
Traffic flow condition	Cross-section traffic flow rate Heavy vehicle percentage
Geometries	Distance to diverge section Distance from merge section Vertical slope
Traffic regulations	Speed limit

2.6.3 Parameter estimation of *LUR* model

Based on the previous analysis of *LUR* on shoulder lane, an exponential function is used to model it through the fundamental relationship between *LUR* and cross-section traffic flow.

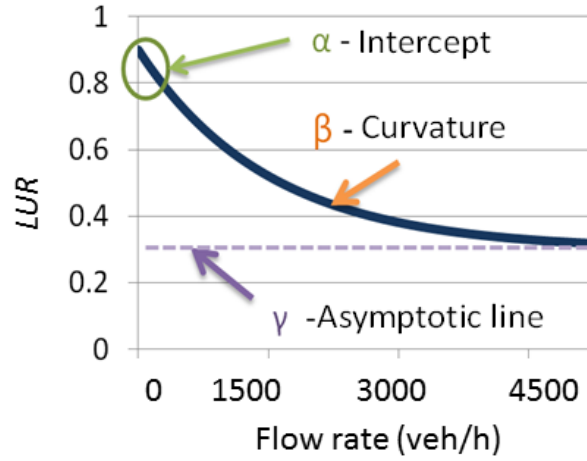


Figure 2.19 *LUR* model parameters

Three parameters are adopted to determine the shape of the curve as shown in Figure 2.19. In Equation (2.2-a), α determines the intercept, β stands for curvature and γ represents the asymptotic line. α , β and γ may vary depending on several influencing factors. Herein the influences of heavy vehicle percentage, slope and distance to diverge section are taken into account to develop the model, as represented in Equations (2.2-a) to (2.2-d).

$$SLFD = (\alpha - \gamma) \exp(\beta FR) + \gamma \quad (2.2-a)$$

$$\alpha = \alpha_0 + \alpha_1 hvr + \alpha_2 \delta_2 uphill_i\% + \alpha_3 \delta_3 uphill_i\% \quad (2.2-b)$$

$$\beta = \beta_0 + \beta_1 hvr + \beta_2 \delta_2 uphill_i\% + \beta_3 \delta_3 uphill_i\% \quad (2.2-c)$$

$$\gamma = \gamma_0 + \gamma_1 hvr + \gamma_4 dd \quad (2.2-d)$$

where, α , β , γ , α_0 , α_1 , α_2 , α_3 , β_0 , β_1 , β_2 , β_3 , γ_0 , γ_1 , γ_4 are estimation parameters. δ_2 is a dummy variable (1, if slope > 0 ; 0, if slope ≤ 0). δ_3 is a dummy variable (1, if slope < 0 ; 0, if slope ≥ 0). FR is cross-section traffic flow with a range from 0 to 4212 (veh/h). hvr stands for heavy vehicle percentage of cross-section. dd (km) means the distance to the nearest hard nose of downstream diverge section. $Uphill_i\%$ (%) is the slope value where detectors are located on uphill ways. $Downhill_i\%$ (%) is the slope value where detectors are located on downhill ways.

Table 2.6 Estimation of LUR model parameters

Parameters	Unit of variables	Speed limit						
		60km/h		80km/h		100km/h		
		Coef.	<i>t</i> value	Coef.	<i>t</i> value	Coef.	<i>t</i> value	
α	α_0	-	0.850	98.82	0.875	277.16	0.886	212.23
	$\alpha_1(hvr)$	-	0.0706	3.91	0.0405	12.93	0.0720	11.01
	α_2	%	-	-	0.0110	7.92	0.00826	3.97
	α_3	%	-	-	-0.00816	-7.09	-	-
β	β_0	-	-0.00410	-10.36	-0.00685	-58.34	-0.00952	-62.91
	$\beta_1(hvr)$	-	-0.00761	-3.51	-	-	0.00401	19.6
	β_2	%	-	-	-0.000267	-8.49	-0.000480	-11.13
	β_3	%	-	-	0.0000967	3.67	0.000230	11.56
γ	γ_0		0.233	7.75	0.299	67.44	0.389	140.7
	$\gamma_1(hvr)$		0.385	2.85	-	-	-0.193	-23.43
	$\gamma_4(dd)$	km	-0.0322	-4.39	-0.00453	-14.63	-0.00453	-17.09
	R^2		0.9969		0.9971		0.9982	
	N		785		5086		4406	

Model parameters at the sections with speed limit 60km/h, 80km/h and 100km/h are separately estimated. Table 2.6 shows the results of model parameter estimation. All the parameters are significant at the 95% confidence levels.

From the estimation results, $\alpha_1(hvr)$ is positive value in each model. The intercept α increases with the increase of hvr , which means that higher hvr result in higher LUR under low traffic flow. $\gamma_4(dd)$ is negative value in each model. The asymptotic line γ increases with the decrease of dd , indicating that LUR gets higher when approaching the diverge section.

$$SLUR_{4-lane}^{60km/h} = (0.617 - 0.3144hvr + 0.0322dd) \exp(-0.00410 - 0.00761hvr)FR + 0.233 + 0.385hvr - 0.0322dd \quad (2.3-a)$$

$$SLUR_{4-lane}^{80km/h} = (0.576 + 0.0405hvr + 0.0110\delta_2i\% - 0.00816\delta_3i\% + 0.00453dd) \exp(-0.00658 - 0.000267\delta_2i\% + 9.67E - 05\delta_3i\%)q + 0.299 - 0.00453dd \quad (2.3-b)$$

$$SLUR_{4-lane}^{100km/h} = (0.497 + 0.265hvr + 0.00826\delta_2i\% + 0.00453dd) \exp(-0.00952 + 0.00410hvr - 0.000480\delta_2i\% + 0.000230\delta_3i\%)q + 0.389 - 0.193hvr - 0.00453dd \quad (2.3-c)$$

The estimated results can be expressed in Equations (2.3-a) to (2.3-c).

2.6.4 Validation of *LUR* model

The section introduces the estimation results by applying the developed models. Figure 2.20 shows the estimation results of *LUR* on shoulder lane on 4-lane expressway for each model with different speed limits. From the results, the models for speed limit 100km/h have the best fitting. Table 2.7 shows goodness of fit by *R* square and *RMSE* of each model. In summary, from the results, it can be seen that the developed models fit well.

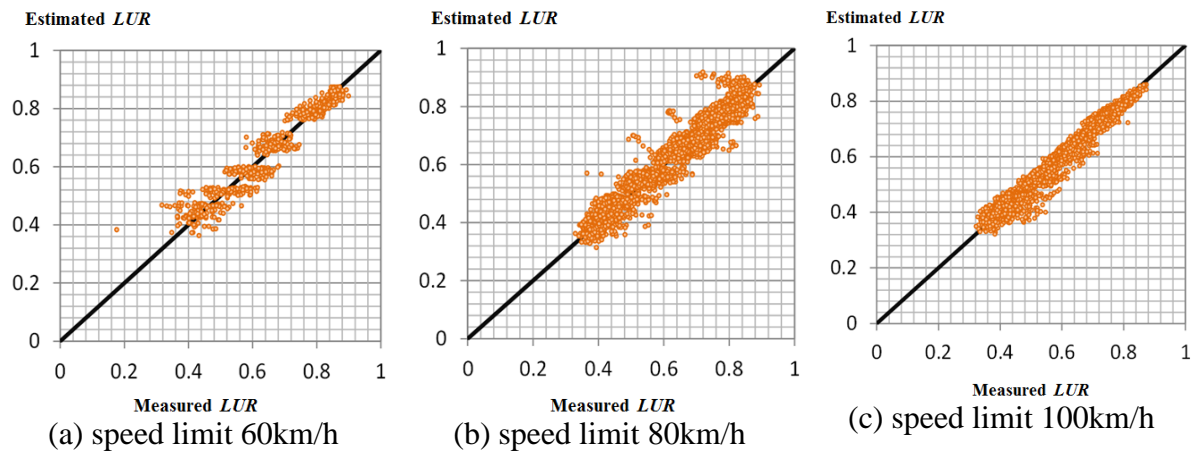


Figure 2.20 Validation results on 4-lane expressway

Table 2.7 Goodness of fit for each developed model

Goodness of fit	4-lane expressway		
	60km/h	80km/h	100km/h
<i>R</i> square	0.9969	0.9971	0.9982
<i>RMSE</i>	0.0380	0.0346	0.0250

2.7 Summary

This chapter introduces the test bed and data preparation for investigation in this study. The preliminary analyses have been conducted to identify the recurrent bottleneck locations in the intercity expressway network of central Japan.

Two groups can be categorized among these types of the identified bottlenecks. One group includes bottlenecks at the interrupted expressway sections like diverge and merge sections.

The other uninterrupted group refers to bottleneck at sag section which is the typical bottleneck type in Japanese intercity expressway network.

Lane specific traffic flow characteristics are discussed particularly for diverge and merge bottlenecks which located at the interrupted expressway sections. Lane usage preference are significantly influenced by the functioning of diverge or merge sections as traffic flows are assigned there. Hence, lane usage preference by drivers apparently varies due to the influence of diverge and merge traffic flow.

With respect to traffic data, traffic flow rates and average speeds on each lane were measured and aggregated at a 5-minute interval at each detector location. The lane based record enables the investigation from the viewpoint of each lane.

To describe the lane-specific characteristics on the multilane expressway, lane utilization rate (*LUR*) is used as a macroscopic variable in this study. *LUR* has been modeled as a function of traffic flow and geometric characteristics for locations in the intercity expressway network of central Japan.

Chapter 3

IDENTIFICATION OF BREAKDOWN OCCURRENCE

3.1 Introduction

This chapter will introduce the methodology of breakdown identification in this study. Identification of breakdown occurrence is the decisive issue to model breakdown probability and discharge flow rate in the following chapters.

With respect to the existing studies, identification procedures treat all lanes of mainline as one unit for an expressway facility, and are mainly conducted through a check of the aggregated data of cross-section. This kind of method can be regarded as a cross-section based one in light of this aggregated cross-section viewpoint. Therefore cross-section based method implies that all lanes of an expressway facility will experience breakdown simultaneously as one unit.

However, it has been well empirically recognized that breakdown actually occurs on a certain lane firstly and then spreads to other lanes of an expressway facility. Accordingly, the time lag is likely to exist between lanes with respect to timing of breakdown occurrence on each lane. More specifically at diverge and merge sections, traffic flows are assigned there which make that mainline traffic flows are generally interrupted by diverge and merge traffic flow there. Hence, lane usage preference by drivers apparently varies due to the influence of diverge and merge traffic flow. Diverge, merge traffic flow and the resulted lane usage preference are regarded as main cause of breakdown occurrence.

Impacted by off-ramp diverge or on-ramp merge traffic flow, possibly breakdown occurrences on each lane would be more significantly different. Furthermore existence of semi-congested state has been observed at diverge bottlenecks, where some lanes are congested and others are not. This semi-congested state is likely to be inappropriately identified as breakdown occurrences on all lanes when averaged across all lanes by existing cross-section based method. For above-mentioned cases, improper identification results through cross-section based method actually do not represent facility capacity. Inappropriate identifications are attributed to its inherent limitation of oversimplification which treats all lanes of mainline as one unit. To sum it up, necessarily, a lane based identification method is required to identify breakdown occurrence particularly at diverge and merge sections which are located at the interrupted intercity expressway facilities.

With respect to sag bottleneck, there are no significant differences between the lane based identification method and cross-section based one. This is attributed to that sag bottlenecks are located at the uninterrupted expressway facilities without impacts from diverge or merge traffic flow.

The remainder of the chapter is organized as follows. At first, the breakdown identification investigation in this study is related to earlier researches described in the literature. Secondly, a lane based method is proposed for breakdown identification at diverge and merge bottlenecks, and its necessity and advantage are presented. Then the extracted breakdown flow rate distributions are analyzed. As for sag bottlenecks, the identification of breakdown still adopts the conventional cross-section based method considering discussions above. The concluding remarks are discussed in the final section.

3.2 Literature review

Review of the relevant literature focuses on the studies which identify breakdown occurrence from viewpoint of each lane. In addition, the commonly used criteria to determine the timing of breakdown occurrence are also reviewed.

Some of the existing studies have investigated breakdown occurrence from viewpoint of each lane either directly or indirectly. Koshi (1986) pointed out that at sag sections, traffic concentrates on median lanes and congestion began there without fully utilizing the available capacity. Xing *et al.* (2005) examined breakdown occurrence at a merge section

of Anagawa IC on Keiyo Expressway in Japan. It was found that breakdown was triggered firstly on median lane and then spread to shoulder lane. Dehman *et al.* (2008) conducted an empirical study to demonstrate a significant difference of breakdown occurrences among lanes.

As for diverge bottleneck, Daganzo *et al.* (1999) reported the possibility of a semi-congested state where some lanes were congested and others were not. Muñoz, J. C *et al.* (2002) stressed similar findings of existence of semi-congested state and attempted to increase awareness of the research community regarding the pernicious effects that saturated off-ramps could have on expressway traffic flow. This research described the behavior of multi-lane expressway traffic, upstream of an oversaturated off-ramp. It was found that semi-congested traffic states, where some lanes were congested and others were not, also existed. Furthermore for congestion across lanes, there existed times lags for breakdown occurrence on each lane. The research attributed cause of above-mentioned phenomena to lane-specific behavior at diverge section as drivers would segregate themselves by destinations.

These related reviews have already implied the significance of applying lane based method for breakdown identification in some degree. More specifically regarding diverge bottlenecks, the related researches have more highlighted effects of lane-specific breakdown characteristics, and lane based method is hence more desirable in this regard.

The most commonly used criteria to identify breakdown occurrence for a facility in practice are based on a critical speed threshold that determines transition from uncongested to congested flow.

Brilon *et al.* (2005) set 70km/h as the critical speed value in their study which was regarded as a fairly representative value for German expressways. Dowling *et al.* (2008) selected a critical speed value of 72 km/h to determine timing of breakdown occurrence. Elefteriadou and Lertworawanich (1995), (2001) set different critical speed values for merging sections and weaving sections as 90 km/h and 80 km/h respectively. They chose these values by observing the boundary between the uncongested and congested flows. They interpreted that weaving sections had typically lower speeds and this was reason why critical speed value was lower there. To be noted here, all these researches concluded that no universal critical speed value could be defined, and that the value only applied to the

expressway facilities on which their researches were conducted. Furthermore there were no discussions on detailed criteria to reliably define critical speed value at a certain expressway facility.

Taken together, some issues can be highlighted as follows. The lane based method is desirable at diverge and merge sections in light of effects of lane-specific breakdown characteristics there. In addition, a concrete and detailed procedure is required to reliably define critical speed value at the studied bottlenecks. Therefore this study aims to adopt the lane based method, and a procedure will be established for defining the site-specific critical speed value.

3.3 Breakdown Identification through the lane based method

This section introduces the lane based method for breakdown identification at diverge and merge bottlenecks.

3.3.1 Data descriptions for lane based method

The lane based identification method will be applied to four diverge bottlenecks and three merge bottlenecks which are introduced in the previous chapter. Along the mainlines, off-ramps and on-ramps of intercity expressway, double-loop detectors are installed approximately every two kilometers. Traffic flow rates and average speeds on each lane were measured and aggregated at a 5-minute interval. These detectors report spot speeds and

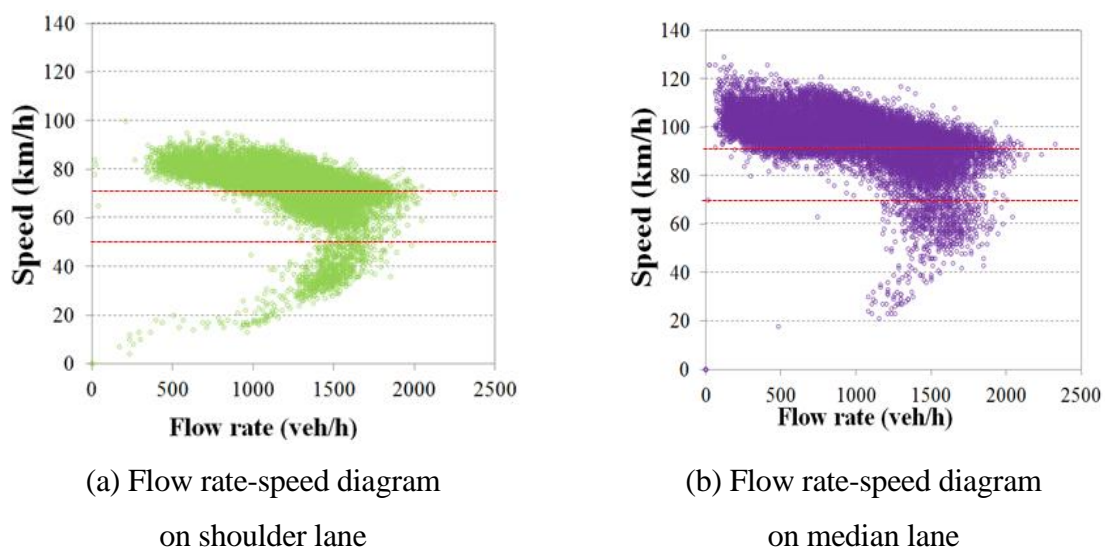


Figure 3.1 Flow rate-speed diagrams of 302.15KP at Toyota diverge bottleneck

traffic counts every 5 minutes on each lane. Detector data were available from 3/1/2008 to 12/31/2009. This kind of data enables the investigation by using the lane based identification method.

3.3.2 Introduction of lane based identification method

To date, most of the existing identification methods have treated all lanes of mainline as one unit for a facility, and are conducted mainly through a check of the aggregated data of cross-section. Such kinds of methods are attributed to cross-section based ones.

In this study, a lane based method is proposed to identify breakdown occurrence on each lane. Identification is based on the following conditions: 1) speed of the subject lane measured at the detector needs to be lower than its critical speed value and 2) this condition continues over 15 minutes to guarantee that queue propagates to upstream.

A procedure to apply the lane based method is introduced as follows. At Toyota diverge bottleneck, mainline of diverge section owns two lanes namely shoulder lane and median lane. Location of 302.15KP (Kilometer Post) has been recognized as bottleneck location as the congested condition is found at its upstream KP location and not found at its downstream KP location in preliminary studies through historical flow rate-speed diagrams.

At this bottleneck location 320.15KP, flow rate-speed distributions on shoulder lane and median lane are illustrated respectively in Figure 3.1. Speed transition regimes from the uncongested to congested conditions apparently differ between two lanes as highlighted in Figure 3.1. Timing of breakdown occurrence on each lane is identified by using lane based method through a critical speed value which will be introduced as follows.

3.3.3 Procedure of lane based method

A process to define optimal critical speed value is introduced as follows. The defining criterion is that optimal critical speed can identify the most significant speed reductions accompanying with occurrences of breakdown events.

Assuming a critical speed v_c , timing of breakdown occurrence is then determined as the interval immediately before the speed becomes lower than v_c and remains over 15 minutes.

Accordingly, a significant speed reduction is expected immediately after this determined timing.

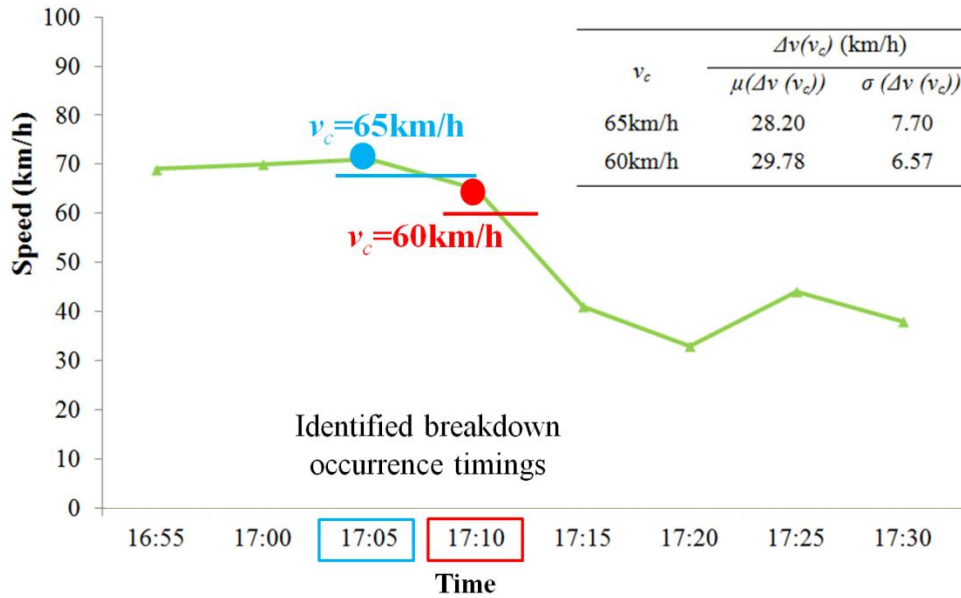


Figure 3.2 Illustration of a breakdown occurrence

As illustrated in Figure 3.2, a breakdown event on shoulder lane on 4/30/2008 at Toyota JCT (numbered as i) is discussed to introduce v_c impact. A significant speed reduction is observed between 17:10 and 17:15.

Firstly, the measured speed reduction $\Delta v_i(v_c)$ by using v_c is computed by Equation (3.1).

$$\Delta v_i(v_c) = v_{before}(v_c, i) - v_{after}(v_c, i) \quad (3.1)$$

where, $v_{before}(v_c, i)$ and $v_{after}(v_c, i)$ are mean speed values of 15-minute intervals (choice of 15-minute considering speed fluctuations) immediately before and after the identified occurrence timing of breakdown i respectively.

Secondly, v_c impact is demonstrated by comparing choices of two representative values (60km/h and 65km/h). The highlighted intervals 17:10 and 17:05 are the determined breakdown occurrence timings by using 60km/h and 65km/h respectively. Identification result by 65km/h is unfavorable as the observed significant speed reduction is not accompanied with its timing. As a result, this inappropriate identification causes lower $\Delta v_i(65)$ compared to 60km/h.

Then all identified values of $\Delta v_i(v_c)$ ($1 \leq i \leq n$, n is the total number of breakdown events) under 60km/h and 65km/h are summed respectively, and their mean and standard deviation (SD), $\mu(\Delta v(v_c))$ and $\sigma(\Delta v(v_c))$, are computed as shown in Figure 3.3. Through 65km/h, the effects of the lower $\Delta v(65)$ due to the improper identification result in smaller $\mu(\Delta v(65))$. Furthermore, frequent identifications of lower $\Delta v(65)$ cause higher value of $\sigma(\Delta v(65))$. Comparably 60km/h results in better results.

Finally, various values of v_c (shoulder lane range: 50-70km/h, median lane range: 70-90km/h) are tested and illustrated in Figure 3.3. For both shoulder lane and median lane, higher $\mu(\Delta v(v_c))$ and lower $\sigma(\Delta v(v_c))$ values exist in medium regions of tested speed ranges. As maximal $\mu(\Delta v(v_c))$ can indicate the most significant $\Delta v(v_c)$, 58km/h and 79km/h are computed as the optimal critical speeds for shoulder lane and median lane respectively.

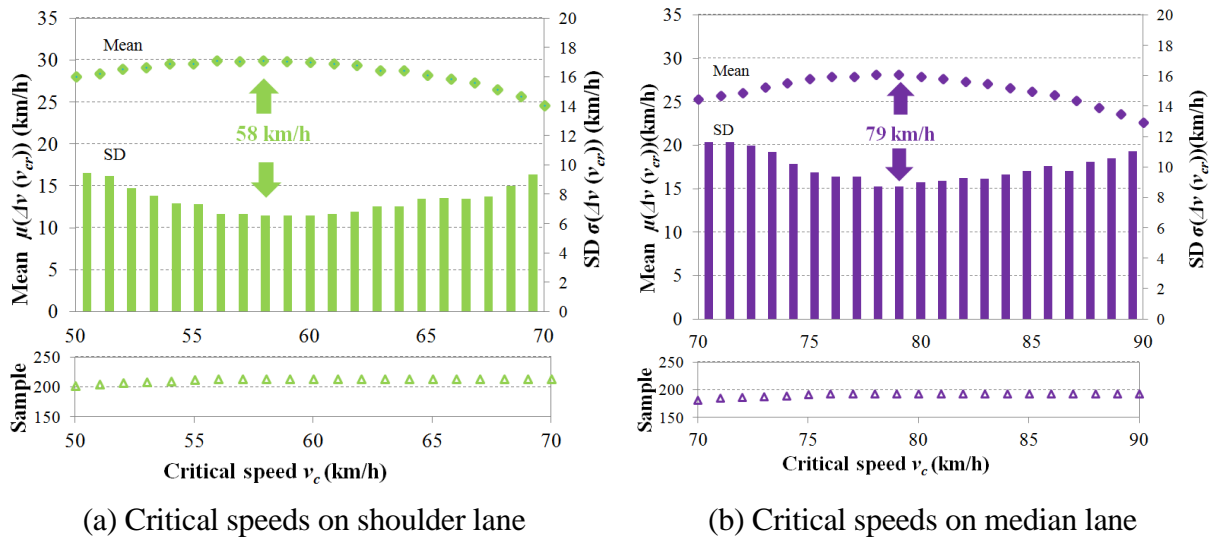


Figure 3.3 Critical speeds on shoulder lane and median Lane

(Note: cases of $\Delta v(v_c)$ value which are lower than 10 km/h are excluded)

The same optimization procedure is also applied to other diverge and merge bottlenecks. In addition, optimal critical speeds for cross-section are also computed as the above-discussed optimization procedure can be applicable to cross-section based method.

3.3.4 Comparison of the identified breakdown events between cross-section and lane based methods

The following parts discuss advantages of the proposed lane based method through a comparison to identification results of cross-section based method. Firstly the numbers of identified breakdown events under two methods are compared.

3.3.4.1 Breakdown type classification and representative examples

At diverge bottlenecks owning a 2-lane mainline, breakdown types are defined by checking breakdown occurrence on each lane and the time lag between them. Definition of breakdown types is as follows. At Toyota diverge bottleneck, three breakdown types are defined as illustrated in Figure 3.4. Type *S* is defined when breakdown only occurs on shoulder lane which is actually semi-congested state. Regarding Type *SAM*, breakdown simultaneously occurs on both shoulder and median lanes. As for Type *STM*, breakdown starts from shoulder lane and then spreads to median lane after a certain time lag.

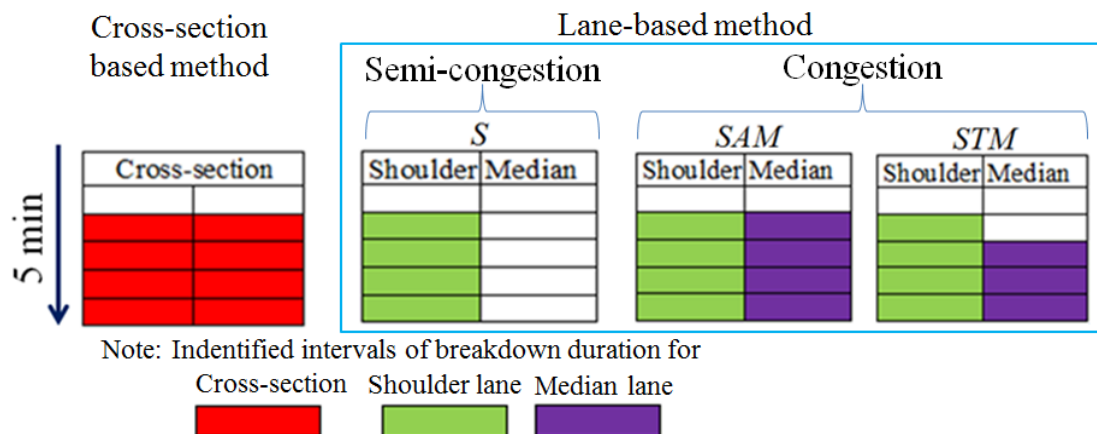


Figure 3.4 Classification of breakdown types at two-lane diverge and merge bottlenecks

Figure 3.5 presents the procedure to apply the lane based identification method. There are four steps in this procedure which enables the classification of the aforementioned breakdown types. In addition, breakdown and discharge flow rate can be extracted.

Figure 3.6(a) and Figure 3.6(b) present two representative examples of Type *S* and *STM*. Speed changes between sequential 5-min periods are plotted, and optimal critical speeds for each lane, cross-section are labeled.

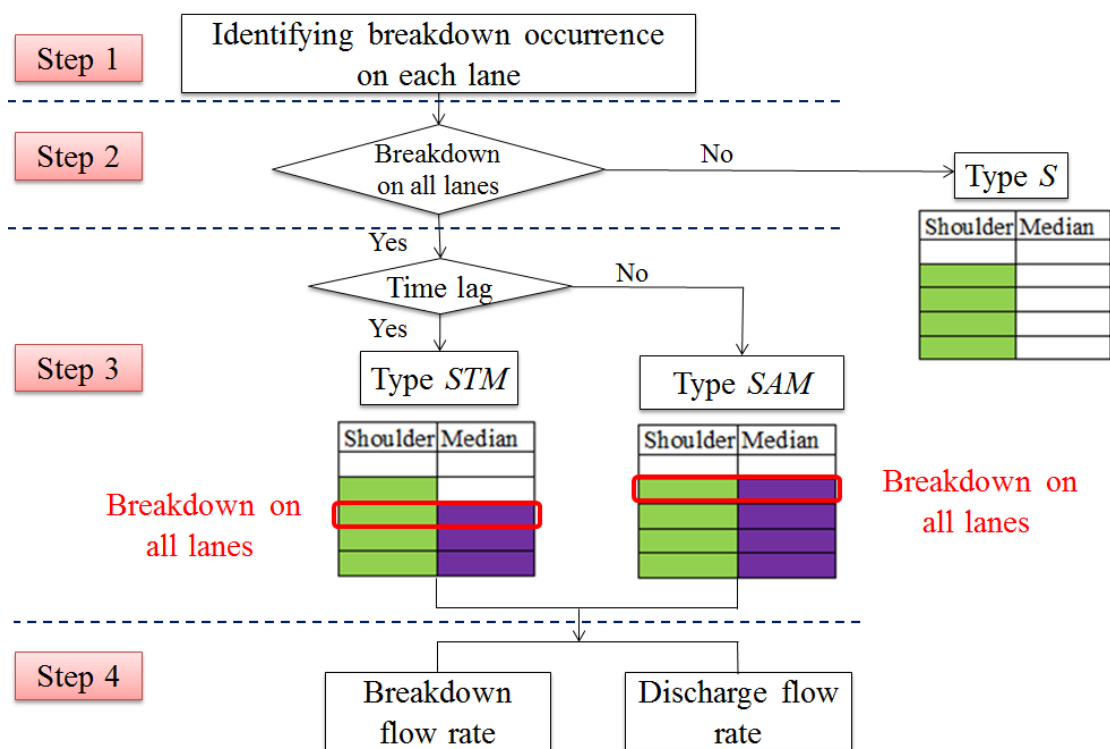


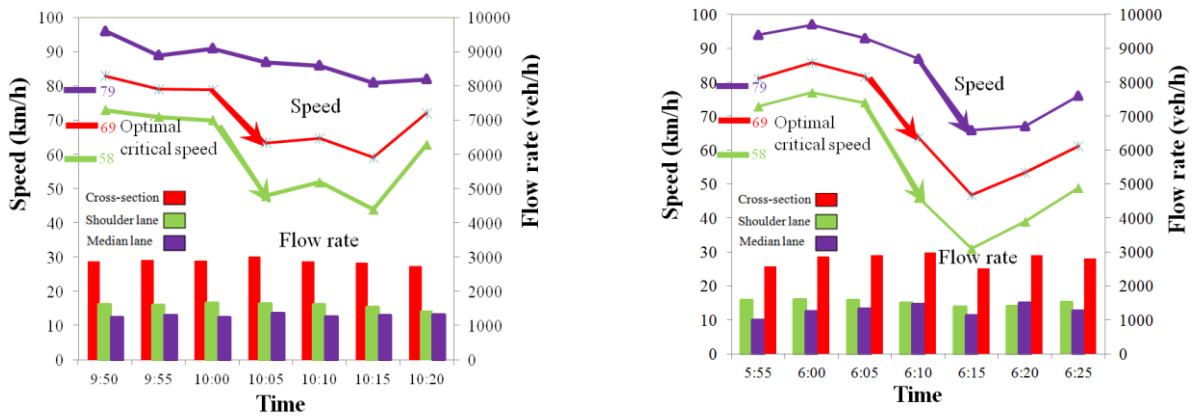
Figure 3.5 Flowchart for applying the lane based identification method

A breakdown event of Type *S* occurred during PM peak hours on 8/13/2008. When using cross-section based method, breakdown occurrence of this facility was identified as the aggregated cross-section speed was found to fall below its critical speed (69 km/h). However through lane based method, only speed on shoulder lane reduced significantly at PM 9:55 below its critical speed (58km/h) and remained for subsequent 15 minutes.

A breakdown event of Type *STM* occurred during PM peak hours on 5/3/2009. When using cross-section based method, the aggregated cross-section speed reduced significantly at 6:05 which would be determined as breakdown occurrence time of all lanes of the diverge facility. However, actually only speed on shoulder lane dropped significantly at 6:05. By applying lane based method, after a time lag of 5 minute, it was found that breakdown occurred on median lane, and 6:10 could be appropriately determined as the interval of breakdown occurrences on all lanes of this diverge facility.

At Nagoya bottleneck with a broader 3-lane mainline, a representative example is illustrated in Figure 3.7. Breakdown occurred on auxiliary lane as speed reduced significantly at AM 17:00. Apparently there were no breakdown occurrences on shoulder lane and median lane due to their lower traffic flow rates. However due to the aggregated

effects, this semi-congested state is improperly treated as breakdown occurrences on all lanes by cross-section based method.



(a) Type S at Toyota diverge bottleneck

(b) Type STM at Toyota diverge bottleneck

Figure 3.6 Representative examples of breakdown types

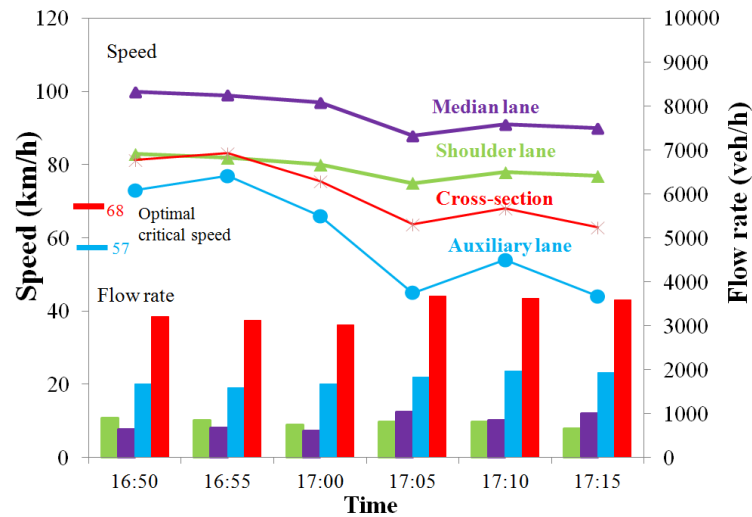


Figure 3.7 A representative example at Nagoya diverge bottleneck

3.3.4.2 Analysis of the identified breakdown events

Analysis of the identified breakdown events are conducted as follows. The optimal critical speeds for each diverge bottlenecks are listed in Table 3.1.

Table 3.1 Optimal critical speeds (km/h) at diverge bottlenecks

Site	Cross-section method	Lane based method		
	Cross-section	Shoulder lane	Median lane	Auxiliary lane
Toyota	69	58	79	
Toki	71	62	80	
Komaki	70	62	78	
Nagoya	68			57

Table 3.2 Identification results at Toyota, Toki and Komaki diverge bottlenecks

Site	(I) identified by both methods (II) only by lane base method	Cross-section based method	Lane based method			
			S	SAM		STM
				Same timing	Not	Same timing
Toyota	(I)	209	15	141	0	8
	(II)	N/A	6	0	0	0
Toki	(I)	36	0	28	0	2
	(II)	N/A	5	0	0	0
Komaki	(I)	27	0	21	0	0
	(II)	N/A	7	0	0	0

At Toyota, Toki and Komaki diverge bottlenecks, the numbers of all types of breakdown are summed in Table 3.2. Regarding Nagoya bottleneck, it is found that breakdown only occurred on auxiliary lane as presented in Table 3.4. At Toyota diverge bottleneck, three different types exist through lane based method among 209 identified breakdown events by using cross-section based method. Sample size of Type *S* is approximately 8% of total samples which is actually semi-congested state. As for Type *STM*, the identified results by using cross-section based method have possibilities of inappropriately determining breakdown occurrence timing for all lanes of the diverge facility in light of existence of a time lag. In total, Type *S* and *STM* account for about 27% of 209 breakdown events which highlights significance of applying lane based method. Similarly at Toki and Komaki diverge bottlenecks, breakdown Type *STM* also could be found to have significant shares.

Impact of diverge rate (*DR*) on the time lag is presented in Table 3.3. Through a comparison of *DR* distributions of type *SAM* and *STM*, it is found that higher *DR* values result in a faster spread of breakdown from shoulder lane to median lane as higher *DR* values cause more frequent decelerations on each lane.

Table 3.3 Impact of DR on time lag of breakdown occurrence on each lane

Contents		SAM	STM	
Time lag(min)		0	5	10
Sample size		141	38	4
Diverge rate (DR)	Mean	0.512	0.484	0.487
	SD	0.048	0.057	0.069

Table 3.4 Identification results at Nagoya diverge bottleneck

(I) identified by two methods (II) only by lane base method	Cross-section based method	Lane based method		
		Shoulder lane	Median lane	Auxiliary lane
(I)	144	0	0	144
(II)	N/A	0	0	25

Comparison results at Nagoya diverge bottleneck further enhance advantage of lane based method as listed Table 3.4. All 144 breakdown events through cross-section based method are found to be only semi-congested states by using lane based method, where auxiliary lane was congested and other lanes were not due to a limit of off-ramp capacity rather than that of mainline.

3.3.4.3 Comparison of Extracted Breakdown Flow Rate between Cross-section and Lane based Methods

This part compares the extracted breakdown flow rate (*BDF*) through two methods. In this study, *BDF* is defined as the flow rate of all lanes observed immediately prior to the interval when all lanes of this diverge facility have experienced breakdown. *BDF* value is adopted as a significant measure to evaluate performance of lane based method since it is quite a critical issue for modeling breakdown probability.

According to above-discussion, at Nagoya diverge bottleneck, all 144 breakdown events have been checked out as semi-congested states. Therefore its mainline *BDF* cannot be measured. Only the extracted *BDF* values at Toyota, Toki and Komaki diverge bottlenecks are focused on in the following analysis. As for Type *SAM*, the identified timings of breakdown occurrences are the same by both methods, thereby its *BDF* values can serve as an analysis basis.

Table 3.5 A comparison between *BDF* values of type *S* and *SAM* at Toyota diverge bottleneck

Contents		<i>S</i>	<i>SAM</i>	<i>t</i>	<i>p</i>
Sample size		15	141	-4.863	0.000
<i>BDF</i> value (veh/h)	Mean	2838	3165		
	SD	324	379		

(Note: confidence level is 95%)

Table 3.6 A comparison between *BDF* values of type *STM* by using two methods

Site	Contents		Cross-section based method	Lane based method	<i>t</i>	<i>p</i>
Toyota	Sample size		42	42	-2.981	0.004
	<i>BDF</i> value (veh/h)	Mean	3042	3149		
		SD	271	325		
Toki	Sample size		8	8	-2.359	0.011
	<i>BDF</i> value (veh/h)	Mean	2784	2895		
		SD	274	261		
Komaki	Sample size		5	5		
	<i>BDF</i> value (veh/h)	Mean	2842	2954		
		SD	278	256		

(Note: confidence level is 95%)

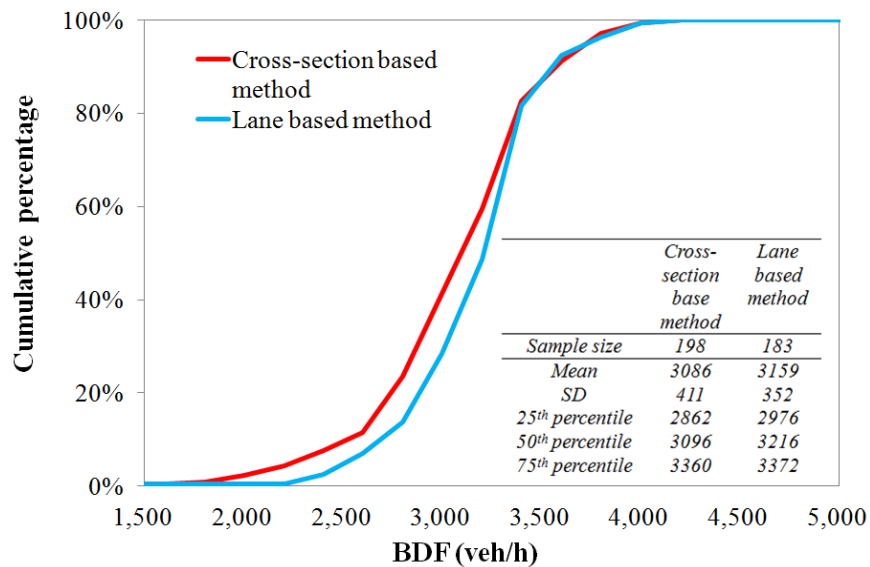


Figure 3.8 The extracted *BDF* dataset by using two methods

Two *BDF* datasets are produced by using two methods respectively. At Toyota diverge bottleneck, 15 breakdown events of Type *S* are incorporated into its *BDF* dataset by using

cross-section based method. However, the extracted *BDF* values of Type *S* are just flow rates of semi-congested states. A comparison to the extracted *BDF* values of Type *SAM* further interprets this improper incorporation. As presented in Table 3.5, at a confidence level of 95%, there is a significant difference between the extracted *BDF* values of Type *S* and *SAM* ($t = -4.863$, $p = 0.000$). In other words, the extracted *BDF* values of Type *S* significantly underestimate diverge facility capacity. Through lane based method, breakdown events of Type *S* can be checked out and excluded from its *BDF* dataset.

Regarding Type *STM*, there is a possibility of inappropriate identification of timing of breakdown occurrence for all lanes through cross-section based method according to above-discussion. The extracted *BDF* values using two methods are compared as presented in Table 3.6. It is found that the extracted *BDF* values by using cross-section based method also significantly underestimate diverge facility capacity ($t = -2.981$, $p = 0.004$). At Toki diverge bottleneck, similar underestimation also exist which are indicated by t test results in Table 3.6. At Komaki diverge bottleneck, similar underestimation is identified as well by comparing mean values.

In summary, the extracted *BDF* datasets using two methods are established. At Toyota diverge bottleneck, distributions of two *BDF* datasets are illustrated in Figure 3.8 which apparently indicates that cross-section based method underestimates *BDF* values.

3.4 The extracted *BDF* distributions at diverge bottlenecks

With respect to diverge bottlenecks, the extracted *BDF* distributions by using the lane based identification method are presented in Table 3.7 and Figure 3.9.

Table 3.7 *BDF* distributions at diverge bottlenecks

Name	Sample		<i>BDF</i> distribution (veh/h)					
	size	<i>Mean</i>	<i>SD</i>	<i>Min</i>	25%	50%	75%	<i>Max</i>
Toyota diverge bottleneck	194	3145	400	2568	2976	3216	3369	4008
Toki diverge bottleneck	36	3253	458	2304	2937	3204	3549	4056
Komaki diverge bottleneck	27	2914	463	2004	2586	3018	3288	3540

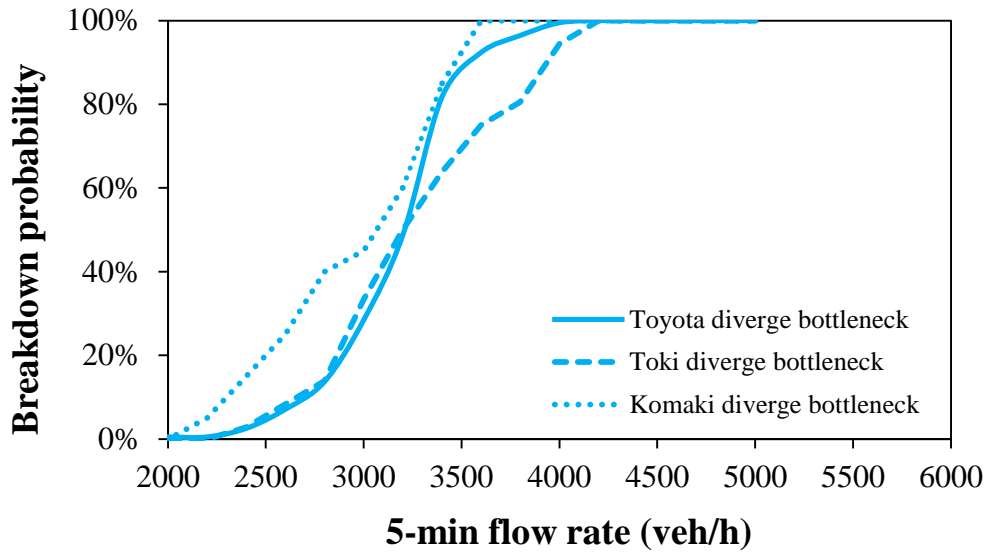


Figure 3.9 The extracted *BDF* distributions at diverge bottlenecks

Based on the statistic analysis, the stochastic nature of breakdown occurrence at diverge bottlenecks can be confirmed. *BDF* values are found to be distributed in wide ranges rather than to be specifically constant values. For example, at Toyota diverge bottleneck, *BDF* distribution has the mean value of 3145 veh/h and standard deviation of 400 veh/h. This means that breakdown for mainline traffic on all lanes can occur stochastically under significantly different traffic demand levels. Similar findings can also be confirmed at Toki and Komaki diverge bottlenecks despite relatively smaller sample sizes there. The *BDF* distributions present basic descriptions on capacities (breakdown flow rates) of these diverge facilities.

3.5 The extracted *BDF* distributions at merge bottlenecks

With respect to merge bottlenecks, lane based breakdown identification method is also applied in the similar way with that for diverge bottlenecks. The extracted *BDF* distributions by using the lane based identification method are presented in Table 3.8 and Figure 3.10.

Table 3.8 *BDF* distributions at merge bottleneck

Name	Sample size	<i>BDF</i> distribution (veh/h)						
		<i>Mean</i>	<i>SD</i>	<i>Min</i>	25%	50%	75%	<i>Max</i>
Toyota merge bottleneck	256	3399	317	2724	3171	3426	3633	4080
Toki merge bottleneck	37	3546	256	2988	3378	3588	3666	4032
Komaki merge bottleneck	196	3040	368	1658	2808	3048	3261	4032

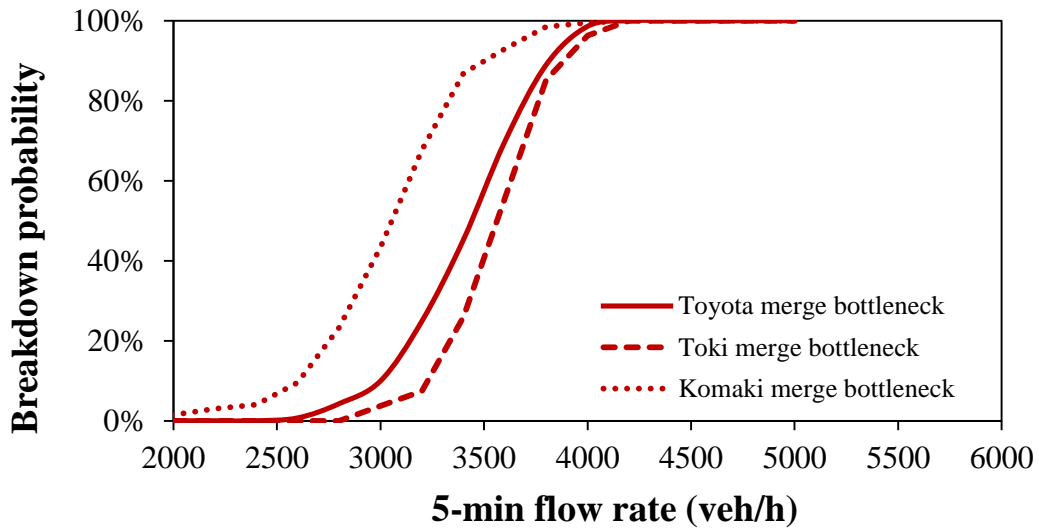


Figure 3.10 The extracted *BDF* distributions at merge bottlenecks

Based on the statistic analysis, the stochastic nature of breakdown at merge bottlenecks can also be confirmed. *BDF* values are found to be distributed in wide ranges rather than to be specifically constant values. For example, at Toyota merge bottleneck, *BDF* distribution has the mean value of 3399 veh/h and standard deviation of 317 veh/h. This means that breakdown for mainline traffic on all lanes can occur stochastically under significantly different traffic demand levels. Similar findings can also be confirmed at Toki and Komaki merge bottlenecks. The *BDF* distributions present basic descriptions on capacities of these merge facilities.

3.6 The extracted *BDF* distributions at sag bottlenecks

With respect to sag bottlenecks, the extracted *BDF* distributions by using the cross-section based identification method are presented in Tables 3.9 to 3.12, Figures 3.11 to 3.14.

Table 3.9 *BDF* distributions at sag bottlenecks on Tomei Expressway of eastbound direction

KP (km)	Sample size	<i>BDF</i> distribution (veh/h)						
		<i>Mean</i>	<i>SD</i>	<i>Min</i>	25%	50%	75%	<i>Max</i>
296.43	132	3387	344	2184	3204	3468	3624	4104
298.43	35	3381	340	2964	3216	3444	3636	3864
290.43	34	2704	375	1740	2538	2682	2955	3528
314.27	38	3306	307	2544	3144	3318	3516	4032

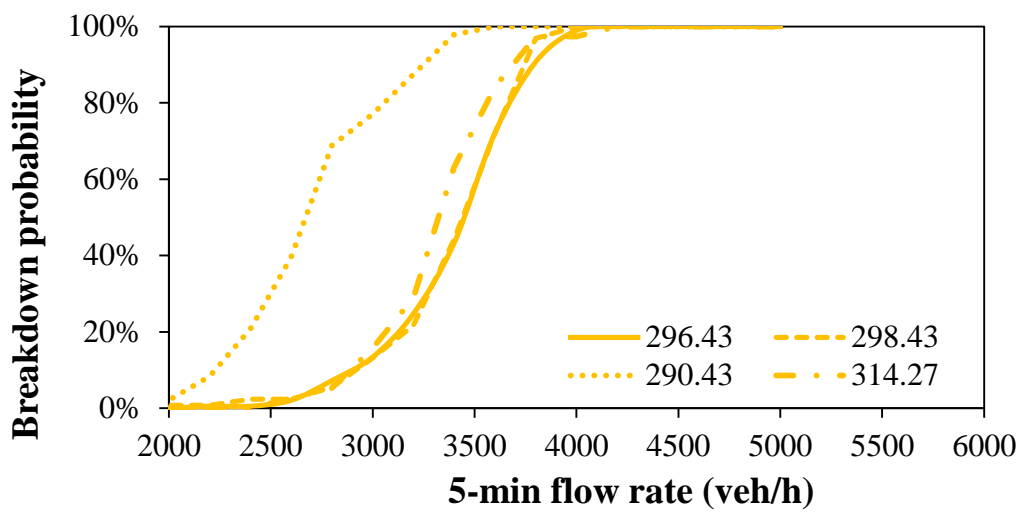


Figure 3.11 The extracted *BDF* distributions at sag bottlenecks on Tomei Expressway of eastbound direction

Table 3.10 *BDF* distributions at sag bottlenecks on Tomei Expressway of westbound direction

KP (km)	Sample size	<i>BDF</i> distribution (veh/h)						
		<i>Mean</i>	<i>SD</i>	<i>Min</i>	25%	50%	75%	<i>Max</i>
294.43	186	3324	353	2184	3108	3360	3576	4044
299.5	20	2986	438	1968	2724	3012	3192	3864
312.01	68	3060	293	2316	2892	3084	3264	3600

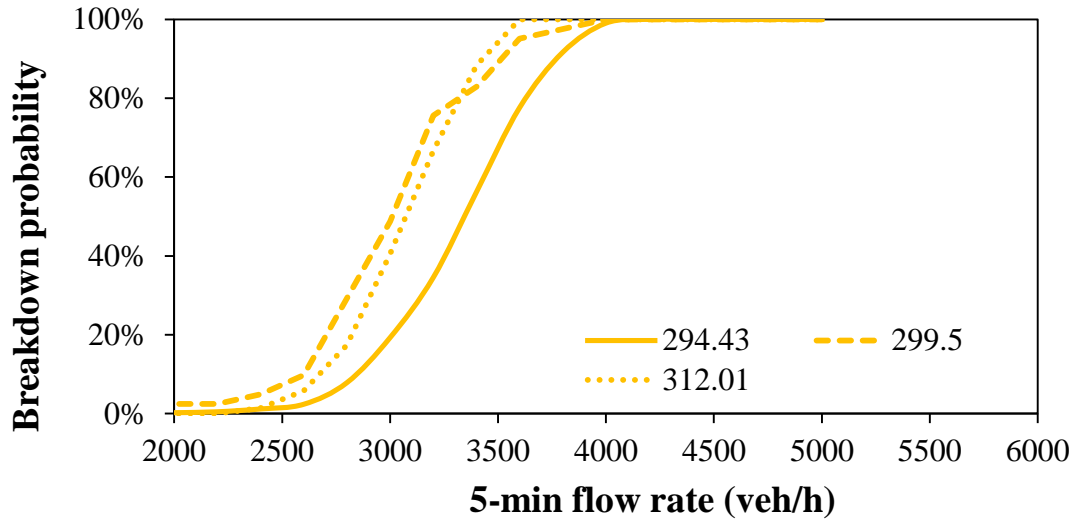


Figure 3.12 The extracted *BDF* distributions at sag bottlenecks on Tomei Expressway of westbound direction

Table 3.11 *BDF* distributions at sag bottlenecks on Higashi-Meihan Expressway

KP (km)	Sample size	<i>BDF</i> distribution (veh/h)						
		<i>Mean</i>	<i>SD</i>	<i>Min</i>	25%	50%	75%	<i>Max</i>
61.5	113	3033	387	2364	2808	3084	3300	3732
67.17	43	2986	343	1536	2796	3000	3213	3720
58.54	62	3099	272	2508	2937	3144	3279	3636

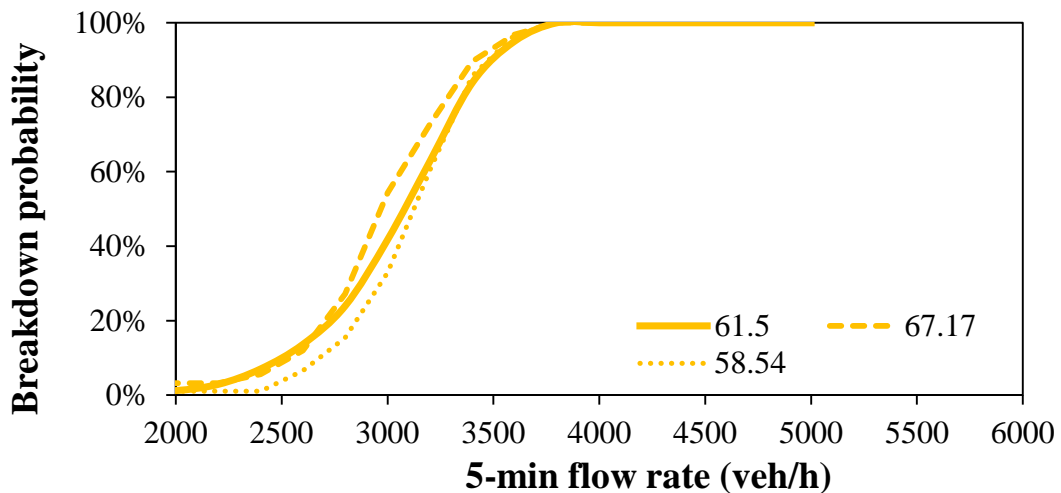


Figure 3.13 The extracted *BDF* distributions at sag bottlenecks on Higashi-Meihan Expressway

Table 3.12 *BDF* distributions at sag bottlenecks on Chuo Expressway

Name	Sample		<i>BDF</i> distribution (veh/h)					
	size	<i>Mean</i>	<i>SD</i>	<i>Min</i>	25%	50%	75%	<i>Max</i>
306.59	16	3131	324	2328	3084	3252	3312	3504
298.44	17	3546	256	2988	3378	3588	3666	4032
306.6	15	2991	459	1992	2700	3048	3324	3696
312.96	17	2883	399	2220	2559	2880	3237	3624
317.49	11	3249	360	2580	3126	3252	3390	3804

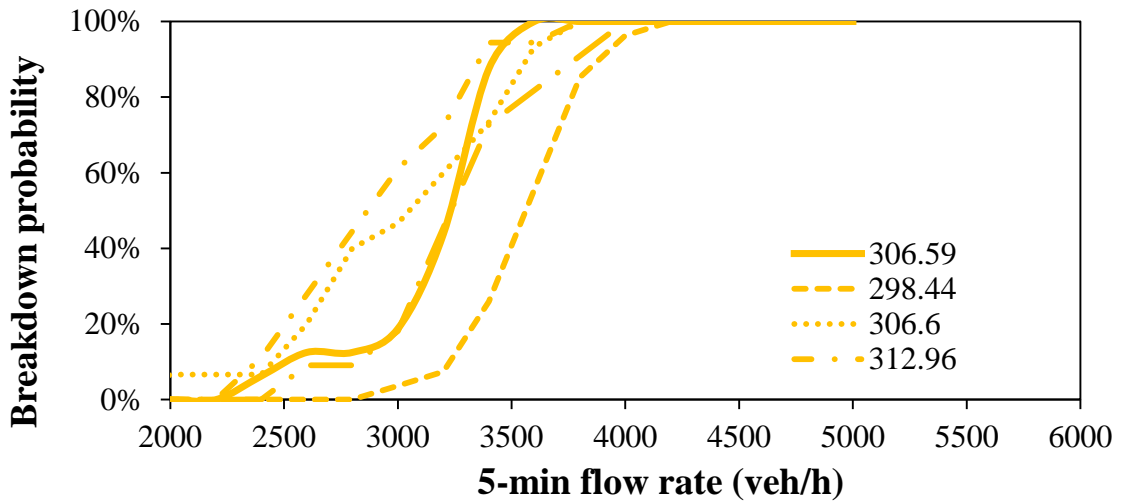


Figure 3.14 The extracted *BDF* distributions at sag bottlenecks on Chuo Expressway

Based on the statistic analysis, the stochastic nature of breakdown at sag bottlenecks can also be confirmed. *BDF* values are found to be distributed in wide ranges rather than to be specifically constant values. For example, at a sag bottleneck at 296.43KP on Tomei Expressway of eastbound direction, *BDF* distribution has the mean value of 3387 veh/h and standard deviation of 344 veh/h. This means that breakdown for mainline traffic on all lanes can occur stochastically under significantly different traffic demand levels. Similar findings can also be confirmed at other sag bottlenecks. The *BDF* distributions present basic descriptions on capacities of these sag bottlenecks.

3.7 Summary

As for modeling breakdown probability and discharge flow rate on multilane intercity expressways, identification of breakdown occurrence is a decisive issue. To date, most of

the existing identification methods have treated all lanes of mainline as one unit for a facility, and are conducted mainly through a check of the aggregated data of cross-section. However, the existing cross-section based method oversimplifies breakdown identification for bottlenecks at expressway facilities where lane usage preferences on each lane significantly differ like nearby diverge and merge sections.

Therefore, with respect to diverge and merge bottlenecks, a lane based method is proposed to identify breakdown on each lane. The timing of breakdown occurrence is determined by a critical speed which is optimized through obtaining the most significant speed reductions accompanying with breakdown occurrences. The proposed lane based method is applied to four diverge bottlenecks and three merge bottlenecks on intercity expressways in Japan.

Superiorities of lane based method are highlighted as follows. Firstly, it can identify and exclude semi-congested cases where some lanes are congested and others are not. At Toyota diverge bottleneck, 15 semi-congested cases are checked out through lane based method among 209 breakdown events which are identified by using cross-section based method. Secondly, timing of breakdown occurrence can be appropriately determined by lane based method which applies to 34 cases for this diverge section. These superiorities significantly improve accuracy of extracting breakdown flow rates which are underestimated by the existing cross-section based method.

With respect to sag bottleneck, there are no significant differences between the lane based identification method and cross-section based one. This is attributed to that sag bottlenecks are located at the uninterrupted expressway facilities without impacts from diverge or merge traffic flow.

Chapter 4

MODELING ON BREAKDOWN PROBABILITY

4.1 Introduction

Breakdown flow rate represents one significant aspect of recurrent bottleneck capacity which is closely related to breakdown occurrence.

Based on empirical observations, it has become evident that breakdown does not necessarily occur at constant flow rate values. The increasing studies have suggested that breakdown occurrence is a stochastic event. Therefore, there is a wide range of flow rates prior to breakdown occurrence at a certain bottleneck location. More and more researches have indicated that traffic flow rate during the time intervals preceding breakdown occurrence (denoted as breakdown flow rate in this study) is distributed in a wide range. It is better represented as a random variable rather than a deterministic value. Thus, breakdown probability model is adopted to describe and quantify breakdown flow rate in light of its stochastic nature.

Furthermore, with respect to the stochastic natures of breakdown occurrence and the resulted breakdown flow rate distribution, impact of traffic flow characteristics and geometries are speculated. To date, analyses supporting this kind of claim are limited.

In addition, with respect to different facility types, parameters of breakdown probability model at each bottleneck are possibly impacted by its site-specific geometries. In this sense, the general breakdown probability model can be developed by considering site-specific geometries for each facility type. This kind of general model enables evaluation of possible

breakdown occurrence at potential bottlenecks which is likely to be triggered by change of traffic demand in future. In this study, there exist several bottlenecks for each facility type in intercity expressway network which have different geometric configurations. This enables the generalization of breakdown probability models.

This chapter has developed a methodology on modeling breakdown probability considering impacts of traffic flow characteristics and geometries. The developed methodology has been adopted at diverge, merge and sag bottlenecks in intercity expressway network of central Japan.

The remainder of the chapter is organized as follows. Firstly, the related researches described in the literature are reviewed.

Secondly, the extracted breakdown flow rate distributions are used which are discussed in the previous chapter. Breakdown probability model is introduced which is based on analyzing the probability of breakdown occurrence at any traffic flow rate level. By using Weibull distribution function, breakdown probability model is established at each bottleneck location at the test bed.

Then, the impacts of traffic flow characteristics and geometries are examined with respect to each facility type. At diverge bottlenecks, lane utilization rate (*LUR*) and diverge rate (*DR*) are chosen as representative influencing factors. Parameters of breakdown probability model are further modeled as functions of *LUR* and *DR*. As for merge bottlenecks, impacts of lane utilization rate (*LUR*) and merge rate (*MR*) are modeled. With respect to sag bottlenecks, impacts of negative and positive slopes are further modeled. By these examinations on impacts of traffic flow characteristics and geometries, the general breakdown flow rate model at each facility type can be developed.

Finally, the concluding remarks are discussed in the final section of this chapter.

4.2 Literature review

Review of the relevant literature focuses on the studies which investigate characteristics of breakdown flow rate. Moreover, studies on impacts of traffic flow and geometric characteristics on breakdown probability are also reviewed.

The currently published version of the Highway Capacity Manual (2010) defines expressway capacity as "the maximum sustained 15-min rate of flow, expressed in passenger cars per hour per lane (pcphpl), that can be accommodated by a uniform expressway segment under prevailing traffic and roadway conditions in a specified direction." Implied in the current definition and understanding of expressway capacity is the notion that the facility will "breakdown" (transition from an uncongested state to a congested state) when demand exceeds a deterministic value. In other words, breakdown flow rate (*BDF*) is regarded as a deterministic value.

However, the increasing researches have suggested that breakdown occurrences are stochastic events which result in wide distribution of breakdown flow rates. Considerable number of researches have adopted breakdown probability model as a preferred measure to describe and quantify stochastic distribution of breakdown flow rates.

Significant studies have been achieved in modeling breakdown based on the empirical data. Brilon *et al.* (2005) conducted empirical analysis of traffic flow patterns, counted at 5-minute intervals over several months and at many sites. It clearly showed that breakdown probability is Weibull-distributed with a nearly constant shape parameter, which represents the variance. This was identified by using the so-called Product Limit Method, which is based on the statistics of lifetime data analysis. It is demonstrated that this method can be applicable to all types of expressways.

Elefteriadou *et al.* (1995), Lorenz. *et al.* (2000), and Persaud *et al.* (2007) proved that the breakdown events at merging sections are not a direct result of peak traffic flow rates. In these studies, breakdown phenomenon was treated as a probabilistic problem. They found that breakdown probability is an increasing function of mainline and on-ramp flow rates. Impact of ramp flow rate on breakdown probability was further investigated by Shawky and Nakamura (2007) by investigating six merging sections in Japan where breakdowns frequently occurred. It was found that by increasing ramp flow rate, breakdown probability increased. Also in Japan, Okamura *et al.* (2006) and Oguchi (2002) empirically investigated the breakdown probability at bottlenecks of expressway basic sections such as sag vertical curves. They also found that the breakdown probability increased with increase of the mainline flow rates as well as the breakdowns occurred over a wide range of flow rates from 210 to 300 veh/5-min/2-lane.

In summary of reviews presented above, some issues can be highlighted. These researches have adequately described breakdown probabilities to offer a basis for understanding stochastic nature of breakdown occurrence. With respect to impacts of traffic condition characteristics, some researches have confirmed impact of merge flow on breakdown probability at merge bottlenecks. This kind of investigation enriches feature of breakdown probability model. However, these kinds of investigations are limited, especially at other bottleneck types like diverge and sag bottlenecks. In addition, up to now, there are no concrete discussions on the general breakdown probability models by incorporating site-specific geometries with respect to each facility type.

4.3 Modeling on breakdown probability

Breakdown probability estimation by using Weibull distribution was originally proposed by Brilon *et al.* (2005). This study also adopts this idea and the cumulative distribution function of Weibull is expressed by a function as shown by Equation (4.1):

$$P(FR) = 1 - e^{-\left(\frac{FR}{\beta}\right)^\alpha} \quad (4.1)$$

where, FR is the traffic flow rate (veh/h), α and β are shape and scale parameters respectively.

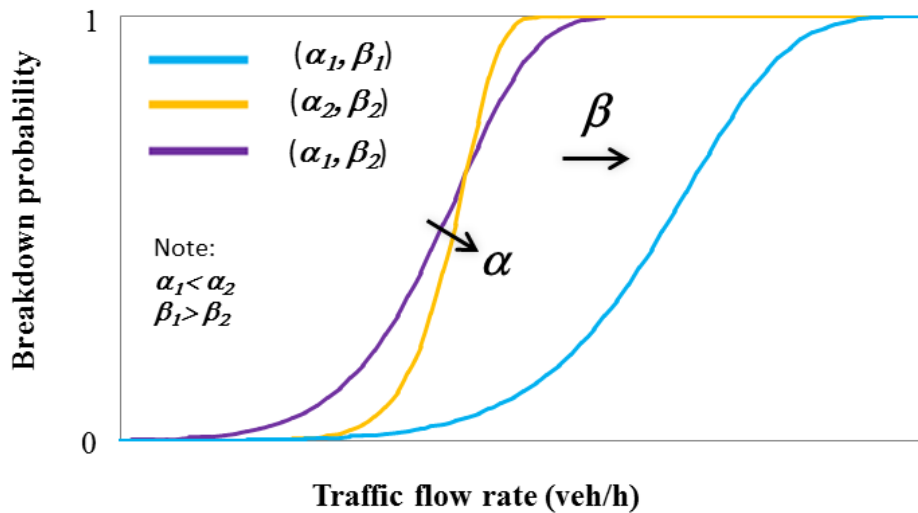


Figure 4.1 Impacts of parameters on breakdown probability distributions

With respect to Weibull distribution, its shape parameter α and scale parameter β determine the variance and position of breakdown probability distribution respectively as illustrated in Figure 4.1.

4.3.1 Breakdown probability models at diverge bottlenecks

With respect to diverge bottleneck, the breakdown probability model has been developed at each bottleneck location as presented in Table 4.1 and Figure 4.2.

Table 4.1 Breakdown probability models at diverge bottlenecks

Name	Sample size	Weibull function	
		α	β
Toyota diverge bottleneck	194	12	4836
Toki diverge bottleneck	36	13	4750
Komaki diverge bottleneck	32	13	4620

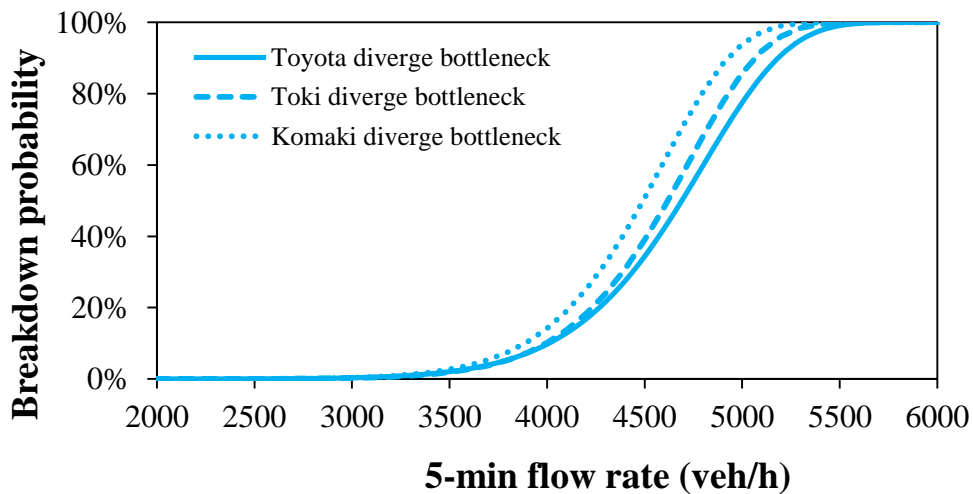


Figure 4.2 Breakdown probability distributions at diverge bottlenecks

The model is based on the extracted *BDF* distributions by using the lane based identification method as described in the previous chapter. Values of the breakdown probability are calculated in terms of the flow rate by comparing the number of breakdown events that occurred at a given value of flow rate with the total number of observations of the same flow rate value.

Based on the modeling results, the stochastic nature of breakdown at diverge bottlenecks can be further confirmed. This breakdown probability model represents the stochastic nature of diverge bottleneck capacity. It stands for the risk of breakdown occurrence at a certain traffic flow rate. Breakdown probability is found to increase with the increase of traffic flow rate. In other words, the possibility that this stochastic capacity is reached becomes high when traffic flow rate increases.

For example, at Toyota diverge bottleneck, its breakdown probability model has the shape parameter (α) of 12 and the scale parameter (β) of 4836. This reflects that breakdown for mainline traffic on all lanes can occur stochastically under significantly different traffic demand levels. Similar findings can also be confirmed at Toki and Komaki diverge bottlenecks despite relatively smaller sample sizes there. These breakdown probability models present basic descriptions and quantifications on capacities at these diverge facilities.

As for the semi-congested states at Toyota and Nagoya diverge bottlenecks, breakdown probability models have also been established.

In addition, it can be found that parameters of breakdown probability model at each diverge bottleneck differ with each other. The differences can be possibly attributed to site-specific geometric configuration like deceleration lane length. These effects will be further discussed in the following parts.

4.3.2 Breakdown probability models at merge bottlenecks

With respect to merge bottlenecks, the breakdown probability model has been developed at each bottleneck location as presented in Table 4.2 and Figure 4.3.

The model is also based on the extracted *BDF* distributions by using the lane based identification method as described in the previous chapter. Values of the breakdown probability are calculated in terms of the flow rate by comparing the number of breakdown events that occurred at a given value of flow rate with the total number of observations of the same flow rate value.

Based on the modeling results, the stochastic nature of breakdown at merge bottlenecks can be further confirmed. This breakdown probability model represents the stochastic nature of diverge bottleneck capacity. It stands for the risk of breakdown occurrence at a certain traffic flow rate. Breakdown probability is found to increase with the increase of traffic flow rate. In other words, the possibility that this stochastic capacity is reached becomes high when traffic flow rate increases.

Table 4.2 Breakdown probability models at merge bottlenecks

Name	Sample size	Weibull function	
		α	β
Toyota merge bottleneck	256	18	4422
Toki merge bottleneck	37	15	4276
Komaki merge bottleneck	196	14	4198

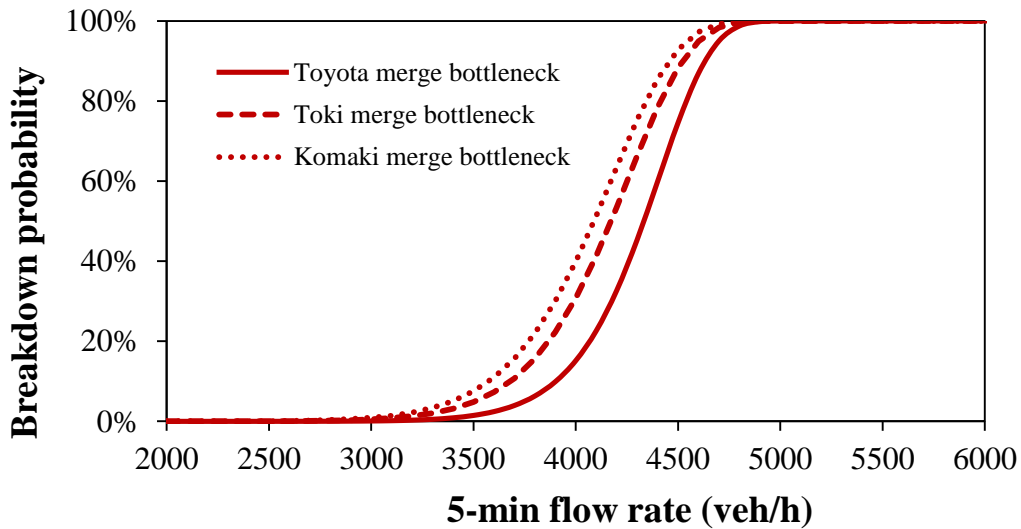


Figure 4.3 Breakdown probability distributions at merge bottlenecks

For example, at Toyota merge bottleneck, its breakdown probability model has the shape parameter (α) of 18 and the scale parameter (β) of 4422. This reflects that breakdown for mainline traffic on all lanes can occur stochastically under significantly different traffic demand levels. Similar findings can also be confirmed at Toki and Komaki merge bottlenecks despite relatively smaller sample sizes there. These breakdown probability models present basic descriptions and quantifications on capacities of these merge facilities.

In addition, it can be found that parameters of breakdown probability model at each merge bottleneck differ with each other. The differences can be possibly attributed to site-specific geometric configuration like acceleration lane length. These effects will be further discussed in the following parts.

4.3.3 Breakdown probability models at sag bottlenecks

With respect to sag bottlenecks, Kobayashi *et al.* (2011) have investigated breakdown probabilities on intercity expressway of central Japan. The breakdown probability model has been developed at each bottleneck location as presented in Table 4.3 and Figure 4.4.

Table 4.3 Breakdown probability models at sag bottlenecks

Number	Expressway	Direction	KP (km)	Sample size	Weibull function	
					α	β
1	Tomei	Eastbound	296.43	132	17	4394
2	Tomei	Eastbound	298.43	35	15	4931
3	Tomei	Eastbound	290.43	34	9	5859
4	Tomei	Eastbound	314.27	38	14	5213
5	Tomei	Westbound	294.43	186	15	4267
6	Tomei	Westbound	298.43	420	10	5203
7	Tomei	Westbound	299.50	30	8	5479
8	Tomei	Westbound	312.01	68	14	4346
9	Higashi-Meihan	Eastbound	61.5	113	13	4362
10	Higashi-Meihan	Eastbound	67.17	43	15	4456
11	Higashi-Meihan	Eastbound	58.54	62	18	4291
12	Chuo	Westbound	306.59	16	19	3951
13	Chuo	Northbound	298.44	17	12	4777
14	Chuo	Southbound	306.6	15	14	4573
15	Chuo	Southbound	312.96	17	11	4335
16	Chuo	Southbound	317.49	11	14	4880

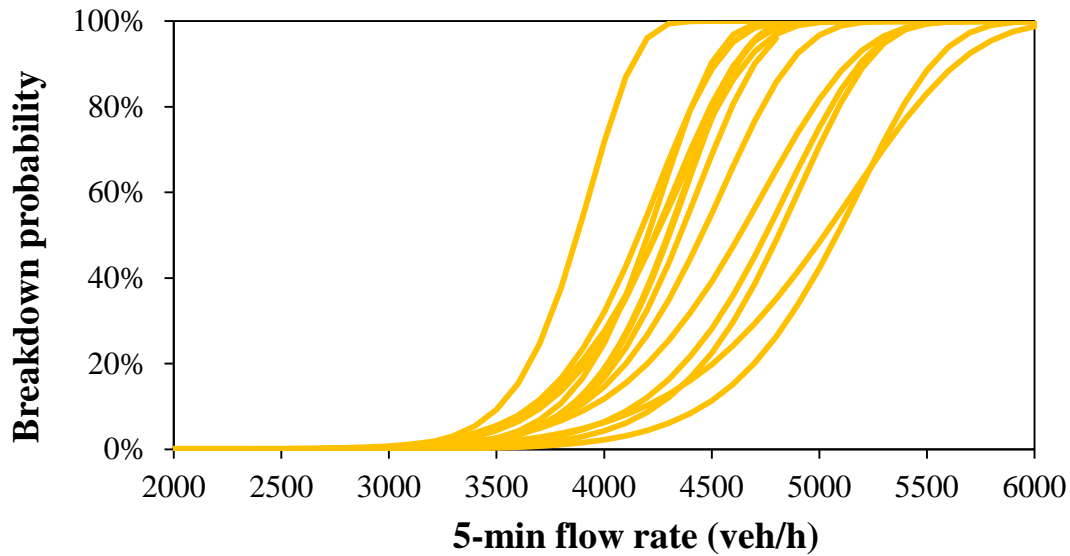


Figure 4.4 Breakdown probability distributions at sag bottlenecks

The model is based on the extracted *BDF* distributions as described in the previous chapter. Values of the breakdown probability are calculated in terms of the flow rate by comparing the number of breakdown events that occurred at a given value of flow rate with the total number of observations of the same flow rate value.

Based on the modeling results, the stochastic nature of breakdown at sag bottlenecks can be further confirmed. This breakdown probability model represents the stochastic nature of sag bottleneck capacity. It stands for the risk of breakdown occurrence at a certain traffic flow rate. Breakdown probability is found to increase with the increase of traffic flow rate. In other words, the possibility that this stochastic capacity is reached becomes high when traffic flow rate increases.

For example, at a sag bottleneck of 296.43KP on Tomei Expressway of eastbound direction, its breakdown probability model has the shape parameter (α) of 17 and the scale parameter (β) of 4394. This reflects that breakdown for mainline traffic on all lanes can occur stochastically under significantly different traffic demand levels. Similar findings can also be confirmed at other sag bottlenecks. These breakdown probability models present basic descriptions and quantifications on capacities of these sag facilities.

In addition, it can be found that parameters of breakdown probability model at each sag bottleneck differ with each other. The differences can be possibly attributed to site-specific

geometric configuration like negative and positive vertical slope values. These effects will be further discussed in the following parts.

4.3.4 Summary of breakdown probability models

Summary of breakdown probability models are illustrated in Figure 4.5. Both diverge and merge bottlenecks belong to the same bottleneck type which are located at the interrupted expressway sections. It is found that breakdown probability distributions of diverge bottleneck apparently are on the right side of those distributions of merge bottleneck.

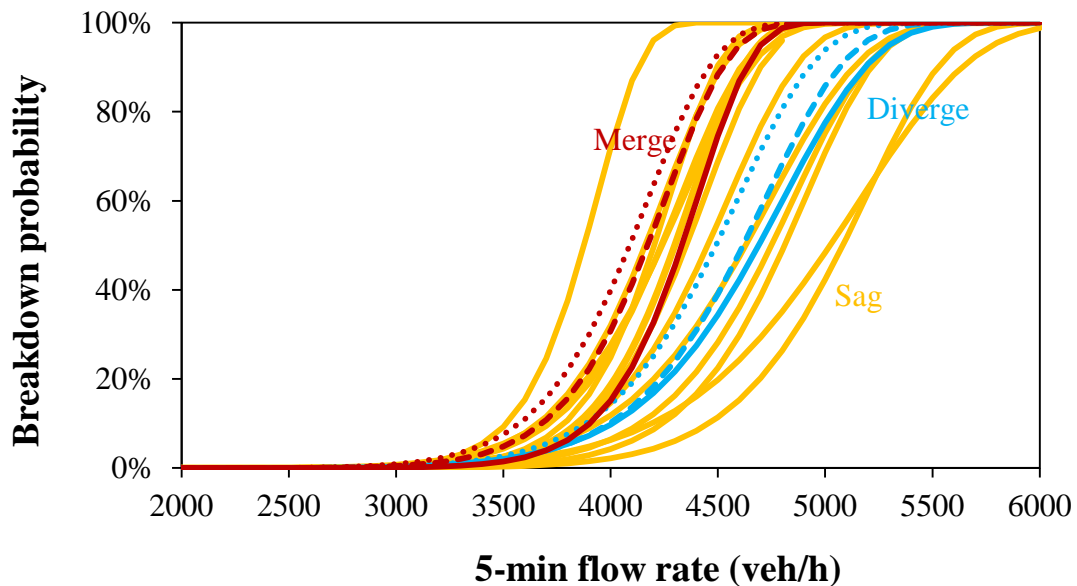


Figure 4.5 Breakdown probability distributions at bottlenecks of different expressway bottleneck types

This represents relatively higher capacities (breakdown flow rate values) at these diverge bottlenecks compared to merge bottlenecks. In other words, at a certain traffic flow rate, the possibility of breakdown occurrence is relatively lower than merge bottlenecks. This effect can be attributed to the fact that diverge traffic flow generally result in less disturbance on mainline traffic comparing to merge flow. As for sag bottlenecks at the uninterrupted intercity expressway sections, breakdown probability distribution varies significantly at each site. These effects are possibly caused by various geometric configurations at different sites.

4.4 Impact of traffic flow characteristics

Breakdown probability is possibly impacted by various aspects of factors, such as weather, lane width, driving population, etc. In this study, impacts from traffic condition characteristics will be focused on due to limitation of sample size.

Parameters (shape parameter α and scale parameter β) of the above developed breakdown probability models are possibly influenced by traffic condition characteristics at bottleneck location. This section will investigate this kind of influence as introduced as follows.

4.4.1 Diverge bottleneck

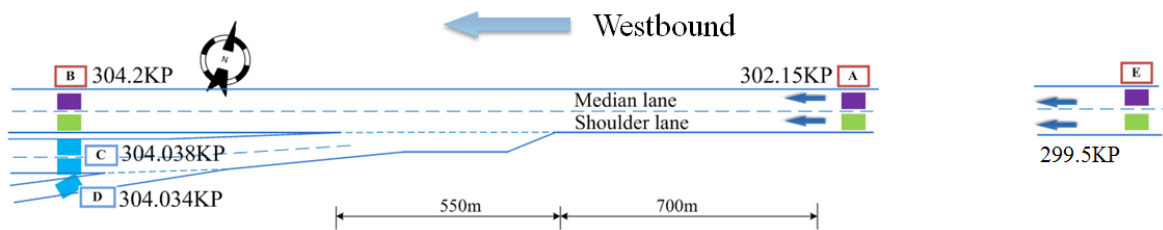


Figure 4.6 Vicinity of Toyota diverge bottleneck

At diverge bottlenecks, diverge traffic flow apparently will impose impact on mainline traffic flow as diverge behaviors will result in deceleration behaviors of mainline traffic flow. This effect is likely to further influence on breakdown occurrence. In addition, as aforementioned, lane-specific breakdown characteristics have significant impacts on breakdown occurrence on each lane. Influences of them will be investigated as follows. Figure 4.6 illustrates vicinity of Toyota diverge bottleneck which will be analyzed.

Figure 4.7 presents the typical distributions of flow rate and speed on each lane in a day (3/28/2009). Also distribution of diverge flow rate is also demonstrated. Two breakdown events occurred during the morning and evening peak hours of this day respectively which were indicated by significant speed drops on both shoulder lane and median lane.

It can be observed that flow rates on shoulder lane and median lane are close with each other especially during peak hours. For ease of diverge behaviors, diverge flow would concentrate on shoulder. It can be found that diverge flow rate is apparently low than flow rate on shoulder lane. This indicates that shoulder lane is shared by both diverge flow and through flow which result in possible breakdown occurrence first there.

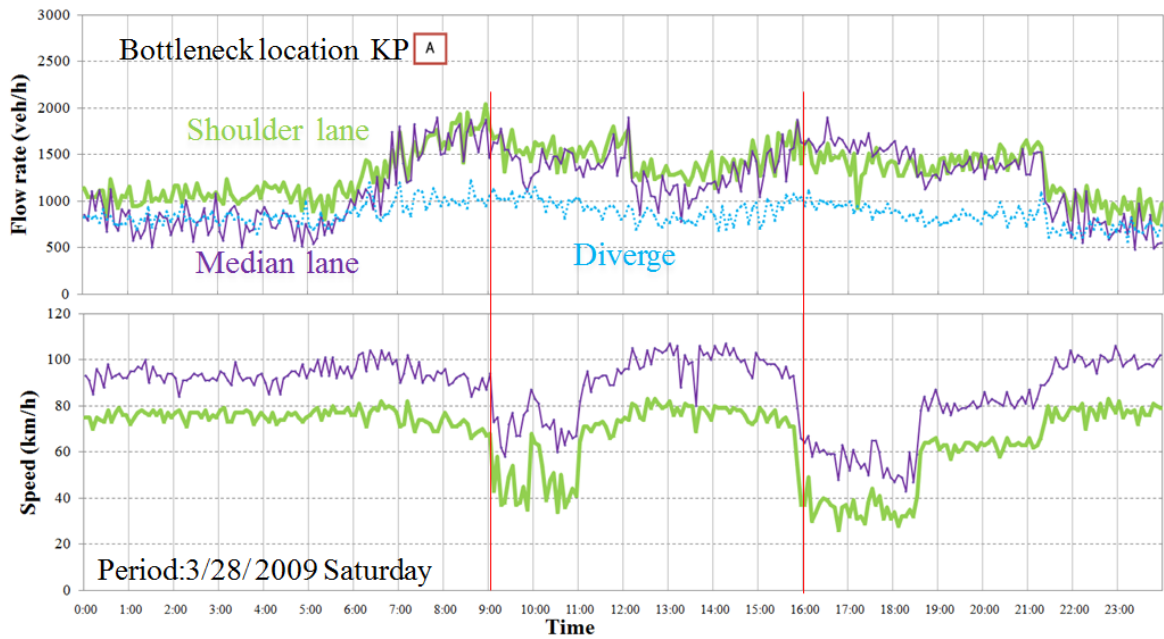


Figure 4.7 Flow rates on each lane and diverge at detector 302.15KP for location of Toyota diverge bottleneck

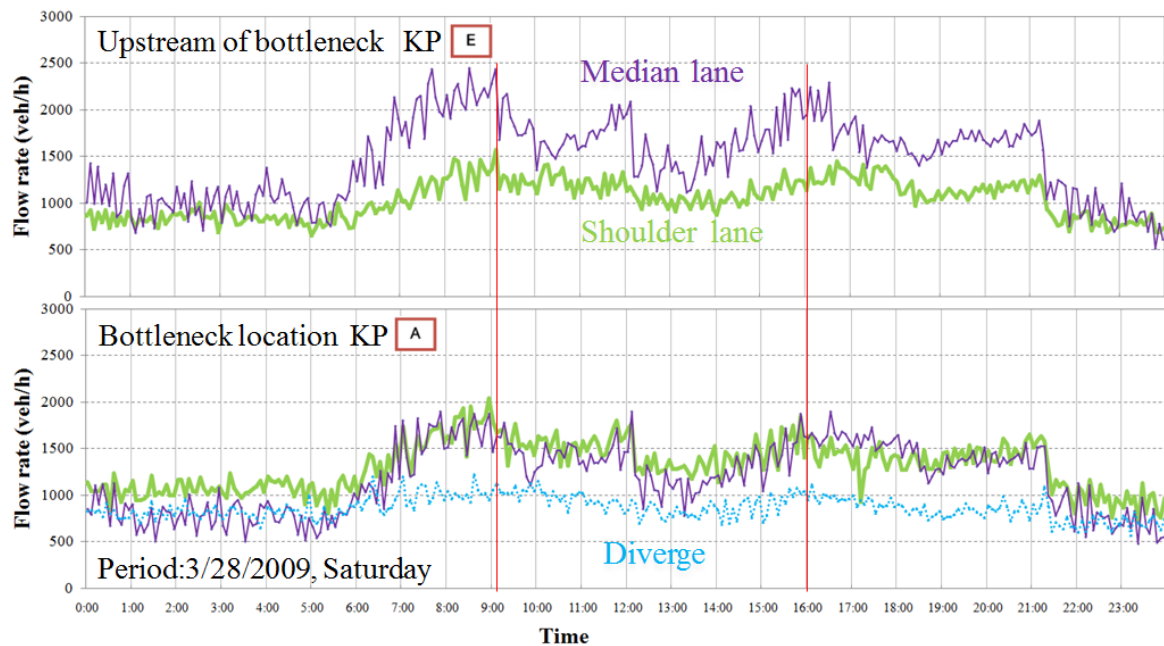


Figure 4.8 Change tendency for flow rates on each lane from upstream to location of Toyota diverge bottleneck

Figure 4.8 presents the comparison between flow rates of bottleneck location and its adjacent upstream location. At upstream location, flow rate on shoulder lane is apparently lower than that on median lane during peak hours. By comparing to bottleneck location,

there is significant shift of flow rate onto shoulder lane. This is attributed to the fact that the diverge drivers would like to shift onto shoulder lane in advance when approaching diverge section for ease of diverge behaviors.

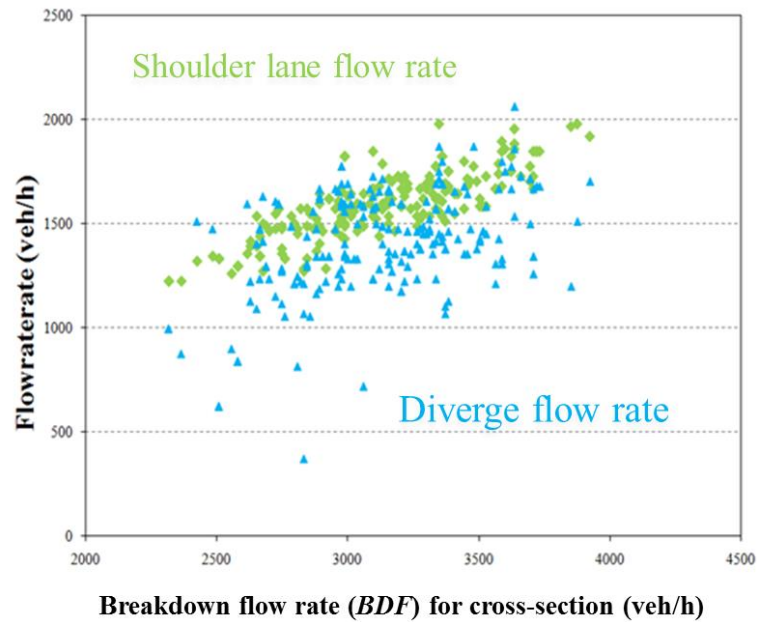


Figure 4.9 Flow rate on shoulder lane and diverge

Figure 4.9 demonstrates the summary of the flow rates on shoulder lane and diverge at the interval when breakdown occurs on both shoulder lane and median lane. It can be found that the distribution of diverge flow rate is apparently lower than that on shoulder lane. It indicates that shoulder lane is shared by both diverge traffic and through traffic.

To sum it up, for diverge bottleneck with left-hand off-ramps as illustrated in Figure 4.6, the overloaded traffic demand and the accompanied diverge flow disturbance are imposed on shoulder lane. While for median lane, its capacity is likely to be underutilized as it mainly serves for through traffic flow there. Thus even for the same traffic demand loaded on mainline, understandably different allocations of demand on each lane will result in difference of breakdown occurrence on each lane. In this sense, lane utilization rate plays an important role in modeling breakdown probability at diverge bottlenecks.

Therefore diverge rate (DR) and lane utilization rate (LUR) are chosen as candidates of the influencing factors for diverge bottlenecks in this study.

4.4.1.1 Diverge rate (DR)

Diverge rate (DR) is used to evaluate impact of diverge traffic flow which represents the proportion of diverge flow from mainline flow. Understandably, with increase of DR at a certain flow rate level, impacts from diverge traffic flow becomes higher. Thanks to Central Nippon Expressway Company Limited (NEXCO), traffic flow data records along the mainlines and off-ramps around these diverge bottlenecks are available. DR can be computed by comparing diverge traffic flow rate to mainline traffic flow rate. For example, at Toyota diverge bottleneck, DR can be calculated by using Equation (4.2).

$$DR = \frac{FR_C + FR_D}{FR_B + FR_C + FR_D} \quad (4.2)$$

where, FR_B , FR_C and FR_D are the measured traffic flow rates on all lanes (veh/h) at detectors with labels of B , C and D in the vicinity of the Toyota diverge bottleneck.

At this diverge bottleneck, during peak hours, values of DR mainly fall into a range from 0.45 to 0.55. It is found that the high diverge flow from mainline to off-ramps exist which is regarded as the major cause of breakdown occurrence there.

4.4.1.2 Lane utilization rate (LUR)

Lane utilization rate (LUR) is adopted to quantify the lane-specific breakdown characteristics at diverge sections. As for the detector data, traffic flow rates were measured and aggregated on each lane. This enables the calculation of LUR based on empirical data. LUR on a certain lane is computed by comparing traffic flow rate on this lane to that on cross-section. For example, at Toyota diverge bottleneck, LUR on shoulder lane is focused on considering its geometric configuration of left-hand off-ramps. LUR on shoulder lane can be calculated by using Equation (4.3).

$$LUR = \frac{FR_S}{FR_S + FR_M} \quad (4.3)$$

where, FR_S and FR_M are the measured traffic flow rates on shoulder lane and median lane respectively in the vicinity of the Toyota diverge bottleneck.

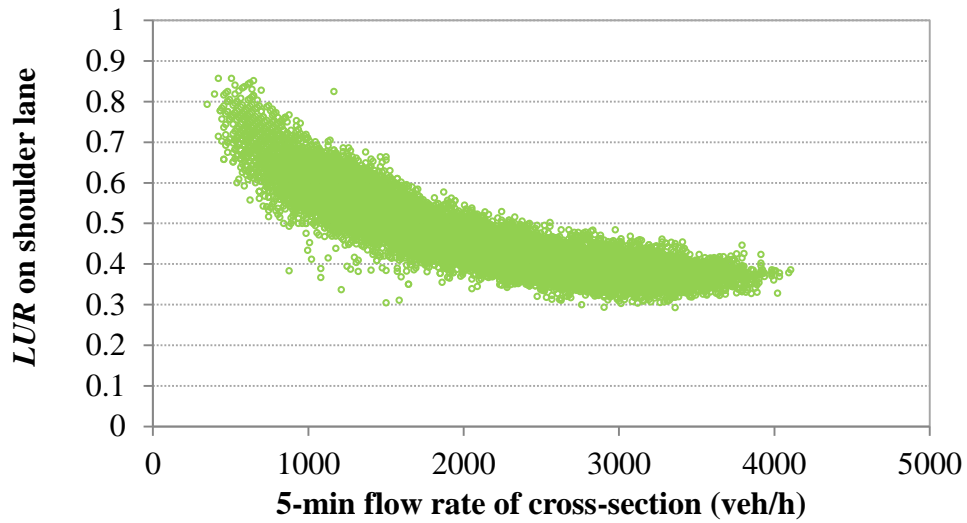


Figure 4.10 *LUR* distribution on shoulder lane at detector 299.5KP for upstream of Toyota diverge bottleneck

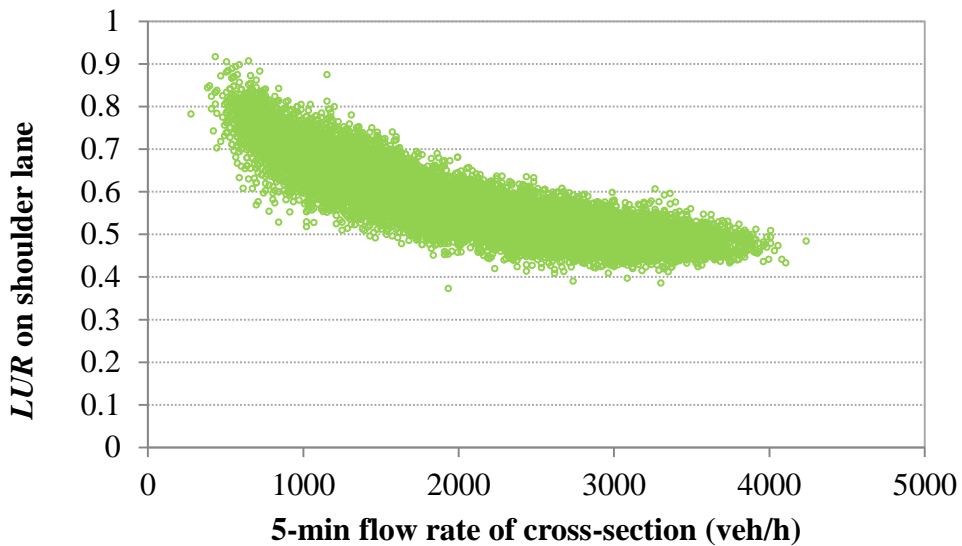


Figure 4.11 *LUR* distribution on shoulder lane at detector 302.15KP for location of Toyota diverge bottleneck

The measured *LUR* distributions around Toyota diverge bottleneck are illustrated in Figures 4.10 and 4.11. At bottleneck location of 302.15KP, its *LUR* values mainly fall into a range from 0.40 to 0.50 under high traffic flow rate levels as shown in Figure 4.8. However, at its adjacent upstream detector location of 299.5KP, *LUR* values are distributed in the relatively lower value region from 0.30 to 0.40 under high traffic flow rate levels. This comparison indicates a significant increase of *LUR* value on shoulder lane when approaching diverge section. This is due to the tendency of traffic flow shift onto shoulder lane for ease of diverge behavior. In addition, *LUR* values will increase after passing this

diverge section. As investigated in the previous chapter, *LUR* on shoulder lane can be further modeled as functions of traffic flow characteristics and geometries. This helps to reproduce the breakdown phenomena at diverge bottlenecks which will be discussed in Chapter 6.

4.4.1.3 Modeling considering impacts of *DR* and *LUR*

With respect to breakdown probability model parameters (shape parameter α and scale parameter β), impacts of *DR* and *LUR* are investigated. Firstly, different ranges of the extracted *BDF* value are classified based on groups of *DR* and *LUR*. Secondly, for each range, parameters (α and β) of Weibull distribution are modeled as listed in Table 3. Then, these parameters are estimated as functions of *DR* and *LUR* in Equation (4.4-a) and (4.4-b) whose *R*-square values are 0.571 and 0.914 respectively. In addition, as illustrated in Figure 4.12, the regression functions perform well according to a comparison between the measured and estimated values. The *t*-values for influencing factors are also indicated in these equations.

$$\alpha = 3.42 \times 10 DR - 2.18 \quad (4.4-a)$$

$t=4.14$ $t=-0.503$

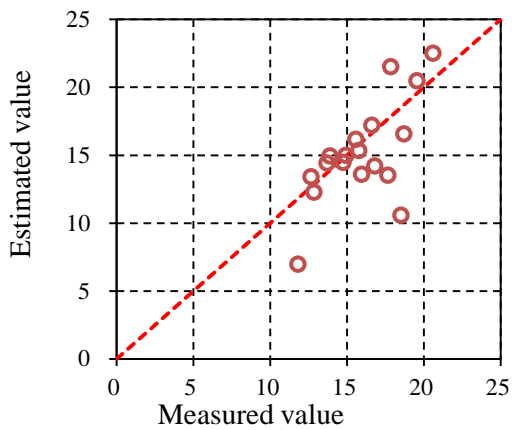
$$\beta = -2.15 \times 10^3 DR + 9.46 \times 10^3 LUR + 8.73 \times 10^2 \quad (4.4-b)$$

$t=-2.64$ $t=8.44$ $t=0.771$

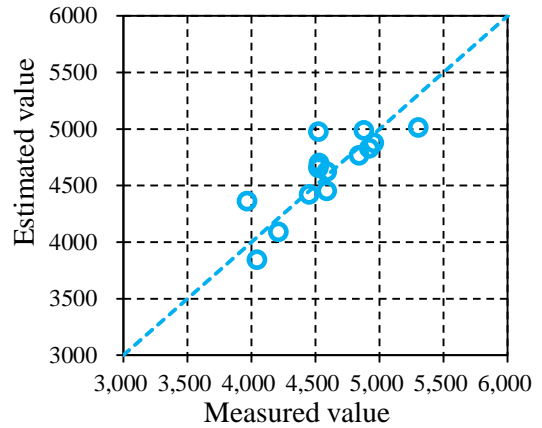
where, *DR* is diverge rate, and *LUR* is lane utilization rate on median lane.

Table 4.4 Impact of *DR* and *LUR* at Toyota diverge bottleneck

<i>DR</i>		<i>LUR</i> for median lane												
		0.38-0.42			0.42-0.46			0.46-0.50			0.50-0.54			
Range	Median	Parameter	0.40		0.44		0.48		0.52					
			No	α	β	No	α	β	No	α	β	No	α	β
0.36-0.40	0.38								(4)	13	4537	(6)	7	6872
0.40-0.44	0.42								(13)	14	4588	(14)	12	5304
0.44-0.48	0.46					(12)	16	3965	(32)	14	4523	(17)	15	4920
0.48-0.52	0.50					(13)	17	4045	(22)	15	4451	(9)	15	4841
0.52-0.5	0.5		(4)	11	4236	(14)	14	4211	(14)	14	4528	(4)	14	4956



(a) Shape parameter α



(b) Scale parameter β

Figure 4.12 A comparison between the measured and the estimated values

4.4.2 Merge bottleneck

With respect to merge bottleneck, Toyota merge bottleneck is used to analyze impacts of traffic flow characteristics as presented in Figure 4.13.

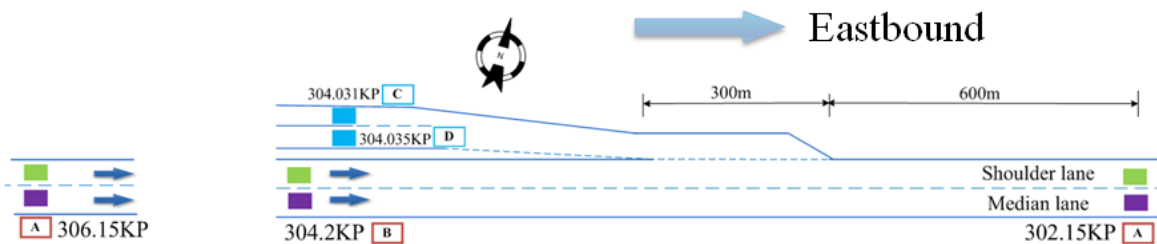


Figure 4.13 Vicinity of Toyota merge bottleneck

4.4.2.1 Merge rate (MR)

Merge rate (MR) is used to evaluate impact of merge traffic flow which represents the proportion of merge flow comparing to mainline flow. Understandably, with increase of MR at a certain flow rate level, impacts from merge traffic flow becomes higher. MR can be computed by comparing merge traffic flow rate to mainline flow rate. For example, at Toyota merge bottleneck, merge rate (MR) is used to evaluate impact of merge flow which is computed by using Equation (4.5).

$$MR = \frac{FR_C + FR_D}{FR_B + FR_C + FR_D} \quad (4.5)$$

where, FR_B , FR_C and FR_D are the measured flow rates on all lanes (veh/h) at detectors with labels of B , C and D in the vicinity of the Toyota merge bottleneck.

At this merge bottleneck, during peak hours, values of MR mainly fall into a range from 0.40 to 0.45. It is found that the high merge flow onto mainline from on-ramps exist which is regarded as the major cause of breakdown occurrence there.

4.4.2.2 Lane utilization rate (LUR)

Lane utilization rate (LUR) is also adopted to quantify the lane-specific breakdown characteristics at merge sections. As for the detector data, traffic flow rates were measured and aggregated on each lane. This enables the calculation of LUR based on empirical data. LUR on a certain lane is computed by comparing traffic flow rate on this lane to that on cross-section. For example, at Toyota merge bottleneck, LUR on shoulder lane is focused on considering its geometric configuration of left-hand on-ramp. LUR on shoulder lane can be calculated by using Equation (4.6).

$$LUR = \frac{FR_S}{FR_S + FR_M} \quad (4.6)$$

where, FR_S and FR_M are the measured traffic flow rates on shoulder lane and median lane respectively in the vicinity of the Toyota merge bottleneck.

4.4.2.3 Modeling considering impacts of MR and LUR

At Toyota merge bottleneck, impacts of MR and LUR are investigated. Firstly, different ranges of the extracted BDF value are classified based on groups of DR and LUR . Secondly, for each range, parameters (α and β) of Weibull distribution are modeled. Then, these parameters are estimated as functions of MR and LUR in Equations (4.7-a) and (4.7-b) whose R -square values are 0.651 and 0.484 respectively. The t -values for influencing factors are also indicated in these equations.

$$\alpha = \underset{t=3.55}{3.01 \times 10} MR - \underset{t=-2.91}{7.39} LUR + \underset{t=1.04}{4.98} \quad (4.7-a)$$

$$\beta = \underset{t=-5.86}{-3.31 \times 10^2} MR - \underset{t=-4.82}{3.76 \times 10^2} LUR + \underset{t=20.1}{4.87 \times 10^3} \quad (4.7-b)$$

where, MR is merge rate, and LUR is lane utilization rate on median lane.

4.5 Impact of geometric characteristics

As illustrated in Figure 4.14, with respect to sag bottlenecks at the uninterrupted expressway sections, breakdown probability distribution varies significantly at each site. These effects are possibly caused by various geometric configurations there. The consequent negative and positive vertical slope values as shown in Figure 4.10 are speculated to impose impacts on parameters (shape parameter α and scale parameter β) of the developed breakdown probability models as discussed above.

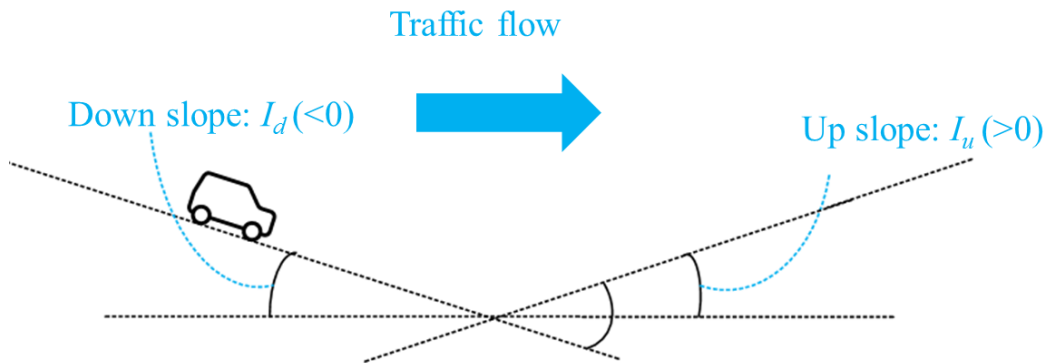


Figure 4.14 Illustration of vertical slope change

Sixteen sag bottlenecks are used for generalizing breakdown probability model. Shape parameter α and scale parameter β are modeled as function of site specific geometric configuration (I_d and I_u) in Equations (4.8-a) and (4.8-b) whose R -square values are 0.395 and 0.547 respectively. The t -values for influencing factors are also indicated in these equations.

$$\alpha = \underset{t=3.55}{-1.00} (I_u - I_d) + 1.5 \times 10 \quad (4.8-a)$$

$$\beta = \underset{t=-4.82}{2.86 \times 10^2} (I_u - I_d) + \underset{t=20.1}{4.06 \times 10^3} \quad (4.8-b)$$

where, I_d is the negative vertical slope value and I_u is the positive vertical slope value.

In addition, shape parameter α and scale parameter β can be further modeled by taking both site specific geometric configuration (I_d and I_u) and lane utilization rate (LUR) into consideration as expressed in Equations (4.9-a) and (4.9-b).

$$\alpha = -1.00(I_u - I_d) + 1.5 \times 10 \quad (4.9-a)$$

$$\beta = 4.69 \times 10^2 (I_u - I_d) LUR + 4.08 \times 10^3 \quad (4.9-b)$$

where LUR is lane utilization rate on median lane.

This general model enables the estimation of breakdown occurrence at potential sag bottlenecks by considering their geometric configuration and traffic condition characteristics.

4.6 Summary

This chapter has developed a methodology on modeling breakdown probability considering impacts of traffic flow characteristics and geometries. The developed methodology has been adopted at diverge, merge and sag bottlenecks in intercity expressway network of central Japan.

Firstly, the extracted breakdown flow rate distributions are used which are discussed in the previous chapter. Breakdown probability model is introduced which is based on analyzing the probability of breakdown occurrence at any traffic flow rate. By using Weibull distribution function, breakdown probability model is established at each bottleneck location at the test bed.

Secondly, the impacts of traffic flow characteristics and geometries are examined with respect to each facility type. At diverge bottlenecks, lane utilization rate (LUR) and diverge rate (DR) are chosen as representative influencing factors. Parameters of breakdown probability model are further modeled as functions of LUR and DR . As for merge bottlenecks, impacts of lane utilization rate (LUR) and merge rate (MR) are modeled. With respect to sag bottlenecks, impacts of negative and positive slopes are further modeled. By these examinations on traffic flow characteristics and geometries, the general breakdown flow rate model at each facility type can be developed.

As for practical application in simulation, the models in this chapter enable estimation of breakdown occurrence at the operational stage. Estimation accuracy can be improved by taking traffic condition characteristics into account. In addition, consideration of geometric characteristics enables the estimation of potential bottleneck.

Chapter 5

MODELING ON DISCHARGE FLOW RATE

5.1 Introduction

Traffic flow rate for breakdown duration (denoted as breakdown flow rate (*DCF*) in this study) is another important aspect of recurrent bottleneck capacity. During the period of breakdown duration, it plays a significant role in evaluating measures of effectiveness for intercity expressway facilities like travel time reliability, queue length and etc.

Discharge flow rate is typically characterized in a deterministic manner by the existing studies. In other words, after breakdown occurs, it is assumed that the queue discharges at a deterministic flow rate. Recently, it has been becoming more and more obvious that such conventional deterministic measurement of discharge flow rate is not sufficient for intercity expressway traffic performance assessment without considering its stochastic nature.

It has been well recognized that breakdown phenomena have significant impacts on intercity expressway performance. To assess influence of breakdown event, its occurrence has been described by breakdown probability models by the considerable number of studies in light of its stochastic nature. With respect to the period of breakdown duration, understandably discharge flow rate is also characterized of stochastic feature which has been confirmed by many empirical observations.

However, few efforts have been made on modeling discharge flow rate by considering its stochastic characteristic. Therefore in this sense, intercity expressway performance for the period of breakdown duration is not adequately represented.

In addition, the relationship between breakdown flow rate and discharge flow rate has not been well understood, which significantly impacts intercity expressway performance accompanied with breakdown phenomena. Existing studies on the investigation of this relationship are to estimate capacity drop due to breakdown occurrence in a deterministic way. However, the stochastic nature of discharge flow rate has not been well interpreted.

Furthermore, there is the speculation on the relationship between breakdown flow rate and discharge flow rate considering the transition between them. As aforementioned, breakdown flow rate is widely distributed due to its stochastic nature. In other words, traffic flow condition prior to breakdown occurrence quite varies. If breakdown is triggered at relatively high breakdown flow rate value, for expressway facility, its carrying ability probably has already been fully utilized. Thus, under such a condition, understandably there is high capacity drop when changing from breakdown flow rate to discharge flow rate. In contrast, when breakdown is triggered at relatively low breakdown flow rate, the inventory carrying ability has not been fully digested. Accordingly this would possibly result in a low capacity drop accompanying breakdown occurrence. To sum it up, breakdown flow rate and discharge flow rate are closely related.

With respect to discharge flow rate, another significant factor is the time-dependent characteristic which needs to be taken into account in analysis. Different from breakdown flow rate, discharge flow rate need to be analyzed for the whole breakdown duration rather than just a specific time interval. The elapsed time of breakdown duration is supposed to impose impact on discharge flow rate as it influences on driver behaviors like driving perception. However, such kind of investigation still remains limited. Therefore this time-dependent feature of discharge flow rate needs to be taken into consideration as well when modeling discharge flow rate.

To sum it up, this chapter has developed a methodology for stochastic modeling on discharge flow rate (*DCF*) by considering its relationship to breakdown flow rate (*BDF*) and the elapsed time of breakdown duration. This methodology has been applied to diverge, merge and sag bottlenecks on intercity expressways of central Japan.

The remainder of the chapter is organized as follows. Firstly, the related researches described in the literature are reviewed.

Secondly, a methodology is developed for stochastic modeling on discharge flow rate (*DCF*). Statistical analysis of discharge flow rate distributions at each time interval indicates: 1) a positive relationship between breakdown and discharge flow rate distributions, and 2) a descending tendency associated with increase of the elapsed time of breakdown duration.

Thirdly, Normal distribution is adopted to describe and quantify stochastic nature of discharge flow rates. Its parameters (mean value and standard deviation) are then modeled as functions of breakdown flow rate and the elapsed time of breakdown duration. The established discharge flow rate models have been validated through Monte Carlo method.

Then, with respect to each facility type, the general discharge flow rate model is developed by considering impacts of site-specific geometric characteristics. At diverge and merge bottlenecks, lengths of deceleration and acceleration lane are taken into account. As for sag bottleneck, negative downhill and positive uphill slopes are considered. Such general discharge flow rate models enable the estimation at potential bottlenecks in intercity expressway network.

The concluding remarks are discussed in the final section of this chapter.

5.2 Literature review

Review of the relevant literature focuses on the studies which investigate characteristics of discharge flow rate. In addition, studies on the relationship between breakdown flow rate and discharge flow rate also reviewed.

Discharge flow rate is another important aspect of bottleneck capacity. It is a significant aspect of bottleneck function which impacts on intercity expressway performance like travel time reliability, breakdown duration and etc. The description and quantification of discharge flow rate have been carried out for several decades.

The current published version of the Highway Capacity Manual (2010) defines expressway capacity as "the maximum sustained 15-min rate of flow, expressed in passenger cars per hour per lane (pcphpl), that can be accommodated by a uniform expressway segment under prevailing traffic and roadway conditions in a specified direction." This definition actually is the description of breakdown flow rate rather than discharge flow rate. For the saturated

period of breakdown duration, there are no specific recommendations to quantify discharge flow rate which possibly will be enhanced in future version.

A number of investigations have proven the existence of different capacities under the congested traffic conditions by comparing the discharge flow rate to the flow rate immediately prior to breakdown occurrence (breakdown flow rate in this study). These differences are generally named as "capacity drop" or "two-capacity" phenomena. There are different hypotheses about the reasons for the capacity drop phenomenon. One significant hypothesis regarding different driving behavior is interpreted as that: drivers in fluent traffic accept shorter headways since they expect to be able to pass the vehicles in front. Once they have given up this idea, they switch to a more safety-conscious style of driving and keep longer headways. The hypotheses and the value of the capacity drop were analyzed by Regler (2004) for the fifteen expressway sections by using different approaches.

Banks *et al.* (1990), Hall and Agyemang-Duah *et al.* (1991) have measured capacity drop values between 3 % and 6 % for different North-American expressways. Ponzlet *et al.* (1996) analyzed traffic flow on German expressways to confirm that this phenomenon existed with a 6 % drop for 5-minute flow rates. Brilon and Zurlinden (2003) analyzed the capacity drop by comparing the stochastic capacity to flow rates in the congested flow. They computed an average of 24 %, which is quite high compared to the results of other researches.

Most of all, regarding relationship between breakdown flow rate and discharge flow rate, capacity drop phenomena have been focused on. In past decades, many studies have compared breakdown flow rate prior to breakdown and the discharge flow rate that follows breakdown (Banks *et al.* (1990, 1991), Hall *et al.* (1991), Urbanik *et al.* (1991), Ringert *et al.* (1993), Elefteriadou *et al.* (1995, 2003), Cassidy *et al.* (1999), Persaud *et al.* (1998, 2001), Zhang *et al.* (2004a, 2004b), Rudjanakanoknad *et al.* (2005), Ma *et al.* (2011)). Most studies have found a decrease in traffic flow rate after breakdown occurrence. These researches have well confirmed that traffic flow rate decreases for transition from uncongested to congested flow.

In the most recent study, Dong and Mahmassani (2011) suggested a linear relationship between queue discharge flow rate and breakdown flow rate. However, most

methodologies are from deterministic viewpoints despite observations of stochastic distribution of discharge flow rate.

With respect to investigation on stochastic nature of discharge flow rate, limited researches have been carried out. Based on field data, Lorenz and Elefteriadou (1995) have demonstrated that the queue discharge flow rate is also stochastic in nature. Elefteriadou *et al.* (2001), Shawky and Nakamura (2007) showed that discharge flow rates followed Normal distribution. These authors have observed the variability of discharge flow rate for breakdown duration. For a more systematic analysis, however, a comprehensive theoretical concept is required.

With respect to the time-dependent characteristic of discharge flow rate, Koshi (1986) pointed out that there was a descending tendency with increase of the elapsed time of breakdown duration at sag bottlenecks in Japan. However, most exiting researches have not taken time-dependent characteristics into account when investing discharge flow rate.

In summary of reviews presented above, some issues can be highlighted. These researches have confirmed the decrease of flow rate (capacity drop) by comparing breakdown and discharge flow rates. The stochastic nature of discharge flow rate need to be taken into consideration when modeling. In addition, impacts from breakdown flow rate and the elapsed time of breakdown duration need to be investigated.

5.3 Statistic analysis of discharge flow rate distributions at bottlenecks

This section introduces statistical analysis of discharge flow rates at diverge, merge and sag bottlenecks. 5-minute detector data of Central Nippon Expressway Company Limited has been used in this research. An initiative analysis was performed to identify the bottleneck sections in intercity expressway network of central Japan. The general information of discharge flow rates at these bottlenecks are discussed as follows.

5.3.1 Diverge bottlenecks

Statistical analysis of the measured discharge flow rates at diverge bottlenecks are listed in Table 5.1. To demonstrate the time-dependent characteristics of discharge flow rate, the mean values, standard deviation (SD) and sample sizes at different intervals (30 minute aggregation for ease of illustration) are analyzed.

Table 5.1 Statistic analysis of *DCF* distributions at diverge bottlenecks

Name	Statistics	<i>BDF</i>	<i>DCF</i> distribution				
			Mean	1st	2nd	3rd	4th
Toyota diverge bottleneck	Mean (veh/h)	3145	2888	3018	2881	2819	2785
	SD (veh/h)	400	357	384	348	324	327
	Sample size	194	194	194	151	110	71
Toki diverge bottleneck	Mean (veh/h)	3253	3080	3273	3130	3075	3019
	SD (veh/h)	2914	307	335	300	236	222
	Sample size	36	36	36	33	27	24
Komaki diverge bottleneck	Mean (veh/h)	2914	2522	2619	2539	2543	2481
	SD (veh/h)	463	458	540	454	389	404
	Sample size	27	27	26	24	22	21

Note: considering limited sample size, stochastic *DCF* model for semi-congestion state at Toyota diverge bottleneck has not been estimated.

The descending tendencies can be observed for both mean values and standard deviation values at each bottleneck location. The decrease of flow rate (capacity drop) can be confirmed. For example, at Toyota diverge bottleneck, with increase of the elapsed time from the first 30 minute to the fourth 30 minute, the mean value decreases from 3018 veh/h to 2785 veh/h. As for standard deviation, it decreases from 384 veh/h to 327 veh/h. There is significant decrease of the flow rate by comparing to mean breakdown flow rate value of 3154 veh/h.

5.3.2 Merge bottlenecks

Statistical analysis of the measured discharge flow rates at merge bottlenecks are listed in Table 5.2. The mean values, standard deviation and sample sizes at different intervals (30 minute aggregation for ease of illustration) are analyzed.

The descending tendencies can also be observed for both mean values and standard deviation values at each bottleneck location. The decrease of flow rate (capacity drop) can be confirmed. For example, at Toyota merge bottleneck, with increase of the elapsed time from the first 30 minute to the fourth 30 minute, the mean value decreases from 3326 veh/h to 3074 veh/h. As for standard deviation, it decreases from 478 veh/h to 304 veh/h. There is significant decrease of the flow rate by comparing to mean breakdown flow rate value of 3399 veh/h.

Table 5.2 Statistic analysis of *DCF* distributions at merge bottlenecks

Name	Statistics	<i>BDF</i>	<i>DCF</i> distribution				
			Mean	1st	2nd	3rd	4th
Toyota merge bottleneck	Mean (veh/h)	3399	3186	3326	3317	3184	3074
	SD (veh/h)	317	450	478	426	303	304
	Sample size	256	256	256	248	214	170
Toki merge bottleneck	Mean (veh/h)	3546	3045	3146	2913		
	SD (veh/h)	256	451	484	439		
	Sample size	37	37	37	15		
Komaki merge bottleneck	Mean (veh/h)	3040	2963	3086	3014	2963	2891
	SD (veh/h)	368	310	325	306	318	302
	Sample size	196	196	196	180	154	121

5.3.3 Sag bottlenecks

Statistical analysis of the measured discharge flow rates at some representative sag bottlenecks are listed in Table 5.3. The mean values, standard deviation and sample sizes at different intervals (aggregation of 30 minute for ease of illustration) are analyzed.

Table 5.3 Statistic analysis of *DCF* distributions at sag bottlenecks

Name	Statistics	<i>BDF</i>	<i>DCF</i> distribution				
			Mean	1st	2nd	3rd	4th
Tomei (westbound) 298.43KP	Mean (veh/h)	3061	3000	3124	3041	2970	2959
	SD (veh/h)	290	189	241	247	240	230
	Sample size	150	150	150	136	126	114
Tomei (westbound) 294.43KP	Mean (veh/h)	3324	3071	3321	3158	3088	3010
	SD (veh/h)	353	219	251	221	210	236
	Sample size	420	420	420	412	389	365
Tomei (eastbound) 296.43KP	Mean (veh/h)	3388	3098	3250	3048	2998	2926
	SD (veh/h)	344	285	247	269	281	337
	Sample size	193	193	193	160	136	107
Higashi-Meihon (eastbound) 61.5KP	Mean (veh/h)	3033	2857	3020	2852	2781	2727
	SD (veh/h)	387	215	221	238	219	182
	Sample size	234	234	234	212	183	158
Higashi-Meihon (eastbound) 67.17KP	Mean (veh/h)	3066	2874	3091	2942	2848	2747
	SD (veh/h)	364	260	300	329	321	279
	Sample size	118	118	118	110	102	90

The descending tendencies can be observed for both mean values and standard deviations values at each bottleneck location. The decrease of flow rate (capacity drop) can be confirmed. For example, at sag bottleneck of 298.43KP on Tomei Expressway of westbound direction, with increase of the elapsed time from the first 30 minute to fourth 30 minute, the mean value decreases from 3124 veh/h to 2959 veh/h. As for standard deviation, it decreases from 241 veh/h to 230 veh/h. There is significant decrease of the flow rate by comparing to mean breakdown flow rate value of 3061 veh/h.

5.4 Stochastic modeling on discharge flow rate

This section introduces how to model the stochastic characteristics of discharge flow rate.

5.4.1 Hypothesis of modeling

Figure 5.1 presents the empirical *DCF* distribution at Toyota diverge bottleneck. A general decreasing tendency can be identified with increase of the elapsed time of breakdown duration.

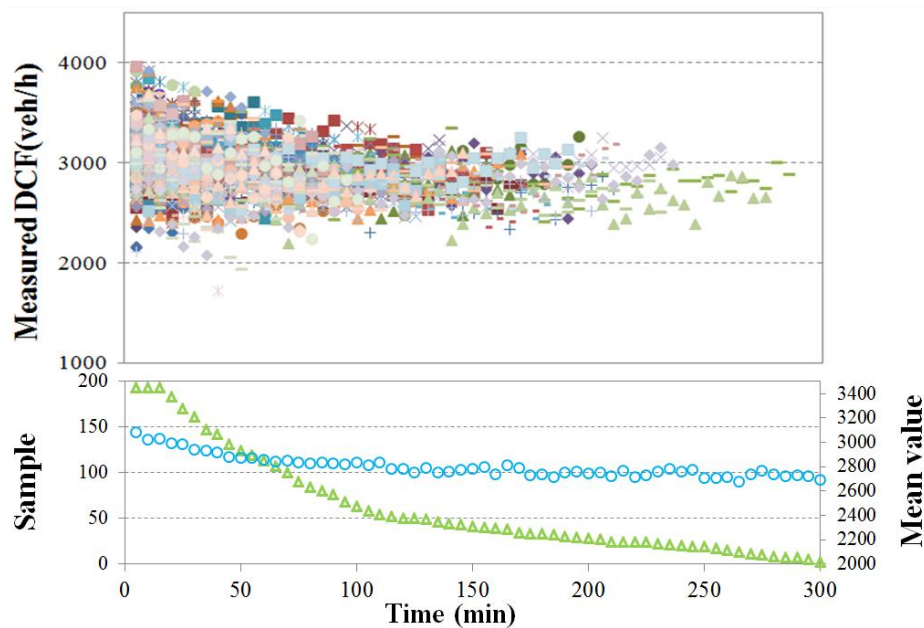


Figure 5.1 Empirical *DCF* distribution at Toyota diverge bottleneck

Figure 5.2 illustrates *DCF* distributions of several representative intervals at Toyota diverge bottleneck. At each interval t , Kolmogorov–Smirnov (*K-S*) test was conducted. *DCF* is found to follow Normal distribution according to *K-S* test values, e.g. 0.037 at the

first 5 minute. Normal distribution parameters at the time interval t are denoted as $\mu(t)$ and $\sigma(t)$ which stand for the mean value and standard deviation respectively.

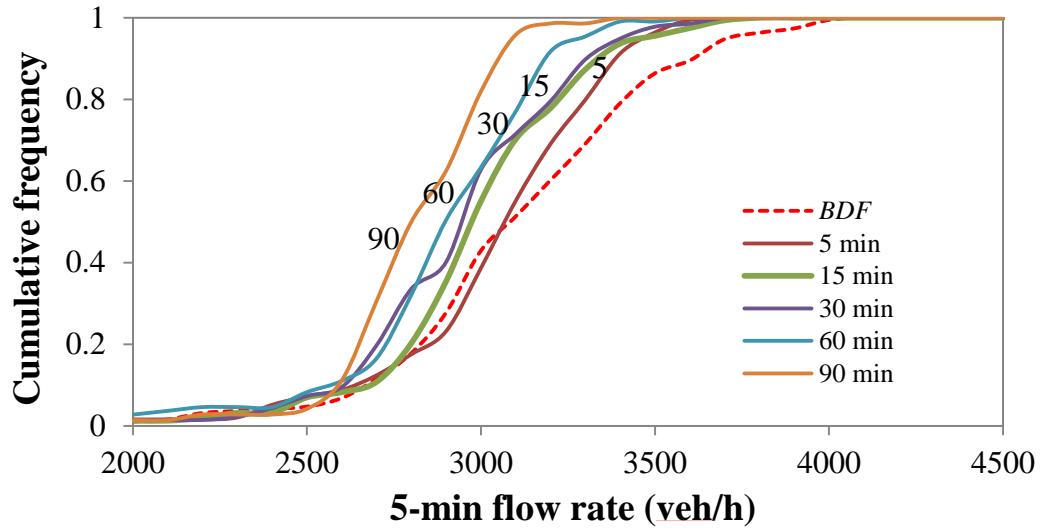


Figure 5.2 Empirical *BDF* and *DCF* distributions at Toyota diverge bottleneck

In Figure 5.2, *DCF* distributions are found of lower values by comparing to the shape of *BDF* distribution. Furthermore, a general decreasing tendency can be identified with the increase of breakdown duration. It suggests that when modeling *DCF*, the following impacts need to be carefully taken into consideration; 1) *BDF* value and 2) the elapsed time t of breakdown duration.

5.4.2 Procedure of modeling

The procedure of stochastic modeling on *DCF* is illustrated in Figure 5.3. At first, *BDF* values are classified into different groups. For each group, mean *BDF* value is adopted as the representative value corresponding to *DCF* distribution of this group. Secondly, impact of breakdown flow rate will be investigated. For each time interval, parameters (mean value and standard deviation) of *DCF* distribution is modeled as functions of breakdown flow rate. Then impact of the elapsed time of breakdown duration will be analyzed. The elapsed time of breakdown duration is further taken into consideration for *DCF* modeling. Finally, *DCF* model is derived based on the above investigations.

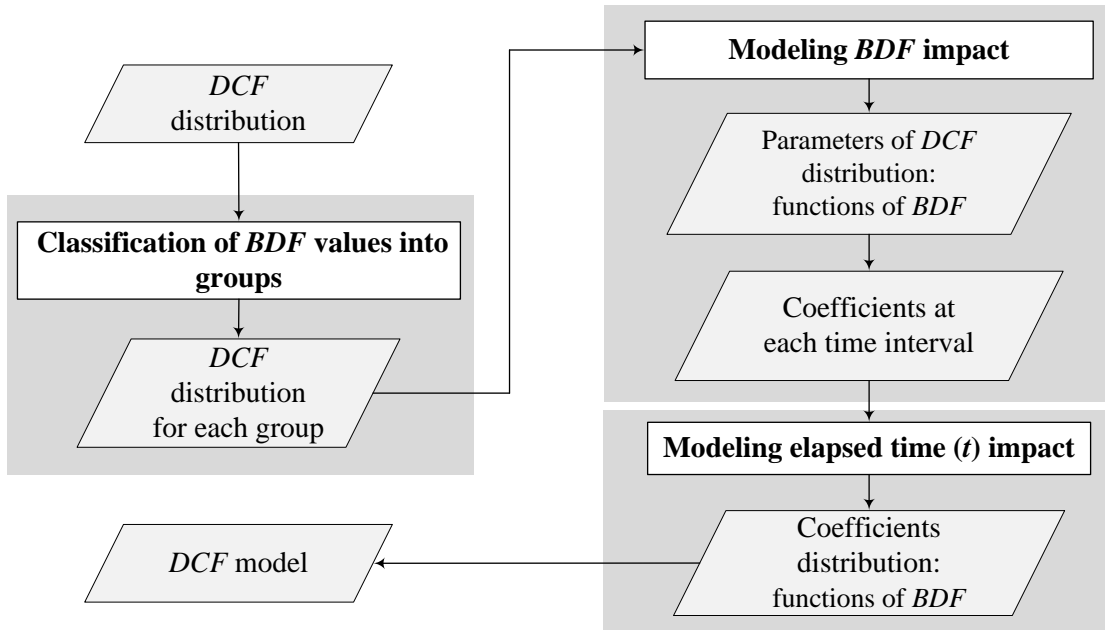


Figure 5.3 Flowchart of stochastic modeling on DCF

5.4.3 Impact of breakdown flow rate (BDF)

To investigate impact of *BDF* values, they are classified into different groups considering sample size at each bottleneck. At Toyota diverge bottleneck, every 10 *BDF* values are classified into a group as presented in Figure 5.4. For each group, mean *BDF* value is adopted as the representative value corresponding to *DCF* distribution of this group.

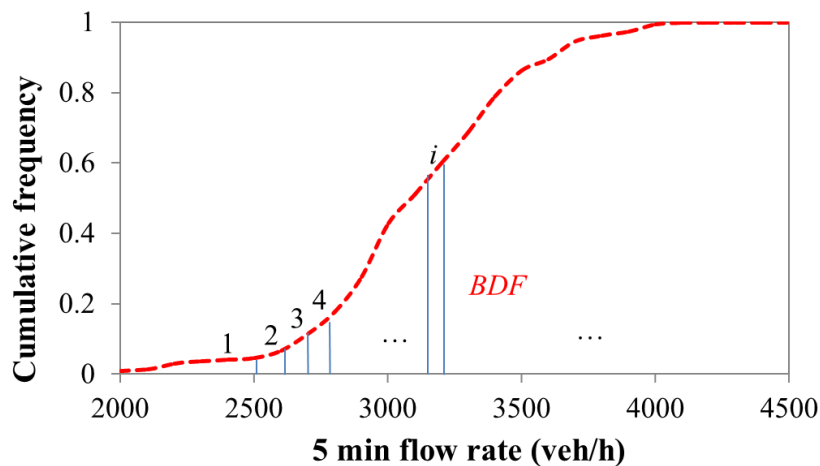
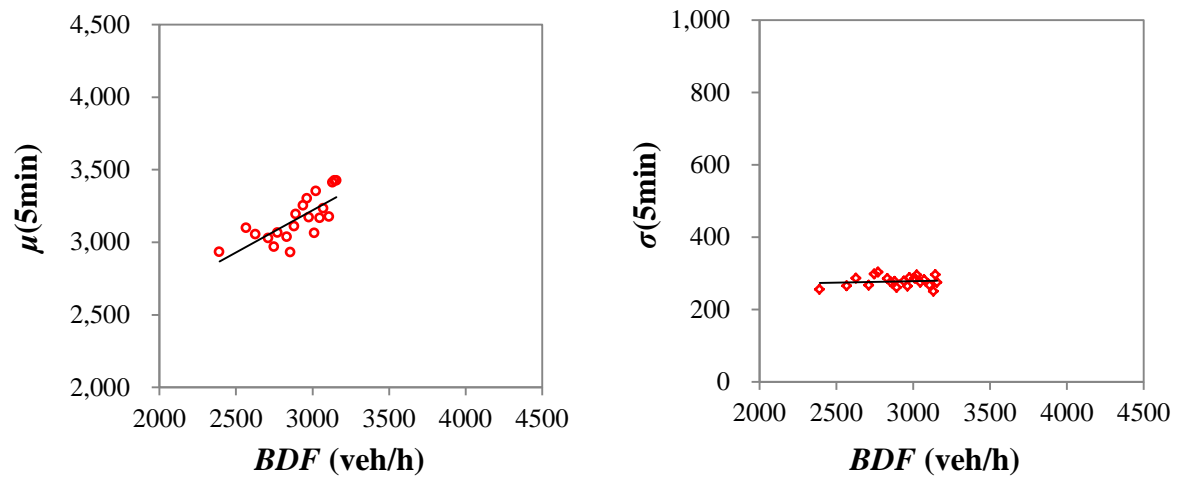


Figure 5.4 Classification of BDF distribution



(a) Mean values

(b) Standard deviations

Figure 5.5 Impact of *BDF* value on *DCF* distribution

Table 5.4 Regression result for the first 5 minute

<i>t</i> =5 minute	Mean values		Standard deviations	
	Coef.	<i>t</i> -value	Coef.	<i>t</i> -value
<i>BDF</i>	5.79×10^{-1}	5.09	8.81×10^{-3}	0.05
Constant	1.48×10^3	4.49	2.52×10^2	5.41
<i>R</i> square	0.577		0.015	

Figure 5.5 presents the relationship between discharge flow rate and breakdown flow rate for the first 5 minute of breakdown duration. A positive relationship can be identified between $\mu(5min)$ and *BDF* according to the *t*-test at a 95% confidence level in Table 5.4. With respect to $\sigma(5min)$, no significant impacts can be identified through *t*-test. Similar findings are also identified in each interval *t* which can be expressed in Equation (5.1-a) and (5.1-b).

$$\mu(t) = a_t \times BDF + b_t \quad (5.1-a)$$

$$\sigma(t) = c_t \quad (5.1-b)$$

where, a_t , b_t and c_t are the coefficients, *t* is the elapsed time of breakdown duration.

5.4.4 Impact of the elapsed time of breakdown duration (t)

The impact of t on DCF distribution is then analyzed in this section. As aforementioned, $\mu(t)$ and $\sigma(t)$ can be expressed as functions of BDF values as shown in Equations (5.1-1) and (5.1-2). Distribution of the estimated coefficients of $\mu(t)$ functions is illustrated in Figure 5.6.

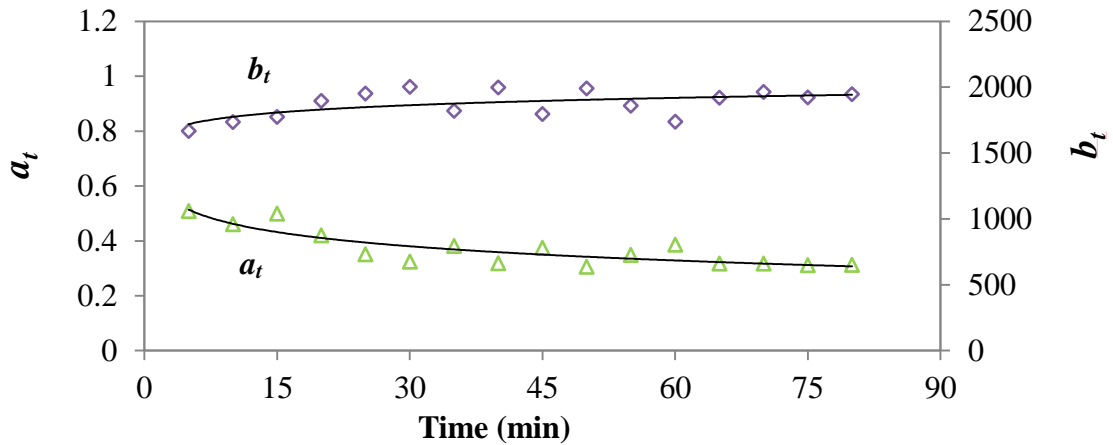


Figure 5.6 Impact of t on mean values of DCF distribution

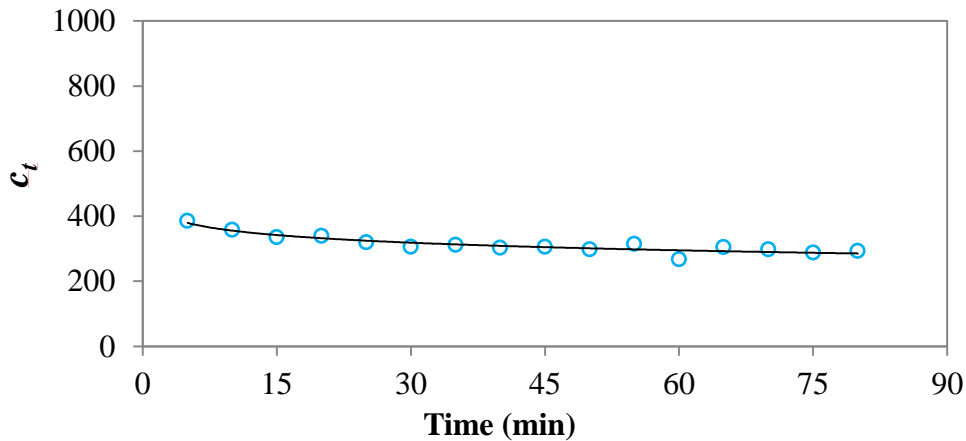


Figure 5.7 Impact of t on standard deviations of DCF distribution

For both a_t and b_t , the changing tendencies are steep in the beginning and then get stable with increase of t . Similar tendency can be found for c_t as shown in Figure 5.7. The characteristics of such tendencies suggest that a logarithmic function is probably applicable as expressed in Equations (5.2-a), (5.2-b) and (5.2-c).

$$a_t = a_1 \ln(t) + a_2 \quad (5.2-a)$$

$$b_t = b_1 \ln(t) + b_2 \quad (5.2-b)$$

$$c_t = c_1 \ln(t) + c_2 \quad (5.2-c)$$

where, a_1 , a_2 , b_1 , b_2 , c_1 and c_2 are coefficients for estimation.

5.4.5 Development of DCF model

DCF model can finally be developed by incorporating Equations (5.2-a), (5.2-b) and (5.2-c) into Equations (5.1-a) and (5.1-b) as shown in Equations (5.3-a) and (5.3-b). Its cumulative function is shown by Equation (5.4).

$$\mu(t) = (a_1 \ln(t) + a_2) \times BDF + b_1 \ln(t) + b_2 \quad (5.3-a)$$

$$\sigma(t) = c_1 \ln(t) + c_2 \quad (5.3-b)$$

$$F(DCF(t)) = \frac{1}{\sqrt{2\pi}\sigma(t)} \int_0^{DCF} e^{-\frac{(x-\mu(t))^2}{2\sigma^2(t)}} dx \quad (5.4)$$

Finally, discharge flow rate (DCF) can modeled in a stochastic way by considering its relationship to breakdown flow rate (BDF) and the elapsed time of breakdown duration (t). The estimated results at each bottleneck are listed in Tables 5.5 to 5.6.

Table 5.5 The estimated parameters for DCF models at diverge bottlenecks

Name	Geometry	a_1	a_2	b_1	b_2	c_1	c_2
Toyota diverge bottleneck	$L_d=550\text{m}$	-0.82×10^{-2}	5.20×10^{-1}	2.27×10^2	1.34×10^3	-2.31×10	4.34×10^2
Toki diverge bottleneck	$L_d=300\text{m}$	-1.61×10^{-1}	4.11×10^{-1}	3.35×10^2	1.16×10^3	-6.67×10	5.40×10^2
Komaki diverge bottleneck	$L_d=250\text{m}$	-1.38×10^{-1}	4.83×10^{-1}	2.40×10^2	9.58×10^2	-7.63×10	7.54×10^2

Note: considering limited sample size, stochastic DCF model for semi-congestion state at Toyota diverge section has not been estimated. L_d : deceleration lane length.

Table 5.6 The estimated parameters for *DCF* models at merge bottlenecks

Name	Geometry	a_1	a_2	b_1	b_2	c_1	c_2
Toyota merge bottleneck	$L_a=500\text{m}$	-2.23×10^{-2}	1.40	5.37×10^2	3.95×10^2	-2.69×10	3.52×10^2
Toki merge bottleneck	$L_a=400\text{m}$	-1.14×10^{-1}	6.70×10^{-1}	2.26×10^2	1.34×10^3	-1.87×10	4.26×10^2
Komaki merge bottleneck	$L_a=325\text{m}$	-1.68×10^{-1}	8.83×10^{-1}	4.29×10^2	6.67×10^2	-1.27×10	3.92×10^2

Note: L_a : acceleration lane length.

Table 5.7 The estimated parameters for *DCF* models at sag bottlenecks

Name	Geometry (I_d, I_u)	a_1	a_2	b_1	b_2	c_1	c_2
Tomei (w) 294.43	(-0.29, 2)	-7.41×10^{-2}	4.93×10^{-1}	9.29×10	2.14×10^3	-3.37×10	4.10×10^2
Tomei (w) 312.04	(-1.5, 0.5)	-2.08×10^{-1}	1.44	3.99×10^2	-3.61×10^2	-3.04×10	4.86×10^2
Tomei (w) 298.43	(-1.5, 0.75)	-1.34×10^{-1}	1.35	2.24×10^2	-7.45	-1.29×10	3.70×10^2
Tomei (w) 296.43	(-1.5, 0.5)	-9.01×10^{-2}	8.39×10^{-1}	6.66×10	1.33×10^3	-3.34×10	4.94×10^2
Tomei (w) 314.2	(-1, 0.97)	-1.14×10^{-1}	6.70×10^{-1}	2.26×10^2	1.34×10^3	-2.35×10	4.26×10^2
Higashi-Meihan (e) 61.5	(-1.26, 0.29)	-8.60×10^{-2}	5.74×10^{-1}	1.06×10^2	1.73×10^3	-4.75	3.06×10^2
Higashi-Meihan (e) 67.17	(-1.64, 2.69)	-1.31×10^{-1}	8.51×10^{-1}	2.34×10^2	1.09×10^3	-2.99×10	4.98×10^2
Higashi-Meihan (e) 58.54	(-0.29, 1.26)	-1.32×10^{-1}	8.34×10^{-1}	2.91×10^2	1.07×10^2	-6.15	3.57×10^2

Note: (e):eastbound, (w):westbound, I_d : negative gradient, I_u : positive gradient

5.4.6 Validation of discharge flow rate (*DCF*) model

The validation of the developed *DCF* model is conducted by following the flowchart shown in Figure 5.8. *DCF* distribution can be generated in a stochastic way through Monte Carlo method based on *BDF* distribution. At Toyota diverge bottleneck, it is found that *DCF* model can well reproduce *DCF* distribution according to Mean Absolute Percentage Error (*MAPE*) value, e.g. 4.13% at the first 5 minute as shown in Figure 5.9.

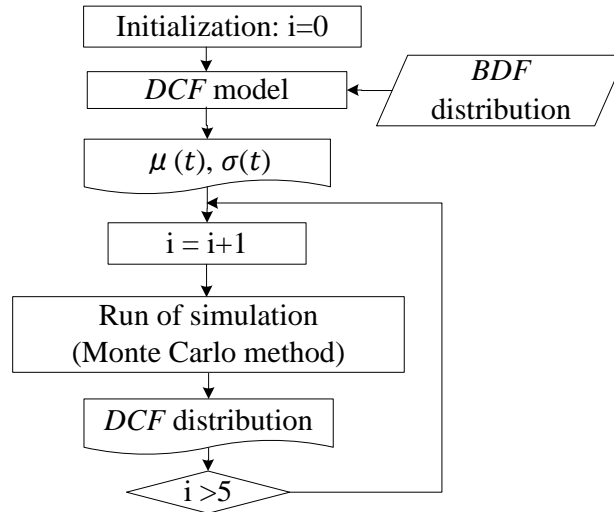


Figure 5.8 Flowchart of *DCF* model validation

The validation procedures have also been conducted at other bottleneck locations. It is found that the developed *DCF* models can generate discharge flow rate in a stochastic way at the acceptable levels.

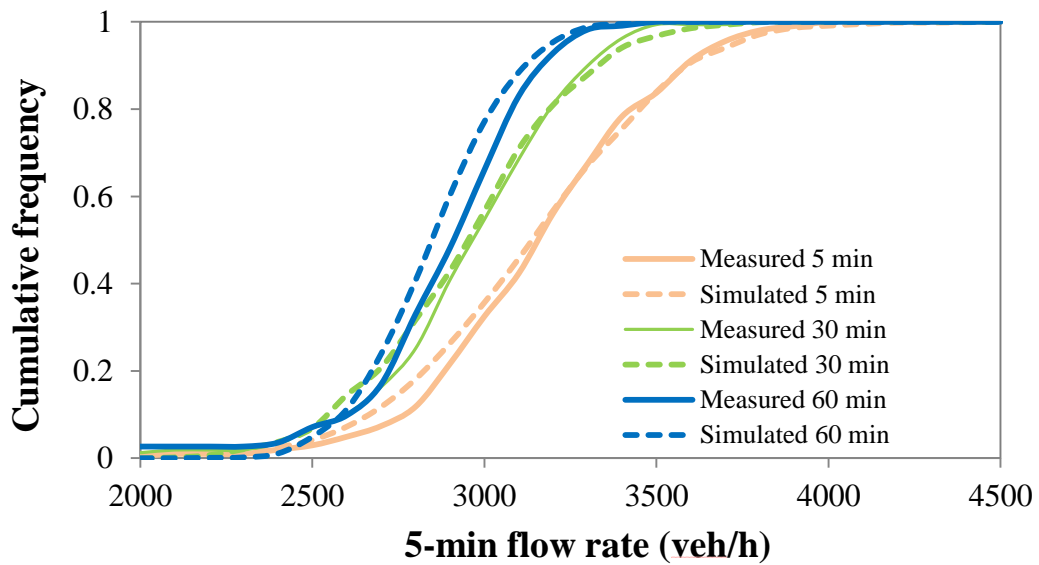


Figure 5.9 Validation of *DCF* model at Toyota diverge bottleneck

5.5 Generalizing *DCF* model

This section will introduce the generalization of *DCF* models by considering site-specific geometric characteristics with respect to each type of intercity expressway facility.

As afore discussed, the developed *DCF* models are listed in Tables 5.5 to 5.7 for diverge, merge and sag bottlenecks respectively. With respect to each bottleneck type, the estimated coefficients of *DCF* models are found to vary at different locations. Possibly, there are the underlying relationship between the *DCF* model coefficients and site-specific geometric configurations. Revealing such a relationship can serve as the basis for generalizing *DCF* models. The general *DCF* model could be used to assess *DCF* distributions at the potential bottleneck locations in intercity expressway network of central Japan.

5.5.1 Diverge bottlenecks

The estimated coefficients of the developed *DCF* models for diverge bottlenecks are listed in Table 5.5. The difference in the site-specific models can be attributed to various geometric characteristics at each site. With respect to geometric configurations at diverge bottleneck, deceleration lane length can be regarded as the dominant influencing factor. This can be attributed to the fact that for breakdown duration, the diverge behaviors of diverge traffic flow are strongly dependent on setting of deceleration lane. The gaps which can be supplied to diverge traffic flow are closely related to length of deceleration lane. Consequently, discharge flow rate are impacted by this length.

Among three diverge bottleneck locations, L_d at Toyota diverge bottleneck (550m) is greater than those at Toki (300m) and Komaki diverge bottlenecks (250m). This is attributed to the consideration on the heavy traffic demand imposed at Toyota junction when designing.

Statistic analysis on *DCF* model coefficients and L_d are presented in Figures 5.10 to 5.12. As aforementioned, a_1 , a_2 , b_1 , and b_2 determine the formation of mean value of *DCF* distribution. a_1 and b_2 are found to be sensitive to L_d value according to their t -values. While for a_2 and b_1 , they can be regarded as constant values according to their t -values. As for c_1 and c_2 , they impact on standard deviation of *DCF* distribution. They are found to be significantly impacted by L_d value.

At diverge bottlenecks, a general *DCF* model is further developed by considering the impact of deceleration lane length as expressed in Equations (5.5-a) to (5.5-f).

$$a_1 = \underset{t=3.59}{2.28 \times 10^{-4}} L_d - \underset{t=13.6}{2.10 \times 10^{-1}} \quad (5.5-a)$$

$$a_2 = 4.71 \times 10^{-1} \quad (5.5-b)$$

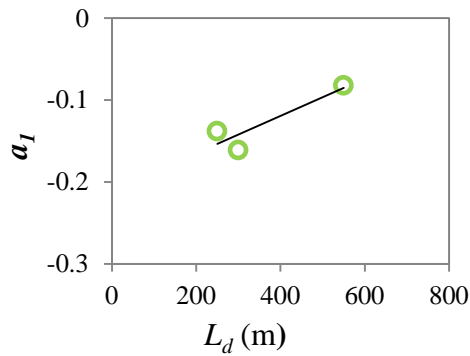
$$b_1 = 2.67 \times 10^2 \quad (5.5-c)$$

$$b_2 = \underset{t=5.13}{1.11} L_d + \underset{t=5.87}{7.48 \times 10^3} \quad (5.5-d)$$

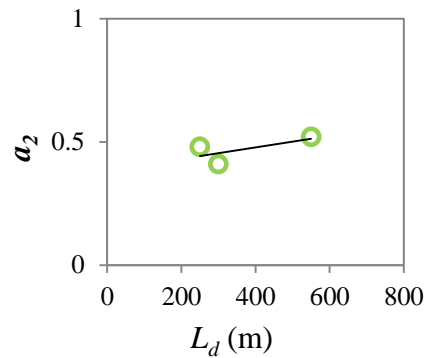
$$c_1 = \underset{t=15.3}{-1.78 \times 10^{-1}} L_d - \underset{t=2.68}{1.20 \times 10^{-2}} \quad (5.5-e)$$

$$c_2 = \underset{t=2.61}{-8.59 \times 10^{-1}} L_d + \underset{t=4.51}{8.91 \times 10^2} \quad (5.5-f)$$

According to the equations, it can be found that longer deceleration lane tends to result in greater *DCF* values as a_1 , a_2 , b_1 and b_2 influence on the coefficients of $\mu(t)$. This tendency can represent the fact that more gaps among the mainline flow due to longer L_d result in less impact from diverge flow on mainline traffic.

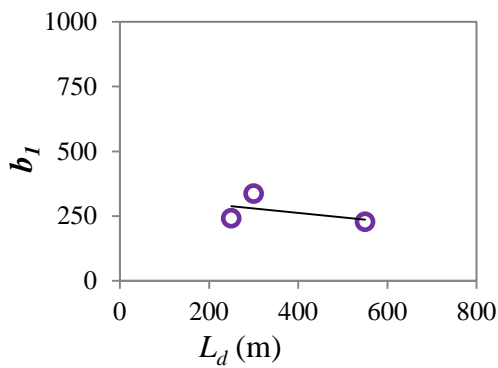


(a) Impact on a_1

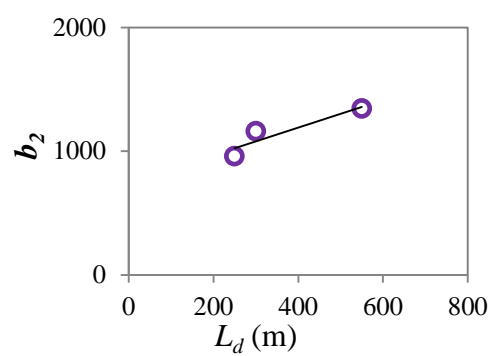


(b) Impact on a_2

Figure 5.10 Impact of deceleration lane length on a_1 and a_2

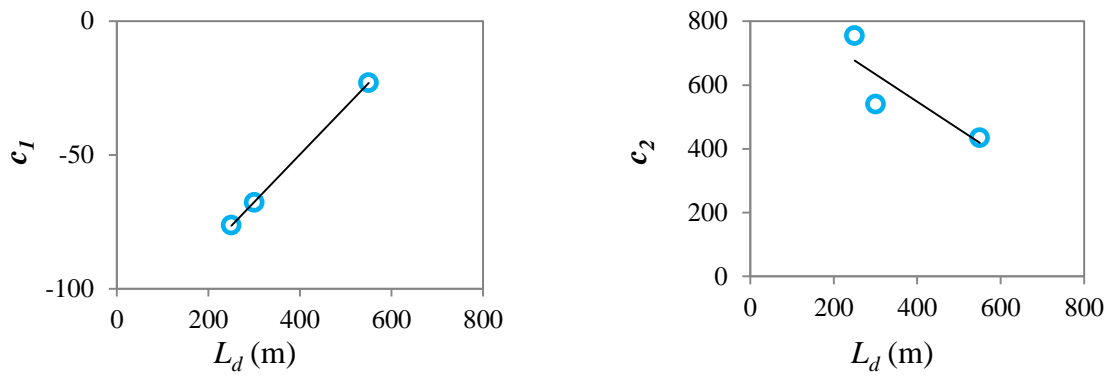


(a) Impact on b_1



(b) Impact on b_2

Figure 5.11 Impact of deceleration lane length on b_1 and b_2



(a) Impact on c_1 (b) Impact on c_2
Figure 5.12 Impact of deceleration lane length on c_1 and c_2

Despite limited sample sizes for diverge bottlenecks, the significant impact of L_d on discharge flow rate models can be revealed.

5.5.2 Merge bottlenecks

With respect to merge bottlenecks, the estimated coefficients of the developed *DCF* models are listed in Table 5.6. The difference in the site-specific models can be attributed to various geometric characteristics at each site. With respect to geometric configurations at merge bottleneck, acceleration lane length can be regarded as the dominant influencing factor. This can be attributed to the fact that for breakdown duration, the merge behaviors of merge traffic flow onto mainline are strongly dependent on setting of acceleration lane. The gaps which can be supplied to merge traffic flow are related to length of acceleration lane. Consequently, discharge flow rate values are related to this length.

Among three merge bottleneck locations, L_a at Toyota merge bottleneck (500m) is greater than those at Toki (400m) and Komaki diverge bottlenecks (325m). This is attributed to the consideration on the heavy traffic demand imposed at Toyota Junction when designing.

As aforementioned, a_1 , a_2 , b_1 , and b_2 determine the formation of mean value of *DCF* distribution. a_1 and b_2 are found to be sensitive to L_d value according to their t -values. While for a_2 and b_1 , they can be regarded as constant values according to their t -values. As for c_1 and c_2 , they impact on standard deviation of *DCF* distribution. They are found to be significantly impacted by L_d value.

At merge bottlenecks, a general *DCF* model is also further developed by considering the impact of acceleration lane length as expressed in Equations (5.6-a) to (5.6-f).

$$a_1 = 1.90 \times 10^{-4} L_a - 7.81 \times 10^{-2} \quad (5.6-a)$$

$$a_2 = 1.49 \times 10^{-3} L_a + 2.67 \times 10^{-1} \quad (5.6-b)$$

$$b_1 = 4.58 \times 10^{-1} L_a + 1.76 \times 10^2 \quad (5.6-c)$$

$$b_2 = -3.27 L_a + 2.12 \times 10^3 \quad (5.6-d)$$

$$c_1 = -2.92 \times 10^{-2} L_a + 5.30 \quad (5.6-e)$$

$$c_2 = -1.29 \times 10^{-1} L_a + 4.52 \times 10^2 \quad (5.6-f)$$

According to the equations, it can be found that longer acceleration lane length tends to result in lower *DCF* values as a_1 , a_2 , b_1 and b_2 influence on the coefficients of $\mu(t)$. This tendency can represent the fact that more gaps among the mainline flow due to longer L_a result in more impact from merge flow on mainline traffic.

Despite limited sample sizes for merge bottlenecks, the significant impact of L_a on discharge flow rate models can be revealed.

5.5.3 Sag bottlenecks

With respect to sag bottlenecks, the estimated coefficients of the developed *DCF* models are listed in Table 5.7. The difference in the site-specific models can be attributed to various geometric characteristics at each site. With respect to geometric configurations at sag bottleneck, the consequent vertical downhill and uphill slopes can be regarded as the dominant influencing factor. This can be attributed to the fact that for breakdown duration, the acceptable headways for traffic flow on mainline are strongly dependent on setting of vertical slope values. Consequently, discharge flow rate values are related to this length.

Among sag bottleneck locations, setting of consequent vertical downhill and uphill slopes are originally impacted by terrains along the expressways. The high values of slopes for sag bottlenecks on Higashi-Meihan expressway are attributed to steep terrains along it.

As aforementioned, a_1 , a_2 , b_1 , and b_2 determine the formation of mean value of *DCF* distribution. a_1 and b_2 are found to sensitive to slope values according to their t -values. While for a_2 and b_1 , they can be regarded as constant values according to their t -values. As

for c_1 and c_2 , they impact on standard deviation of *DCF* distribution. They are found to be significantly impacted by slope value.

At merge bottlenecks, a general *DCF* model is further developed by considering the impact of slope values as expressed in Equations (5.7-a) to (5.7-f).

$$a_1 = -6.27 \times 10^{-2} I_u - 6.70 \times 10^{-2} \quad (5.7-a)$$

$t=4.07$ $t=-1.38$

$$a_2 = 2.96 \times 10^{-1} L_u + 6.67 \times 10^{-1} \quad (5.7-b)$$

$t=3.27$ $t=0.785$

$$b_1 = 1.79 \times 10^2 I_d + 3.93 \times 10^2 \quad (5.7-c)$$

$t=2.28$ $t=1.91$

$$b_2 = -7.92 \times 10^2 I_u + 1.61 \times 10^3 \quad (5.7-d)$$

$t=-2.69$ $t=2.35$

$$c_1 = 3.43 \times 10 I_d - 3.60 \times 10 I_u + 4.94 \times 10 \quad (5.7-e)$$

$t=-2.75$ $t=2.19$

$$c_2 = -1.86 \times 10^2 I_d + 2.15 \times 10^2 I_u + 9.97 \quad (5.7-f)$$

$t=-2.75$ $t=2.19$

Through the general model at sag bottleneck, the significant impact of the consequent vertical downhill and uphill slopes on discharge flow rate models can be revealed.

5.6 Summary

Discharge flow rate is another important aspect of bottleneck capacity. During the period of breakdown duration, it plays a significant role in evaluating measures of effectiveness for intercity expressway performance like travel time reliability, queue length and etc.

This chapter has developed a methodology for stochastic modeling on discharge flow rate (*DCF*) by considering its relationship to breakdown flow rate (*BDF*) and the elapsed time of breakdown duration. This methodology has been applied to diverge, merge and sag bottlenecks on intercity expressways of central Japan.

Firstly, statistical analysis of discharge flow rate distributions at each time interval indicates: 1) a positive relationship between breakdown and discharge flow rate distributions, and 2) a descending tendency associated with the increase of the elapsed time of breakdown duration.

Secondly, Normal distribution is adopted to describe and quantify stochastic nature of discharge flow rates. Its parameters (mean value and standard deviation) are then modeled as functions of breakdown flow rate and the elapsed time of breakdown duration. The established discharge flow rate models have been validated through Monte Carlo method.

Finally, with respect to each facility type, the general discharge flow rate model is developed by considering impacts of site-specific geometric characteristics. At diverge and merge bottlenecks, lengths of deceleration and acceleration lane are taken into account. As for sag bottleneck, negative downhill and positive uphill slopes are considered. Such general discharge flow rate models enable the estimation at potential bottlenecks in intercity expressway network.

To sum it up, this chapter has developed a methodology for stochastic modeling on discharge flow rate (*DCF*) by considering its relationship to breakdown flow rate (*BDF*) and the elapsed time of breakdown duration.

With respect to practical application in simulation, the developed stochastic *DCF* models enable the performance evaluation for breakdown duration in a stochastic way. Advantages of the developed models are highlighted as follows which improve evaluation accuracy. The relationship between breakdown and discharge flow rates is taken into account. Furthermore, a descending tendency of discharge flow rate is modeled with increase of elapsed time of breakdown duration.

Chapter 6

SIMULATION OF BREAKDOWN PHENOMENA BY APPLYING THE DEVELOPED MODELS

6.1 Introduction

This chapter introduces the simulation of breakdown phenomena by applying the developed breakdown probability and discharge flow rate models.

As aforementioned, breakdown flow rate and discharge flow rate represent two distinct aspects of bottleneck capacity which are significant indicators to represent breakdown phenomena. By applying the developed models, breakdown phenomena can be simulated. Such a simulation tool would help to plan countermeasures to alleviate breakdown occurrence like traffic demand management, lane usage recommendation.

Performance of intercity expressways is significantly affected by breakdown phenomena at bottleneck locations in the network. Strategies such as traffic demand management or lane usage recommendation might mitigate breakdown phenomena and improve overall traffic operations on critical expressway segments. Efficiency of such congestion relief schemes is generally evaluated based on the empirical comparison between performances before and after scheme application. However, for expressway authority, it is very significant to evaluate the impact of congestion relief schemes on intercity expressway performance before implementing them in real conditions.

Therefore, a simulation tool is required to reproduce breakdown phenomena. In the previous chapters, breakdown flow rate and discharge flow rate have already been modeled

which are significant indicators to represent expressway breakdown phenomena. By applying the developed models, breakdown phenomena can be simulated which can serve as the basis to evaluate the aforementioned relief schemes. This kind of reproduction can be realized by incorporating the developed stochastic models. Based on the arriving traffic demand, the breakdown occurrence can be generated in a stochastic way by using the developed breakdown probability model. As for breakdown duration, it can be estimated through discharge flow rate model.

In this chapter, the developed stochastic breakdown probability and discharge flow rate models will be applied to simulate the breakdown phenomena at the bottleneck locations.

6.2 Simulation of breakdown phenomena at the bottlenecks

This section introduces the methodology for simulation of breakdown phenomena by incorporating the developed stochastic models. Simulation is carried out by following the framework as illustrated in Figure 6.1.

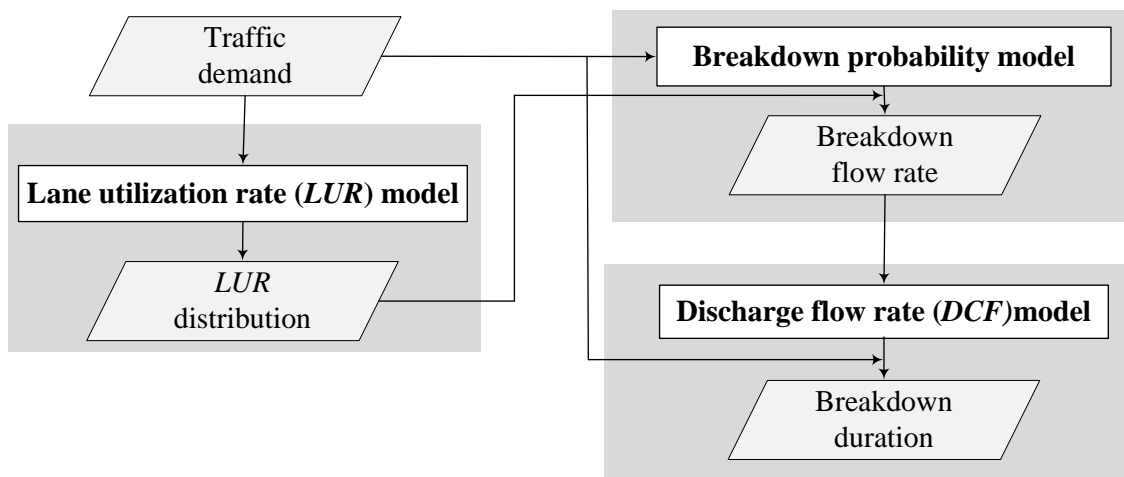


Figure 6.1 Simulation framework

Firstly, traffic demand is set for simulation which is the basic input of the whole simulation procedure. Lane utilization rate is computed by using the *LUR* model as described in Chapter 2.

Secondly, breakdown occurrence is generated in a stochastic way by applying breakdown probability model. With respect to diverge and merge bottlenecks, impacts from lane usage preference are considered. Also from the simulated results of breakdown occurrence, the

breakdown flow rate distribution can be reproduced which is necessary input of discharge flow rate model.

Finally, breakdown duration is determined by using the stochastic discharge flow rate model. After the judged timing of breakdown occurrence, the developed *DCF* model can generate *DCF* distribution for each interval. Then a comparison is conducted between the cumulative discharge flow rate and arriving traffic demand from upstream. The interval will be determined as breakdown end when cumulative traffic flow can be dissipated.

6.3 Simulation at diverge bottleneck

This section introduces the simulation of breakdown phenomena at diverge bottleneck by following the procedure as described above.

6.3.1 Bottleneck location for simulation

Toyota diverge bottleneck is considered as a test bed for the simulation of breakdown phenomena.

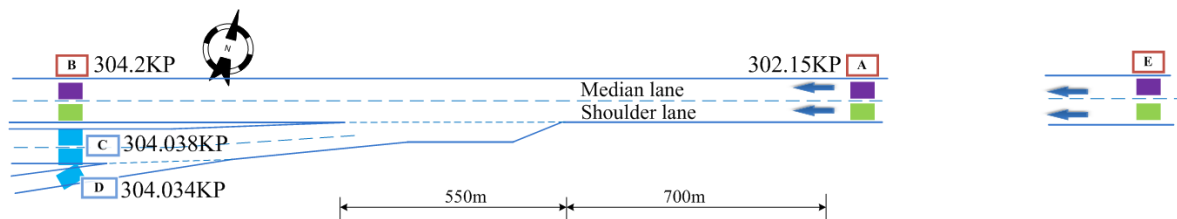


Figure 6.2 Test bed location and position of detectors in vicinity of Toyota diverge bottleneck

As shown in Figure 6.2, its mainline has two lanes, namely shoulder lane and median lane (at this diverge section, its mainline has been broadened to three lanes by fully utilizing shoulder from 10/21/2011). At this section, frequent breakdown events have been observed due to high diverge traffic flow which aims at using Shin-Meishin Expressway due to its better driving perception and shorter distance after its operation in March, 2008. Westbound directional AADT (Average Annual Daily Traffic Volume) of the test bed stays about 48,200 (veh/day) in 2009, resulting in extended congested hours. AADT of diverge flow reach about 28,200 (veh/day) which is approximately 45% of mainline flow of westbound direction. This high diverge flow level is regarded as the main cause of

breakdown occurrence at this diverge section. Simulation covers the period from 3/1/2008 to 12/31/2009.

There are double loop detectors installed on this segment (almost every 2 km) whose schematic locations are presented in Figure 6.2. These detectors report spot speeds and traffic counts every 5 minutes on each lane. Detector data were available from 3/1/2008 to 12/31/2009.

6.3.2 Input of simulation procedure

This section introduces the input of traffic demand for the simulation procedure. The traffic data at the adjacent upstream detector location (299.5 KP) is used. As the traffic flow rate at the congested conditions cannot represent traffic demand, the traffic flow rate is analyzed by referring to detector location (302.15 KP). With respect to the duration of a breakdown event, if queue propagates to the location at 299.5 KP, its upstream detector locations are checked to find the location which is not impacted by queue propagation. Then the flow rate at this detector location is regarded as traffic demand input for this breakdown duration. The traffic demand data during the period from 3/1/2008 to 12/31/2009 will be used for simulation.

6.3.2.1 Traffic demand

The traffic demand data are extracted as described above. Figure 6.3 presents traffic demand distribution of cross-section for one week from 3/3/2008 to 3/9/2008.

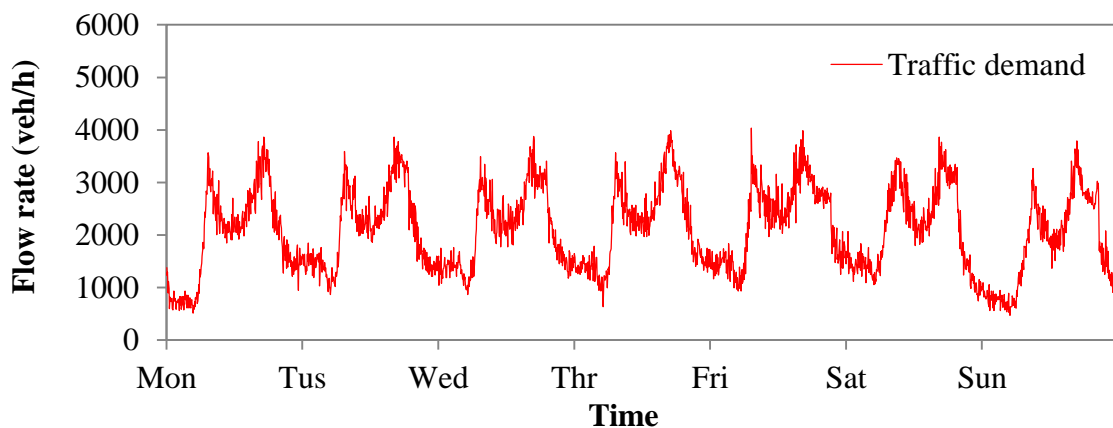


Figure 6.3 Traffic demand distribution at Toyota diverge bottleneck

During this week, there are five working days from Monday to Friday without national holidays which can be regarded as weekdays/non-holidays. Saturday and Sunday are treated as weekends/holidays. The peak traffic flow can be found for both morning and evening peak hours on each day of this week. Traffic demands on Saturday and Sunday are relatively lower than those from Monday to Friday especially for morning periods.

Heavy vehicle are also the significant input for simulation. Toyota diverge bottleneck is located on Tomei Expressway which is the corridor expressway characterized of high demand of heavy vehicles as described before. Heavy vehicles significantly influence on lane utilization rate as discussed in *LUR* model which will play a significant role in breakdown probability model.

Figure 6.4 illustrates heavy vehicle flow rate for the same period with the traffic demand in Figure 6.3 from 3/3/2008 to 3/9/2008. By comparing to Figure 6.3, peak hours of heavy vehicle demand do not bring into correspondence with those of the whole traffic demand. In addition, heavy vehicle demands on Saturday and Sunday are significantly lower than those from Monday to Friday. The heavy vehicle demand will also be used for the simulation.

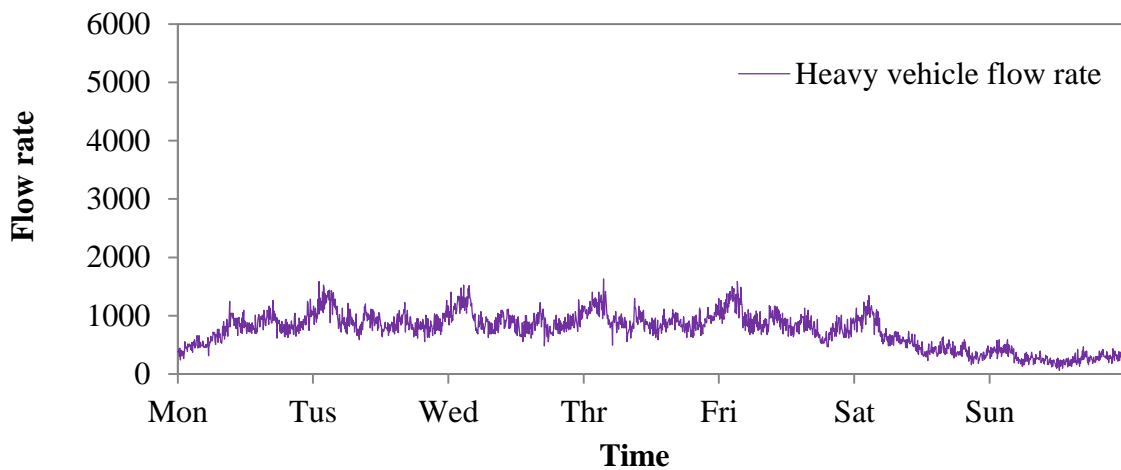


Figure 6.4 Heavy vehicle distribution at Toyota diverge bottleneck

6.3.2.2 Lane utilization rate

As discussed before, *LUR* is a significant influencing factor on breakdown occurrence as expressed in Equation (2.1) in chapter 2. On multilane expressways, especially nearby

diverge and merge sections, lane usage preference by drivers differs toward each lane due to the influence of diverge and merge traffic flow.

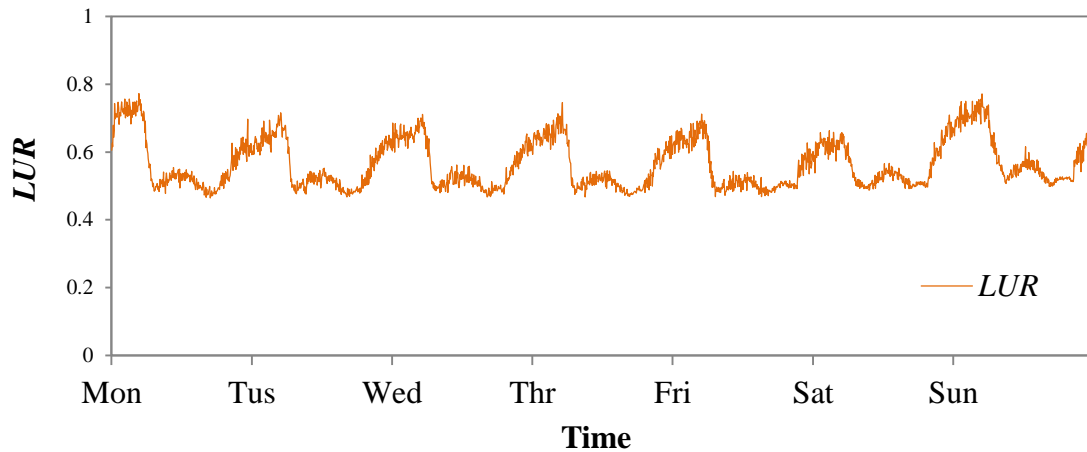


Figure 6.5 The simulated *LUR* on shoulder lane at Toyota diverge bottleneck

Lane utilization rate (*LUR*) is adopted to describe such a lane preference, which is defined as the proportion of traffic flow on individual lanes out of the cross-section flow. As expressed in Equations (2.2-1) to (2.2-4), *LUR* at bottleneck location (302.15 KP) can be expressed as a function of traffic demand of cross-section, heavy vehicle percentage, distance to diverge section and etc. When approaching diverge section, *LUR* on shoulder lane increases while traffic demand and heavy vehicle demand can be regarded to keep constant (without impacts of off-ramps and on-ramps).

Figure 6.5 demonstrates the simulated *LUR* on shoulder lane during one week at Toyota diverge bottleneck. This estimated *LUR* distribution on shoulder lane is based on the input of traffic demand and heavy vehicle demand and etc. It can be found that *LUR* on shoulder lane reaches about 0.5 for both morning and evening peak hours on each day of this week. This indicates that high proportion of traffic demand is allocated on shoulder lane which is likely to be the significant contribution to breakdown occurrence there. In addition, quite high *LUR* on shoulder lane are estimated during midnight which is attributed to very high heavy vehicle percentage during that period. The estimated *LUR* distribution will serve as basis of breakdown probability model as illustrated in simulation framework in Figure 6.1.

6.3.2.3 Diverge rate

High diverge traffic flow is regarded as a significant influencing factor for breakdown occurrence at diverge bottleneck. Diverge rate (DR) is used to evaluate impacts of diverge traffic flow which represents the proportion of diverge traffic flow from mainline flow. The measured DR value is used for simulation as expressed by Equation (6.1).

$$DR = \frac{FR_C + FR_D}{FR_B + FR_C + FR_D} \quad (6.1)$$

where, FR_B , FR_C and FR_D are measured flow rates on all lanes (veh/h) at detectors with labels of B , C and D in the vicinity of Toyota diverge bottleneck.

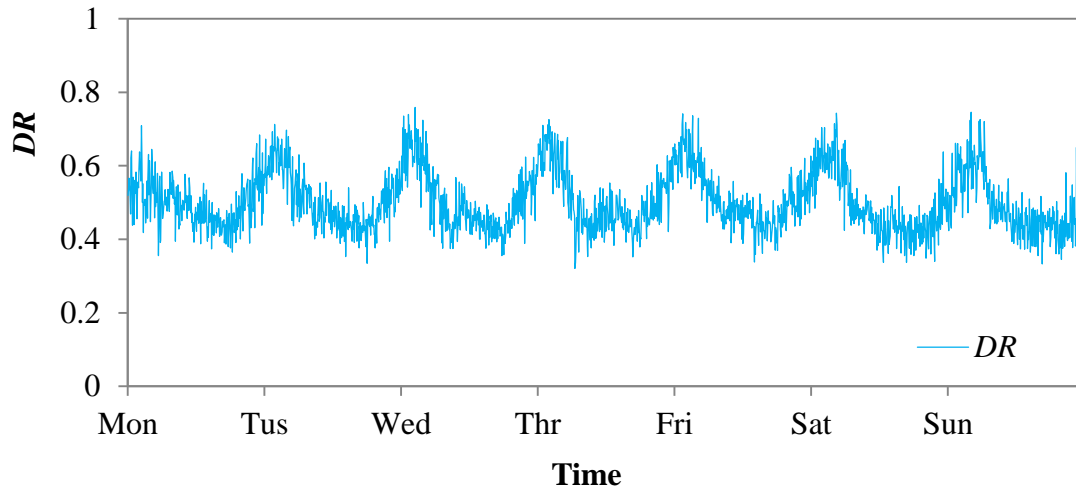


Figure 6.6 The measured DR at Toyota diverge bottleneck

Figure 6.6 illustrates the measured DR at Toyota diverge bottleneck during one week from 3/3/2008 to 3/9/2008. It can be found that DR values are approximately over 0.45 during both morning and evening peak hours on each day of this week. This indicates that high proportion of traffic demand diverge onto off-ramp which are likely to impose significant impact on mainline traffic flow. In addition, quite high DR values are observed during midnight which is attributed to very high heavy vehicle percentage during that period. The measured DR distribution will also serve as the basis of breakdown probability model as illustrated in simulation framework in Figure 6.1.

6.3.3 Breakdown occurrence

The section will introduce the estimation of breakdown occurrence by using the developed breakdown probability model based on the arriving traffic demand.

6.3.3.1 Stochastic model

As described in previous chapters, breakdown probability model is adopted to quantify stochastic natures of breakdown occurrence and distribution of *BDF* values. Breakdown probability model are established by using Weibull distribution as expressed in Equation (6.2).

$$P(FR) = 1 - e^{-\left(\frac{FR}{\beta}\right)^\alpha} \quad (6.2)$$

Where *FR* is the traffic flow rate (veh/h), α and β are shape and scale parameters respectively.

Through the inverse of Weibull distribution of breakdown probability model, capacity (*BDF*) can be described as random value as expressed in Equation (6.3). Breakdown occurrence can be determined when capacity is lower than the arriving traffic demand. In this way, breakdown occurrence can be generated in a stochastic way.

As for shape and scale parameters (α and β), they are not constant values. Actually, they are influenced by traffic flow characteristics as expressed by Equations (6.4-a) and (6.4-b).

$$c = \beta(-\ln(\mu))^{\frac{1}{\alpha}} \quad (6.3)$$

$$\alpha = 3.42 \times 10 \underset{t=4.14}{DR} - 2.18 \underset{t=-0.503}{} \quad (6.4-a)$$

$$\beta = -2.15 \times 10^3 \underset{t=-2.64}{DR} + 9.46 \times 10^3 \underset{t=8.44}{LUR} + 8.73 \times 10^2 \underset{t=0.771}{} \quad (6.4-b)$$

where, *DR* is diverge rate, and *LUR* is lane utilization rate on median lane.

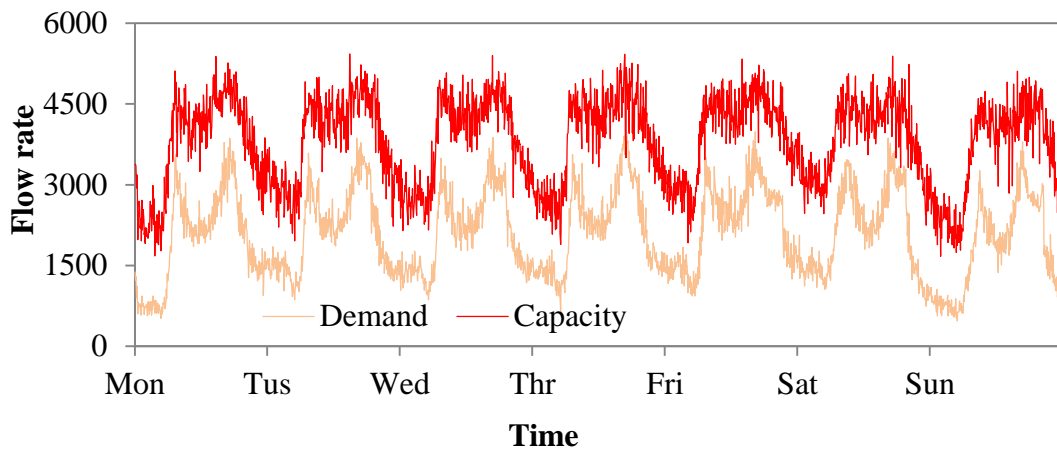


Figure 6.7 Capacity and demand distributions at Toyota diverge bottleneck

Table 6.1 Number of breakdown occurrences

Measured	Simulated	
	Mean of 20 runs	Standard deviation of 20 runs
194	180	13

Figure 6.7 demonstrates the estimated capacity (*BDF*) during one week from 3/3/2008 to 3/9/2008. This stochastic distribution is generated by using Monte Carlo method based on Equations (6.3), (6.4-1) and (6.4-2). Also the arriving traffic demand is illustrated in Figure 6.7. Breakdown occurrence is dependent on the comparison between this capacity distribution and traffic demand distribution. Breakdown occurrence can be judged when capacity is lower than the arriving demand. In this way, breakdown occurrence can be generated in a stochastic way.

6.3.3.2 The simulated number of breakdown occurrence

Number of breakdown occurrence during the period from 3/1/2008 to 12/31/2009 is computed by counting the simulated breakdown occurrences. 20 runs of simulation are performed through Monte Carlo method. With respect to the simulated number of breakdown occurrence, the mean value is calculated as 180 by aggregating results of 20 simulation runs as listed in Table 6.1. Standard deviation is computed as 13. These results are found to well reproduce the measured number of breakdown occurrence (194).

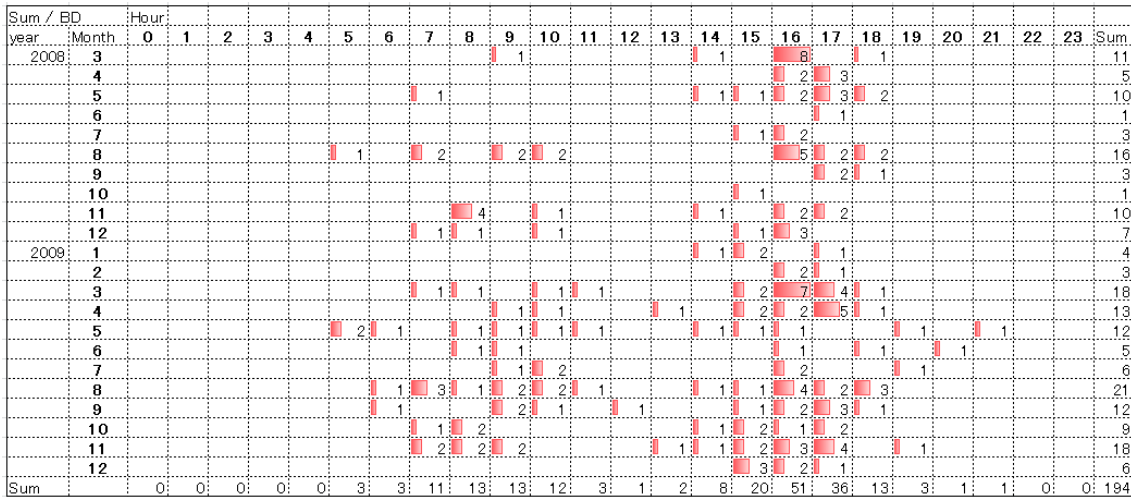


Figure 6.8 The measured frequency distribution of breakdown occurrence

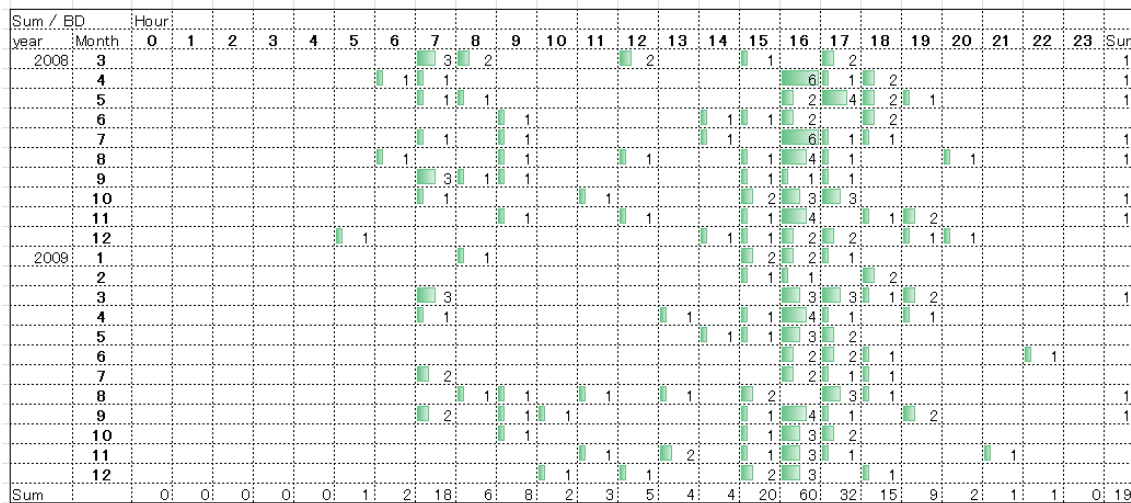


Figure 6.9 The simulated frequency distribution of breakdown occurrence

6.3.3.3 Time-dependent breakdown frequency

This section will discuss the time-dependent characteristics of breakdown occurrence. With respect to each bottleneck location, the arriving traffic demand is generally characterized of time-dependent features, like morning or evening peak hours. The features will possibly result in time-dependent distribution of breakdown occurrence.

Monthly traffic flow characteristics possibly impact on breakdown distribution. Figure 6.8 presents the measured frequency distribution of breakdown occurrence from 3/1/2008 to 12/31/2009. It can be found that breakdown occurrence during each month differs

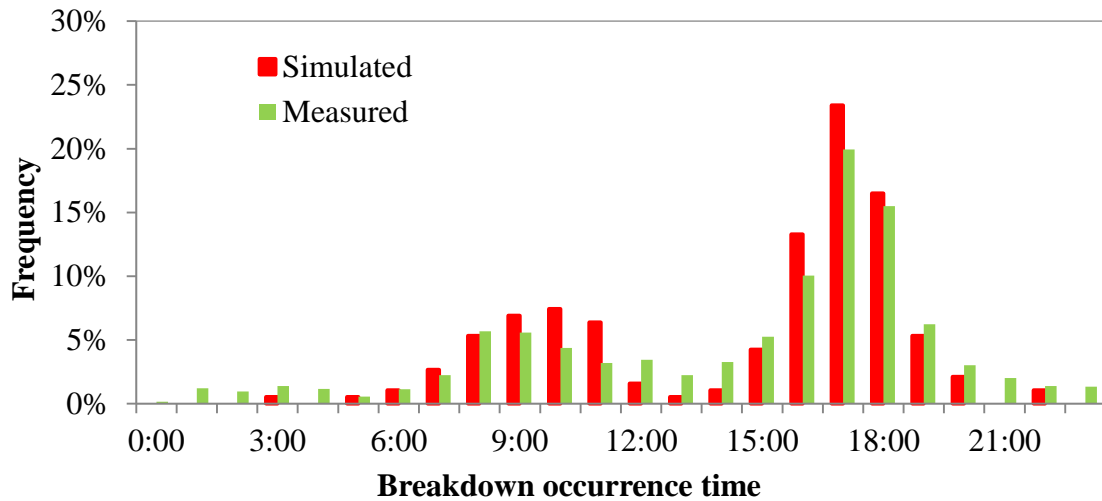


Figure 6.10 Time-dependent distribution

significantly. The simulated frequency distribution can generally represent this feature as illustrated in Figure 6.9.

At Toyota diverge bottleneck, apparently high traffic demands appear during the periods of both morning and evening peak hours as shown in Figure 6.3. Especially for evening peak hours, high traffic demands can be observed for each day. As a result, the measured breakdown occurrences concentrate during the periods as shown in Figure 6.10. High proportion of breakdown occurrences is during the period from AM 16:00 to AM 18:00.

This kind of time-dependent characteristics of breakdown occurrence can also be reproduced by using simulation. As presented in Figure 6.10, the distribution of the simulated breakdown occurrence is shown for each hour of a day. It can be found that the high proportion of the simulated breakdown occurrences is also during the period from AM 16:00 to AM 18:00. For morning peak hours, some underestimation exists for the simulated result by comparing to the measured distribution. On the whole, this time-dependent frequency can be reproduced at an acceptable level ($MAPE=11.4\%$).

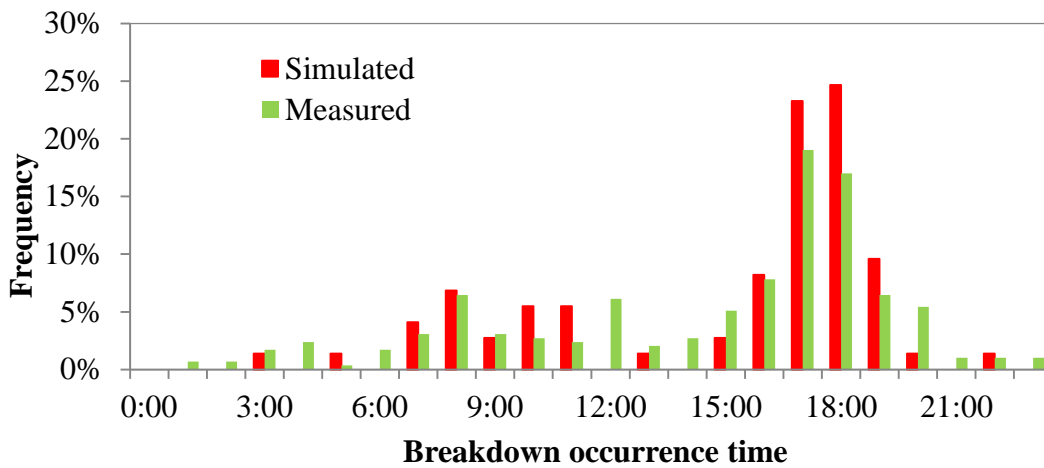


Figure 6.11 Breakdown frequency on weekdays/non-holidays

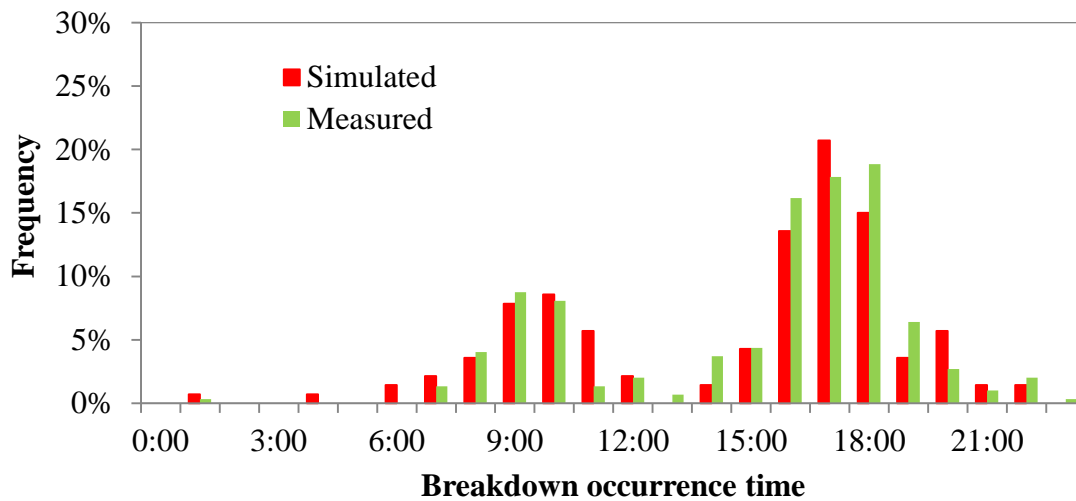


Figure 6.12 Breakdown frequency on weekends/holidays

In order to rationally evaluate simulation performance, the analysis period is further classified into two categories: weekdays/non-holidays and weekends/holidays. Distributions of traffic demand, especially heavy vehicle demand are different for these two categories. This is likely to result in different time-dependent frequency for each category.

Figures 6.11 and 6.12 show the measured breakdown occurrences on weekdays/non-holidays and weekends/holidays respectively. By comparing the measured distributions of them, it is found that for weekends/holidays, the proportion of breakdown occurrence during morning peak hours is relatively high. This is attributed to the concentration of traffic demand for that period on weekends/holidays.

The simulated time-dependent frequencies are also demonstrated in Figure 6.11 and 6.12 respectively. By comparing them, it is found that simulation performs better for weekends/holidays by comparing its *MAPE* value (8.57%) to that (13.24%) of weekdays/non-holidays.

6.3.3.4 The simulated *BDF* distribution

This section introduces the reproduction of breakdown flow rate in a stochastic way. As aforementioned, *BDF* value is an important aspect of bottleneck capacity which has significant impacts on *DCF* distribution. Figure 6.13 demonstrates the measured *BDF* distribution which indicates a wide range of *BDF* values. This kind of stochastic nature also needs to be reproduced by using simulation.

In simulation, breakdown occurrence is generated in a stochastic way. The flow rate which triggers the breakdown occurrence is defined as the simulated *BDF* value.

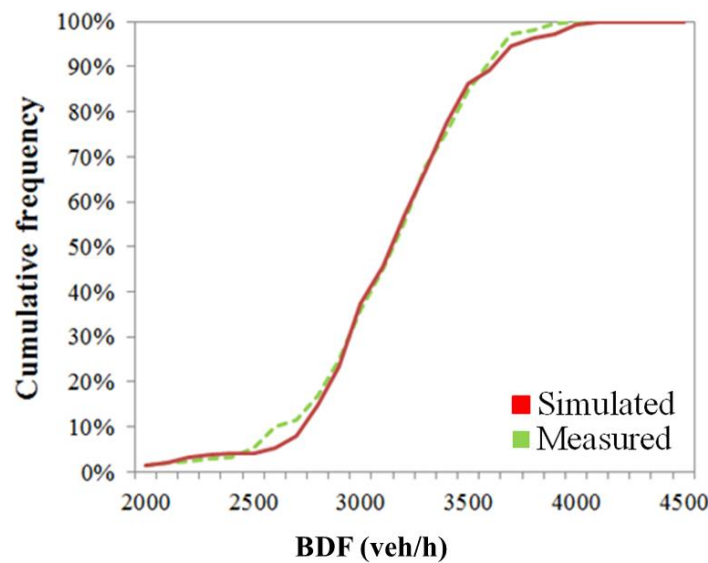


Figure 6.13 Comparison between the measured and simulated *BDF* distributions

Figure 6.13 presents the simulated *BDF* distribution by aggregating results of 20 runs of simulation through Monte Carlo method. By comparing to the measured *BDF* distribution which is also shown in Figure 6.13, it is can be found that the simulated *BDF* distribution can fit well. For the ranges of low and high *BDF* values, there are some underestimations or overestimations possibly due to very low proportion of such values. On the whole, the

simulation can reproduce well *BDF* distribution at an acceptable level ($MAPE=5.64\%$). The simulated *BDF* values will serve as the base of *DCF* model.

6.3.4 Breakdown duration

This section discusses the estimation of breakdown end by computing breakdown duration. Breakdown duration plays a significant role in impacting the intercity expressway performance. As discussed in the previous chapter, there is a descending tendency with the increase of breakdown duration. As for drivers, their driving perceptions deteriorate towards long duration of breakdown which is likely to contribute to traffic accident occurrence. The method to estimate breakdown duration will be discussed as follows.

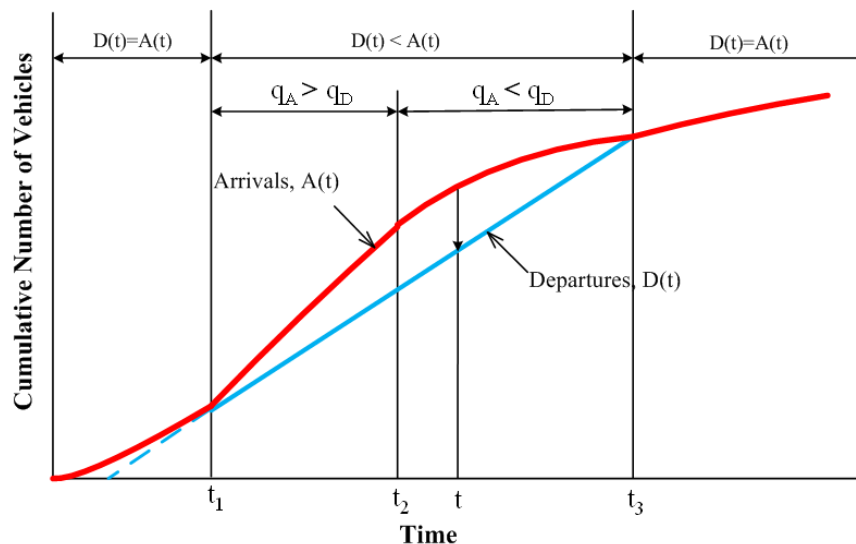


Figure 6.14 Estimation method of breakdown duration

6.3.4.1 Determining method of breakdown duration

Estimation of the breakdown duration is based on the comparison between discharge flow rate and the arriving traffic demand. The formation and dissipation of queue after the breakdown occurrence can be introduced as illustrated by using Figure 6.14. *DCF* represents the ability of bottleneck to dissipate the queued vehicles. Once breakdown occurs, with respect to *DCF*, generally there is a descending tendency. As for the arriving traffic demand, it possibly still remains at a high level. These effects will result in the formation of queue. The queue will extend as long as the arriving traffic demand is above the *DCF* value. When the arriving traffic demand decreases below the *DCF* value, the

queue starts to dissipate. The end of breakdown is the time when all the cumulative traffic demand can be dissipated.

For the simulation, the estimation of breakdown duration is performed in the way as follows. Firstly, once breakdown occurs, *DCF* model will be used to generate *DCF* value in a stochastic way through Monte-Carlo method based on the simulated *BDF* value. Also time-dependent characteristic of *DCF* is considered. Secondly, the generated *DCF* value and the cumulative arriving demand from upstream are compared. Finally, the interval is determined as breakdown end when all the cumulative traffic flow can be dissipated.

6.3.4.2 The determined result

Figure 6.15 presents the comparison between the measured and simulated breakdown durations.

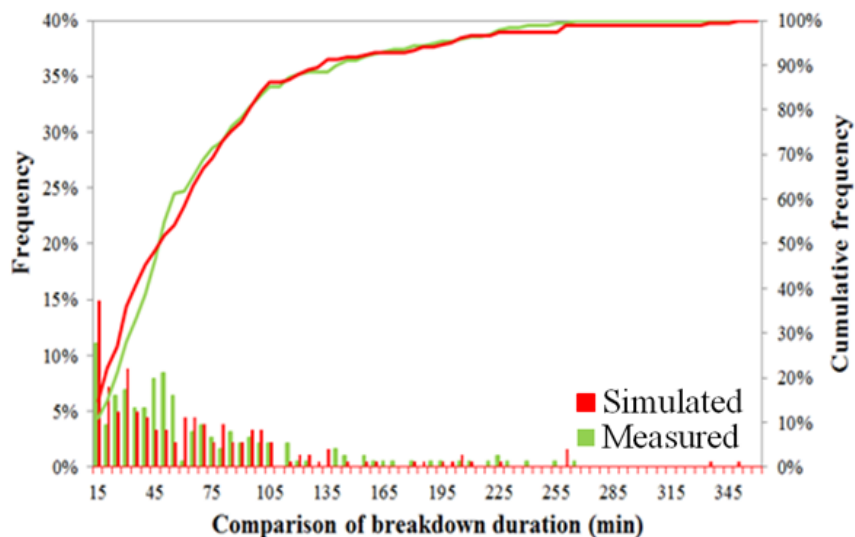


Figure 6.15 Comparison between the measured and simulated breakdown duration

With respect to the measured distribution, it is found that values of breakdown duration are distributed in quite a wide range. High proportion of values concentrates in the range which is lower than two hours. While for the long duration cases, their distribution is quite scattered. This is attributed to the combined effects from stochastic characteristics of arriving traffic demand and discharge flow rate. By performing the simulation, a general tendency can be reproduced whereas some underestimation or overestimation exists.

6.4 Simulation at merge bottleneck

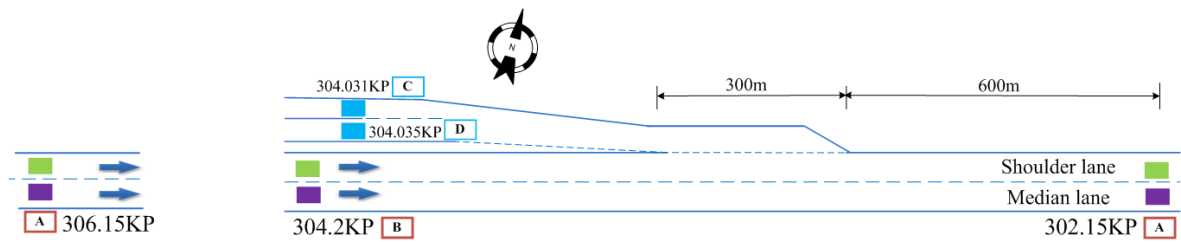


Figure 6.16 Test bed location and position of detectors in vicinity of Toyota merge bottleneck

Simulation is also performed in the similar way as described above. Figure 6.16 demonstrates the layout of Toyota merge bottleneck which is located on Tomei Expressway of eastbound direction.

6.4.1 Input of simulation procedure

The traffic demand data during the period from 3/1/2008 to 12/31/2009 will be used for simulation.

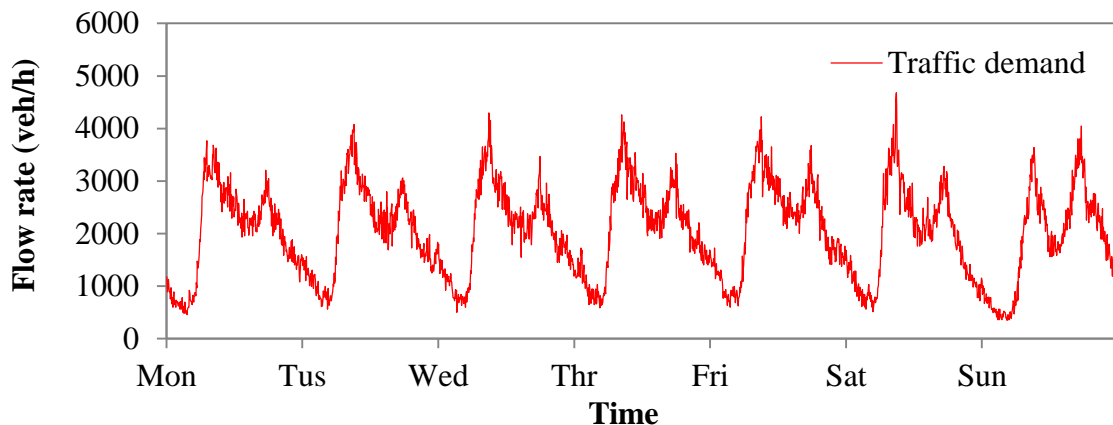


Figure 6.17 Traffic demand distribution at Toyota merge bottleneck

Figure 6.17 presents the traffic demand distribution at Toyota merge bottleneck for one week from 3/3/2008 to 3/9/2008. The apparent high traffic demand appear during peak hours of both morning and evening peak hours as shown in Figure 6.17. Especially for morning peak hours, high demands can be observed for each day. This is the tide traffic phenomena on Tomei Expressway by comparing to the traffic demand distribution at Toyota diverge bottleneck which is located on Tomei Expressway of westbound direction.

As described in the previous chapters, with respect to breakdown probability model, its shape and scale parameters (α and β) are not constant values. Actually, they are influenced by traffic flow characteristics as expressed by Equations (6.5-a) and (6.5-b).

$$\alpha = \underset{t=3.55}{3.01 \times 10} MR - \underset{t=-2.91}{7.39} LUR + \underset{t=1.04}{4.98} \quad (6.5-a)$$

$$\beta = \underset{t=-5.86}{-3.31 \times 10^2} MR - \underset{t=-4.82}{3.76 \times 10^2} LUR + \underset{t=20.1}{4.87 \times 10^3} \quad (6.5-b)$$

where, MR is merge rate, and LUR is lane utilization rate on median lane.

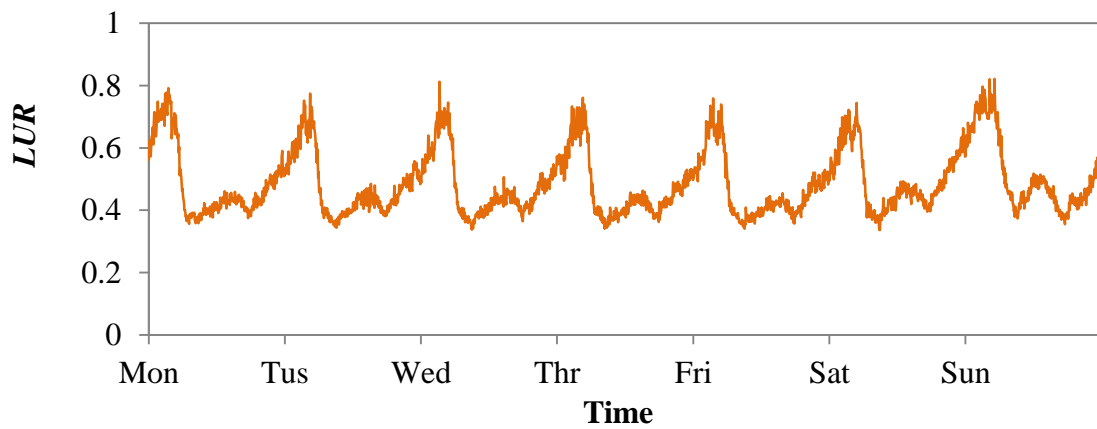


Figure 6.18 The simulated LUR on shoulder lane at Toyota merge bottleneck

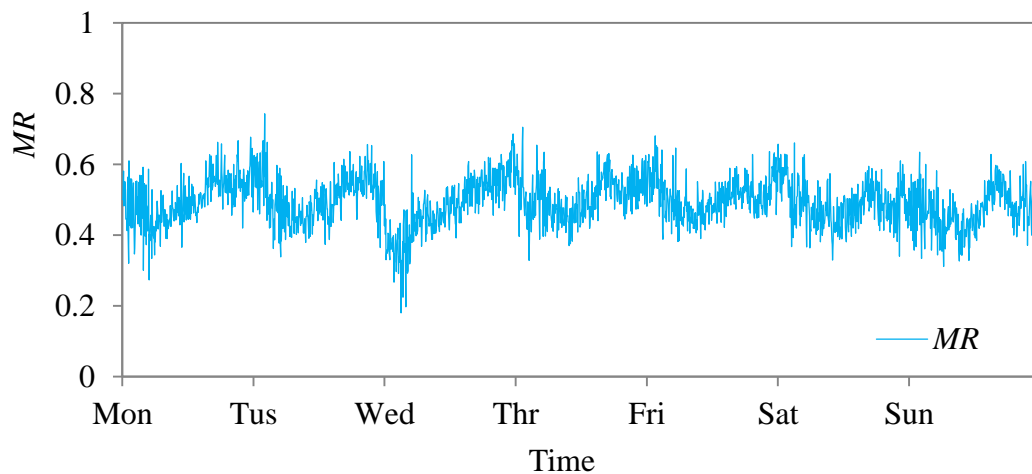


Figure 6.19 The measured MR at Toyota merge bottleneck

LUR will be reproduced in the similar way as described in the previous section. Figure 6.18 demonstrates the simulated LUR on shoulder lane during one week at Toyota merge bottleneck. This estimated LUR distribution on shoulder lane is based on the input of

traffic demand and heavy vehicle demand and etc. It can be found that *LUR* on shoulder lane stays about 0.4 for both morning and evening peak hours on each day of this week. This indicates that high proportion of traffic demand is allocated on shoulder lane which is likely to be the contribution of breakdown occurrence there. The estimated *LUR* distribution will serve as basis of breakdown probability model as illustrated in simulation framework in Figure 6.1.

Figure 6.19 illustrates the measured *MR* distribution at Toyota merge bottleneck during one week from 3/3/2008 to 3/9/2008. It can be found that *MR* values are approximately over 0.45 during both morning and evening peak hours on each day of this week. This indicates that high proportion of traffic demand merge onto on-ramp which is likely to impose significant impact on mainline traffic flow. The measured *MR* distribution will also serve as basis of breakdown probability model as illustrated in simulation framework in Figure 6.1.

6.4.2 Output of simulation procedure

This section discusses the time-dependent characteristics of breakdown occurrence.

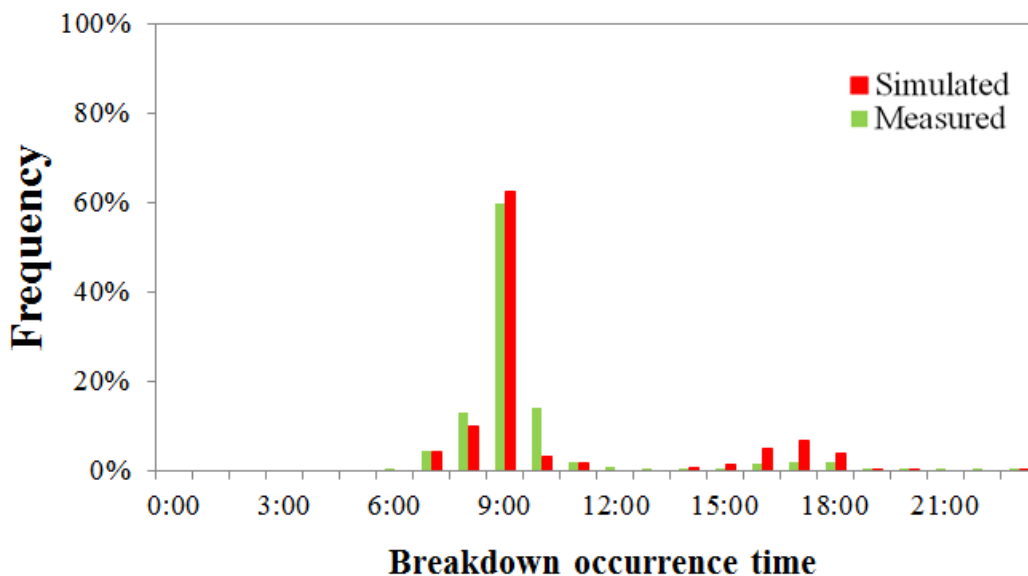


Figure 6.20 Time-dependent breakdown frequency at Toyota merge bottleneck

With respect to each bottleneck location, the arriving traffic demand is generally characterized of time-dependent features, like morning or evening peak hours. The features will possibly result in time-dependent distribution of breakdown occurrence.

At Toyota merge bottleneck, the apparently high traffic demands appear during peak hours of both morning and evening peak hours as shown in Figure 6.20. Especially for morning peak hours, high demands can be observed for each day. As a result, the measured breakdown occurrences concentrate during the periods as shown in Figure 6.20. High proportion of breakdown occurrences is in the period from PM 9:00 to PM 11:00. This is attributed to the tide traffic phenomena on Tomei Expressway by comparing to the traffic demand distribution at Toyota diverge bottleneck.

This kind of time-dependent characteristics of breakdown occurrence can also be reproduced by simulation. As presented in Figure 6.22, the distribution of the simulated breakdown occurrence is shown for each hour of a day. It can be found the high proportion of the simulated breakdown occurrences is also in the period from PM 9:00 to PM 11:00. For evening peak hours, some underestimation exists for the simulated result comparing to the measured distribution. On the whole, this time-dependent frequency can be reproduced at an acceptable level ($MAPE=10.74\%$).

6.5 Simulation at sag bottleneck

Simulation is also performed in the similar way as described above. Figure 21 demonstrates the layout of a sag bottleneck which is located on Tomei Expressway of eastbound direction between Toyota JCT and Okazaki IC.



Figure 6.21 Sag bottleneck between Toyota JCT and Okazaki IC on Tomei Expressway of eastbound direction

6.5.1 Input of simulation procedure

Similarly to diverge and merge bottlenecks, for sag bottlenecks, the traffic demand data during the period from 3/1/2008 to 12/31/2009 will be used for simulation.

6.5.2 Output of simulation procedure

This section will discuss the time-dependent characteristics of breakdown occurrence. With respect to each bottleneck location, the arriving traffic demand is generally characterized of time-dependent features, like morning or evening rush hours. The features will possibly result in time-dependent distribution of breakdown occurrence.

At this sag bottleneck location, the apparent high traffic demand appear during peak hours of both morning and evening peak hours as shown in Figure 6.22. Especially for morning peak hours, high demands can be observed for each day. As a result, the measured breakdown occurrences concentrate during the periods as shown in Figure 6.23. High proportion of breakdown occurrences is during the period from PM 9:00 to PM 11:00.

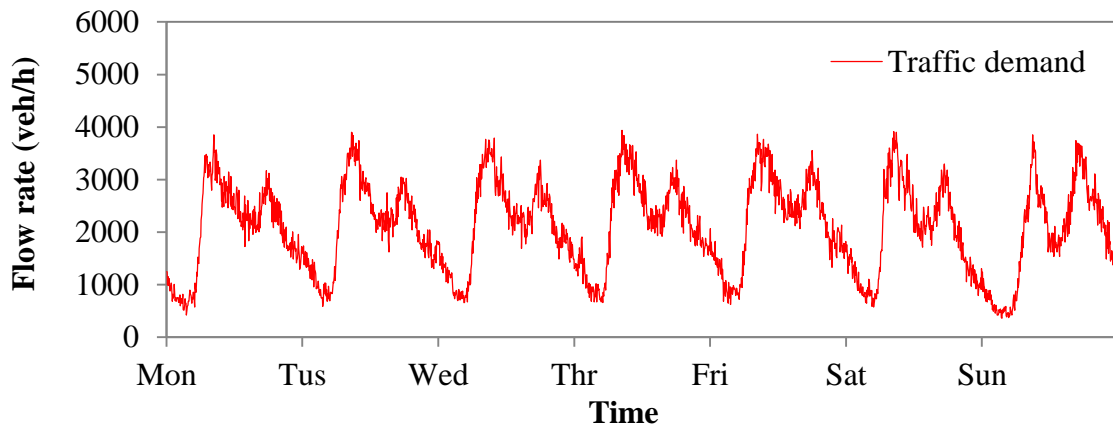


Figure 6.22 Traffic demand distribution at sag bottleneck

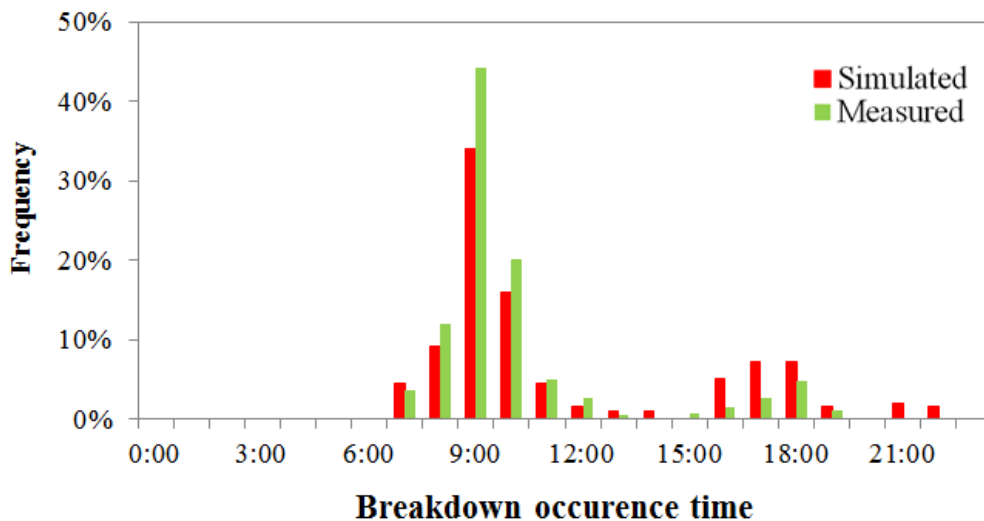


Figure 6.23 Time-dependent breakdown frequency at sag bottleneck

This kind of time-dependent characteristics of breakdown occurrence can also be reproduced by using simulation. As presented in Figure 6.23, the distribution of the simulated breakdown occurrence is shown for each hour of a day. It can be found the high proportion of the simulated breakdown occurrences is also in the period from PM 9:00 to PM 11:00. For evening peak hours, some underestimation exists for the simulated result by comparing to the measured distribution. On the whole, this time-dependent frequency can be reproduced at an acceptable level ($MAPE=9.46\%$).

6.6 Summary

In this chapter, a methodology has been developed to simulate breakdown phenomena by incorporating breakdown probability and discharge flow rate models. The developed methodology is applied to diverge, merge and sag bottlenecks respectively.

Performance measures like the number of breakdown occurrence, time-dependent breakdown occurrence, breakdown duration are adopted to evaluate simulation result. Furthermore, at diverge and merge sections, lane usage preference characteristic are taken into account in simulation by adopting *LUR* model considering lane-specific characteristics there.

It is found that the reproduction of breakdown phenomena can be statistically acceptable. For example, at Toyota diverge bottleneck, there are 180 simulated breakdown events during the period (3/1/2008 to 12/31/2009). Comparing to the measured 194 breakdown events, this result is statistically acceptable.

The applications of the developed methodology at merge and sag bottlenecks are also found to achieve statistically acceptable simulation results.

The investigation in this chapter verifies the effectiveness of the developed models for simulation in practice.

Chapter 7

CASE STUDY BY APPLYING THE DEVELOPED MODELS

7.1 Introduction

This chapter introduces the case study by applying the developed models. The selected test bed is located on Tomei Expressway of westbound direction from Okazaki IC to Toyota JCT.

As aforementioned, performance of intercity expressways is significantly affected by breakdown phenomena at bottleneck locations in the network. As for breakdown phenomena, they are impacted by traffic flow characteristics which are supposed to be changeable in future. Such changes are possibly related to change of expressway network, adjustment of charge schemes and etc.

It is quite important to estimate change of breakdown phenomena accompanying with change of traffic flow characteristics. Especially for traffic operations on critical expressway segments, the knowledge on breakdown probability distribution is quite required. Evaluation of performances of the critical expressway segments is significant for expressway authorities at the operational stage in practice.

As aforementioned, the relationships between breakdown and discharge flow rates have been generalized by referring to the site-specific geometries with respect to each facility type. This enables breakdown probability estimation at different locations on intercity expressway which helps to construct the map of the breakdown probability which is discussed above.

This chapter aims to investigate the issues mentioned above by conducting the case study at the test bed.

7.2 Descriptions of test bed

Figure 7.1 presents the position of test bed in the intercity expressway network of central of Japan. It is located at the section on Tomei Expressway between Okazaki IC and Toyota JCT of westbound direction.

The test bed is found to be the critical expressway segment as high traffic demand has been loaded. The test bed has experienced serious breakdown according to the empirical observations during the period from 3/1/2008 to 12/31/2009. The breakdown phenomena have occurred at Toyota diverge bottleneck and sag bottlenecks which are located along the test bed. Figures 7.2 to 7.4 present the views of this test bed from Okazaki IC to Toyota JCT. As for sag bottleneck, Inano *et al.* (2008) has identified the successive sag bottleneck locations along this test bed.

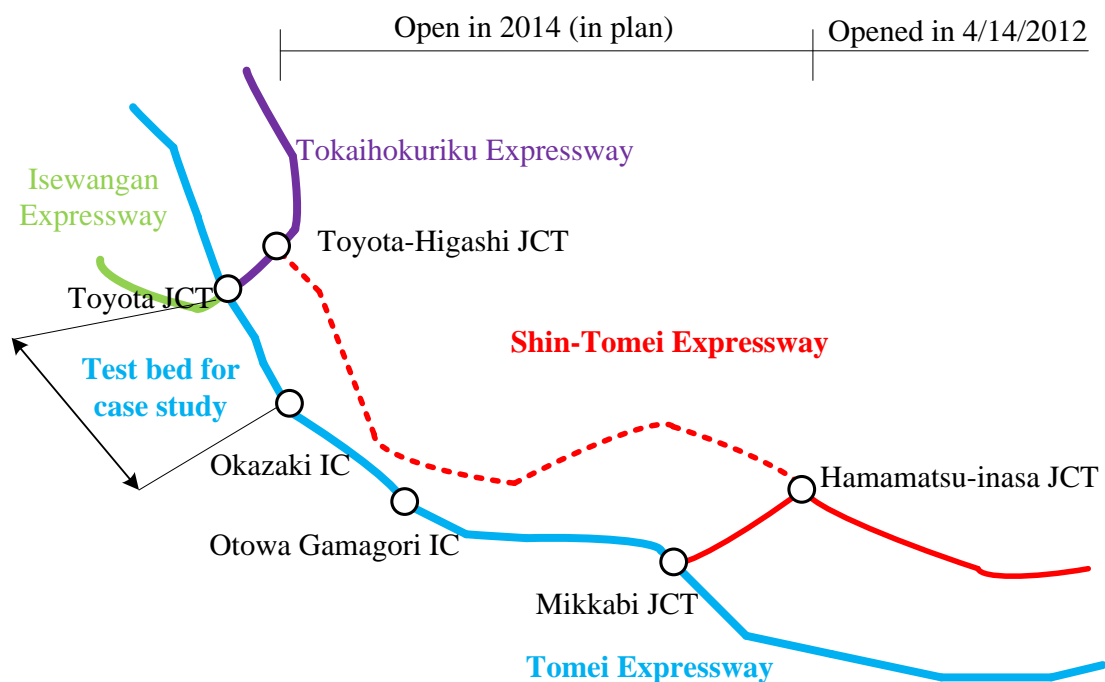


Figure 7.1 Location of test bed for case study

Traffic flow characteristics are likely to change due to the change of expressway network. With respect to Shin-Tomei Expressway, its section between Hamamatsu-inasa JCT to

Gotonba JCT was opened on 4/14/2012. More traffic demands were supposed to be attracted onto Tomei Expressway possibly through Mikkabi JCT. To avoid consequently more breakdown occurrence, a project has been conducted by NEXCO at the section between Otowa Gamagori IC and Toyota JCT. This section has been broadened from the two-lane configuration to three-lane configuration by fully utilizing shoulder which was put into use from 10/21/2011. It will serve as the temporary application until 2014 when the section of Shin-Tomei Expressway between Toyota-Higashi JCT and Hamamatsu-inasa JCT is opened in plan.



(a) View 1



(b) View 2

Source: <http://fumi.ninja-x.jp/TOMEI6.html>

Figure 7.2 Views nearby Okazaki IC



(a) View 1



(b) View 2

Source: <http://fumi.ninja-x.jp/TOMEI6.html>

Figure 7.3 Views between Okazaki IC and Toyota JCT



(a) View 1

(b) View 2

Source: <http://fumi.ninja-x.jp/TOMEI6.html>

Figure 7.4 Views nearby Toyota JCT

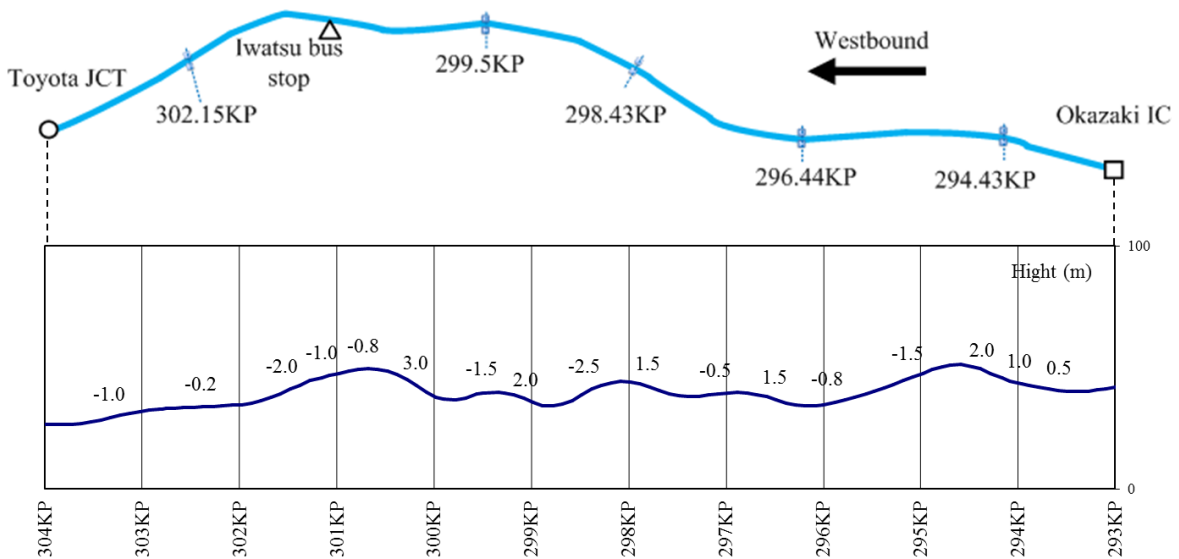


Figure 7.5 Configuration of test bed

The configurations of vertical slope changes and horizontal alignment are also illustrated in Figure 7.5. It can be found that value of vertical slope varies along this section which is regarded as the major influencing factors on breakdown probability model.

7.3 Distribution of breakdown probability at the test bed

This section will introduce the development of distribution map of breakdown probability at the test bed.

The case study is conducted for two-lane configuration. With respect to traffic flow characteristics, they are supposed to change accompanying with change of expressway network. Changes may mainly fall into some aspects as follows. Firstly, traffic demand will possibly be impacted as drivers would prefer to the better driving perception on Shin-Tomei Expressway. Secondly, as for heavy vehicle, it is more influenced by the charging schemes on different expressways. As result, lane utilization rate will be impacted as descried in Chapter 2.

Therefore, breakdown probability distribution will be developed by considering the traffic flow characteristics as described above. As for this test bed, there exist two types of facilities, namely diverge section at Toyota JCT and sag sections. Breakdown probability will be computed for them respectively.

With respect to diverge bottleneck, breakdown probability model has been developed in Chapter 4 as expressed in Equations (4.4-a) and (4.4-b). As for sag sections along the test bed, site-specific breakdown probability model is be established by using Equations (4.8-a) and (4.8-b) considering vertical negative and positive slope values as illustrated in Figure 7.5.

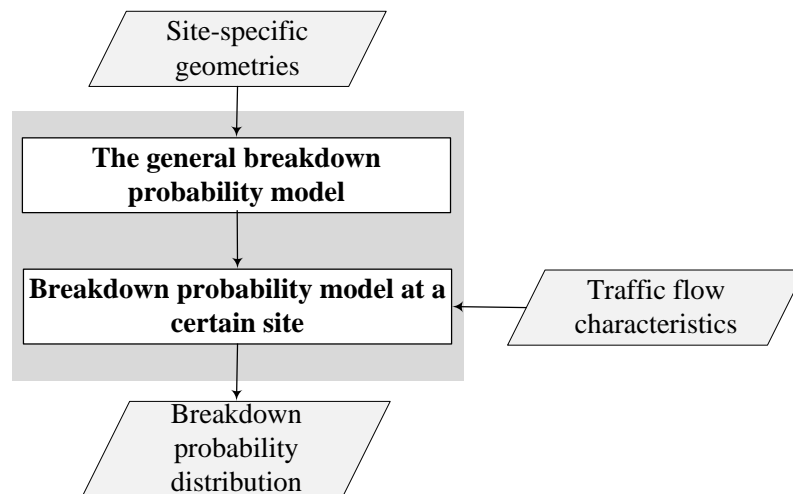


Figure 7.6 Procedure to develop breakdown probability distribution

The procedure to develop breakdown probability distribution is presented in Figure 7.6. Firstly, site-specific geometries are measured for the input of the general breakdown probability. Secondly, shape and scale parameters are calculated by using the estimated

breakdown probability model at a certain site. Finally, breakdown probability distributions are computed by using the estimated considering traffic flow characteristics.

7.3.1 Output of simulation procedure

Breakdown probability distributions will be developed by considering the change of traffic flow. Traffic demand plays the dominant role in determining breakdown occurrence. At a certain site, breakdown probability will increase with increase of traffic demand. The sensitivity of breakdown probability regarding traffic demand is dependent on site-specific breakdown probability model.

Scenarios are designed to develop breakdown probability distributions under different levels of traffic demand. Figure 7.7 presents breakdown probability distributions for traffic demands from 3000 veh/h to 3800 veh/h by assuming the constant heavy vehicle percentage of 15%.

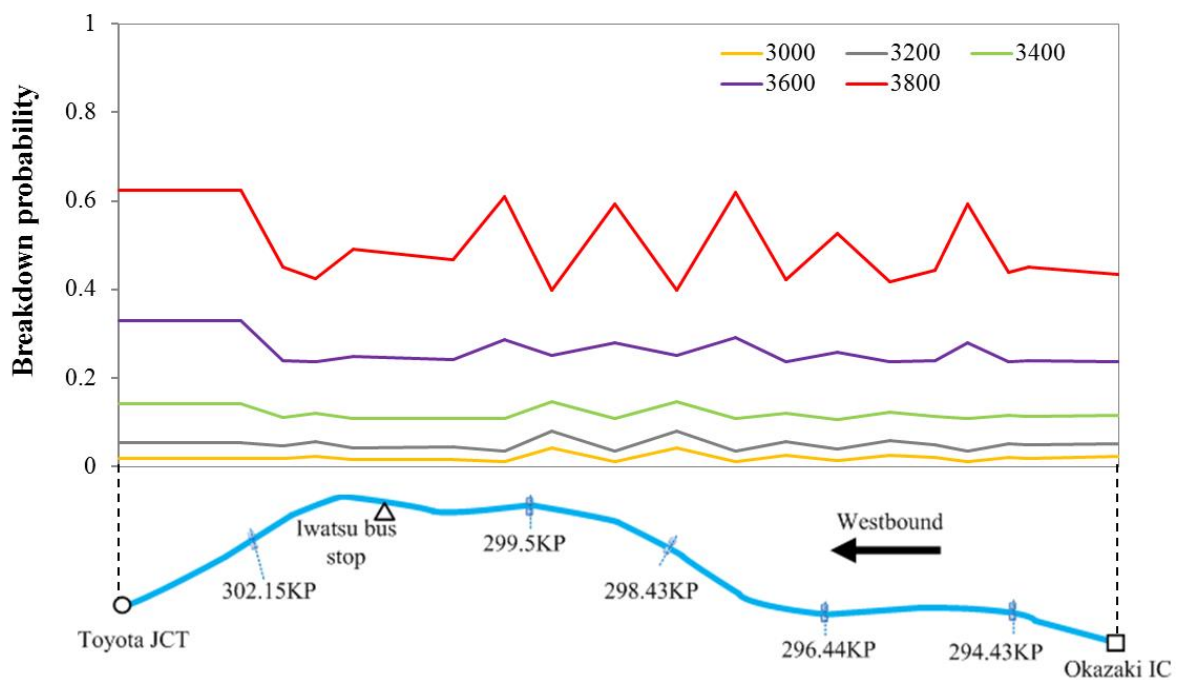


Figure 7.7 Breakdown probability distributions regarding traffic demand (heavy vehicle percentage=15%)

It can be found that breakdown probability increases with the increase of traffic demand for each specific site. When traffic demand increases from 3000 veh/h to 3800 veh/h, there are significant increases of breakdown probability values.

As for traffic operations on this critical expressway segment, the results can be interpreted by using the terms of risk of breakdown occurrence. When traffic demand of 3000 veh/h is loaded on this test bed, quite low risk of breakdown occurrence can be caused as breakdown probability value approaches 0 along the test bed.

The risk of breakdown occurrence becomes high under high traffic demand levels. For example, under the traffic demand of 3600 veh/h, the risk of breakdown occurrence is relatively high as breakdown probability value is approximately above 0.2 along the test bed. Moreover, the relatively higher risks can be found at several sites. One site is located nearby 302KP which is actually the location of Toyota diverge bottleneck. Under this traffic demand of 3600 veh/h, this location has relatively higher risk compared to other locations along test bed. In addition, attentions also need to be paid to those sites like nearby 294KP, 298KP and 299KP where high values of breakdown probability values can also be identified.

When traffic demand level reaches 3800 veh/h, quite high risk of breakdown occurrence can be found as breakdown probability values become high which are approximately above 0.4 along the test bed. This high risk need to be avoided for this critical expressway segment.

Breakdown relief scheme can be proposed regarding traffic demand management (TDM). This kind of relief scheme can be realized by managing traffic demand especially for peak hours through traffic policies like higher charge rates during peak hours.

Figures 7.8 and 7.9 present breakdown probability distributions regarding traffic demand when heavy vehicle percentages are set as 5% and 25% respectively. Similar tendencies can be found as discussed above.

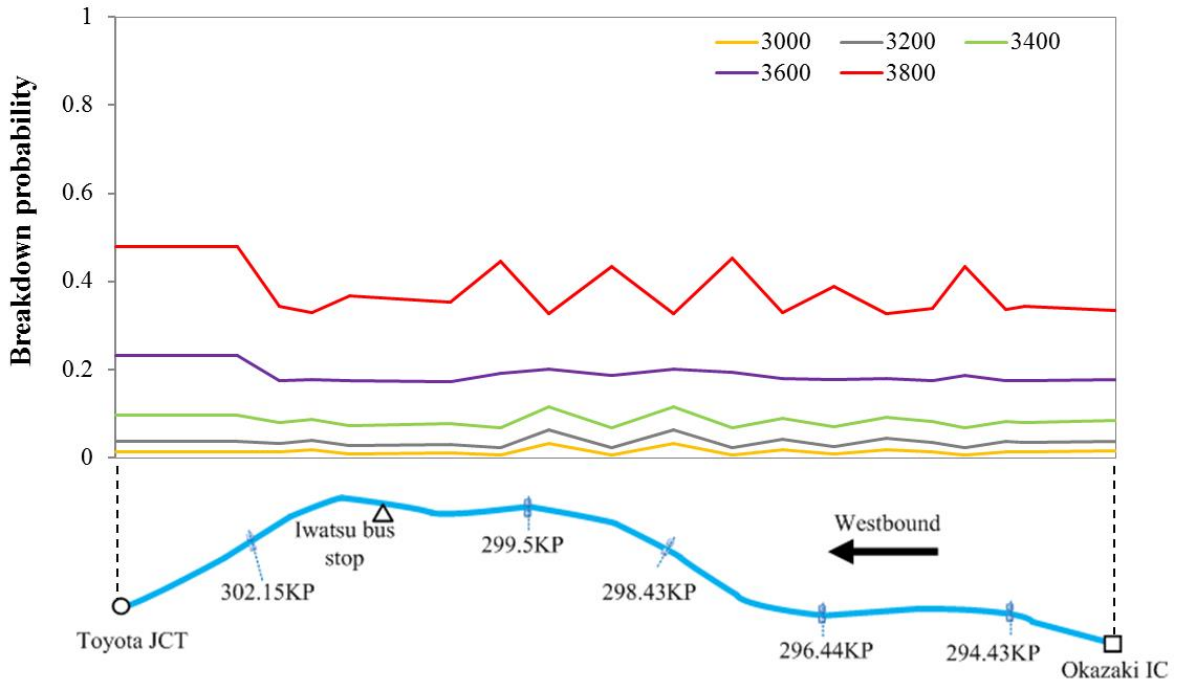


Figure 7.8 Breakdown probability distributions regarding traffic demand (heavy vehicle percentage=5%)

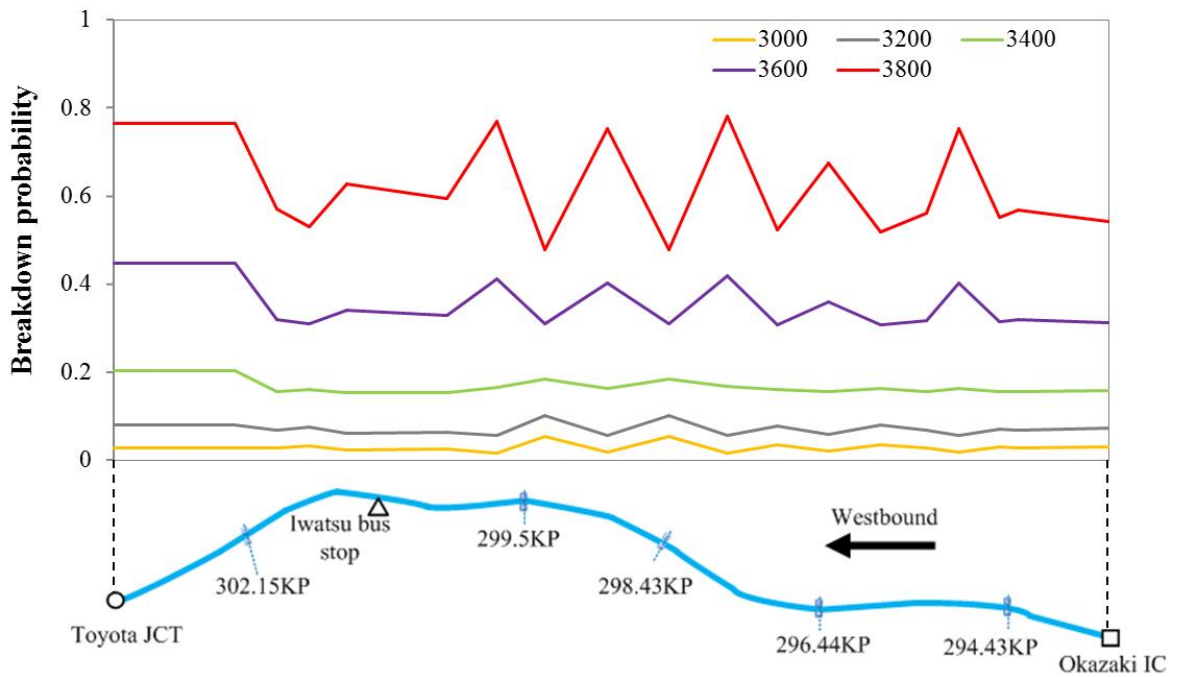


Figure 7.9 Breakdown probability distributions regarding traffic demand (heavy vehicle percentage=25%)

7.3.2 Impact of heavy vehicle percentage

Breakdown probability distributions will be developed by considering the change of heavy vehicle percentage. Heavy vehicle percentage influences breakdown occurrence by considering its impact on lane utilization rate (*LUR*) as described in Chapter 2. The sensitivity of breakdown probability regarding heavy vehicle percentage is dependent on site-specific breakdown probability model.

Scenarios are designed to develop breakdown probability distributions under different levels of heavy vehicle percentage. Figure 7.10 presents breakdown probability distributions for heavy vehicle percentages from 5% to 25% by assuming the constant traffic demand of 3500 veh/h.

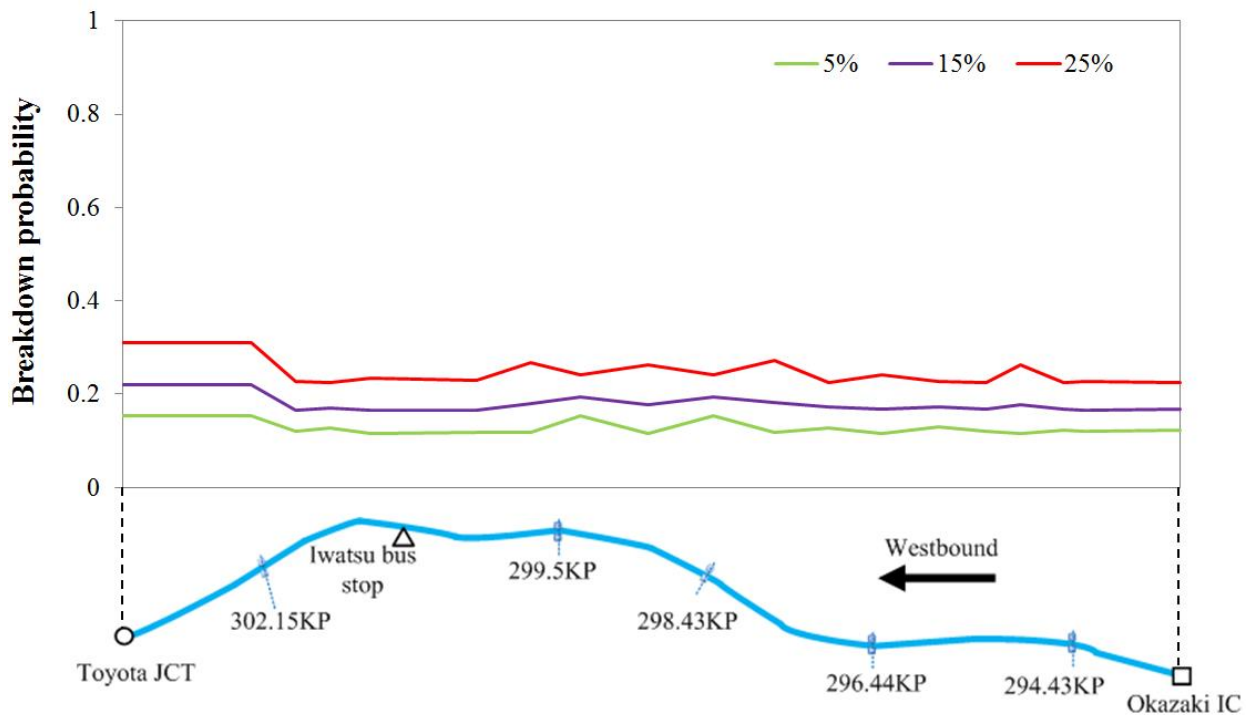


Figure 7.10 Breakdown probability distributions regarding heavy vehicle percentage (traffic demand=3500 veh/h)

It can be found that breakdown probability increases with the increase of heavy vehicle percentage for each specific site. When heavy vehicle percentage increases from 5% to 25%, there are significant increases of breakdown probability values.

As for traffic operations on this critical expressway segment, the results can also be interpreted by using the terms of risk of breakdown occurrence. When heavy vehicle

percentage of 5% is loaded on this bed, relatively low risk of breakdown occurrence can be caused as breakdown probability value approaches 0.1 along the test bed.

The risk of breakdown occurrence becomes high under high heavy vehicle percentage levels. For example, under the heavy vehicle percentage of 15%, the risk of breakdown occurrence is relatively high as breakdown probability value is approximately above 0.2 along the test bed. Moreover, the relatively higher risks can be found at several sites. One site is located nearby 302KP which is actually the location of Toyota diverge bottleneck. Under heavy vehicle percentage of 15%, this location has relatively higher risk compared to other locations along test bed. When heavy vehicle percentage reaches 25%, quite high risk of breakdown occurrence can be found as breakdown probability value become high which are approximately above 0.25 along the test bed. This high risk needs to be avoided for this critical expressway segment.

Breakdown relief scheme can be proposed to control heavy vehicle percentage. This kind of relief scheme can be realized by control of heavy vehicle especially for peak hours through traffic policies like different charge rates on different expressway or different periods.

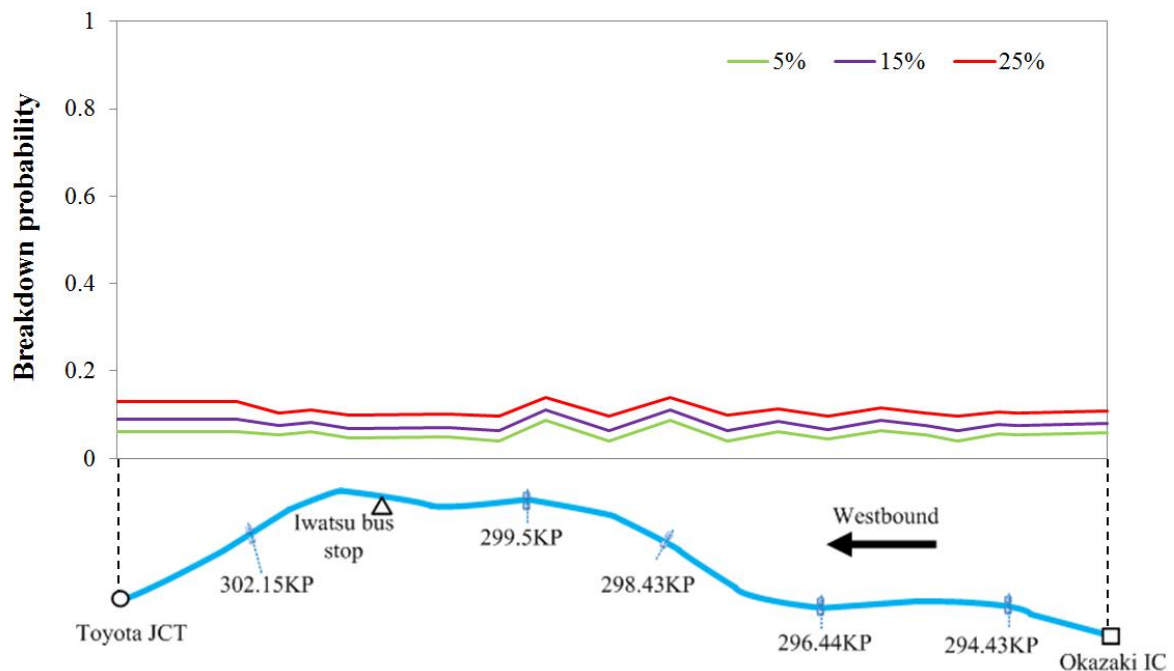


Figure 7.11 Breakdown probability distributions regarding heavy vehicle percentage (traffic demand=3300 veh/h)

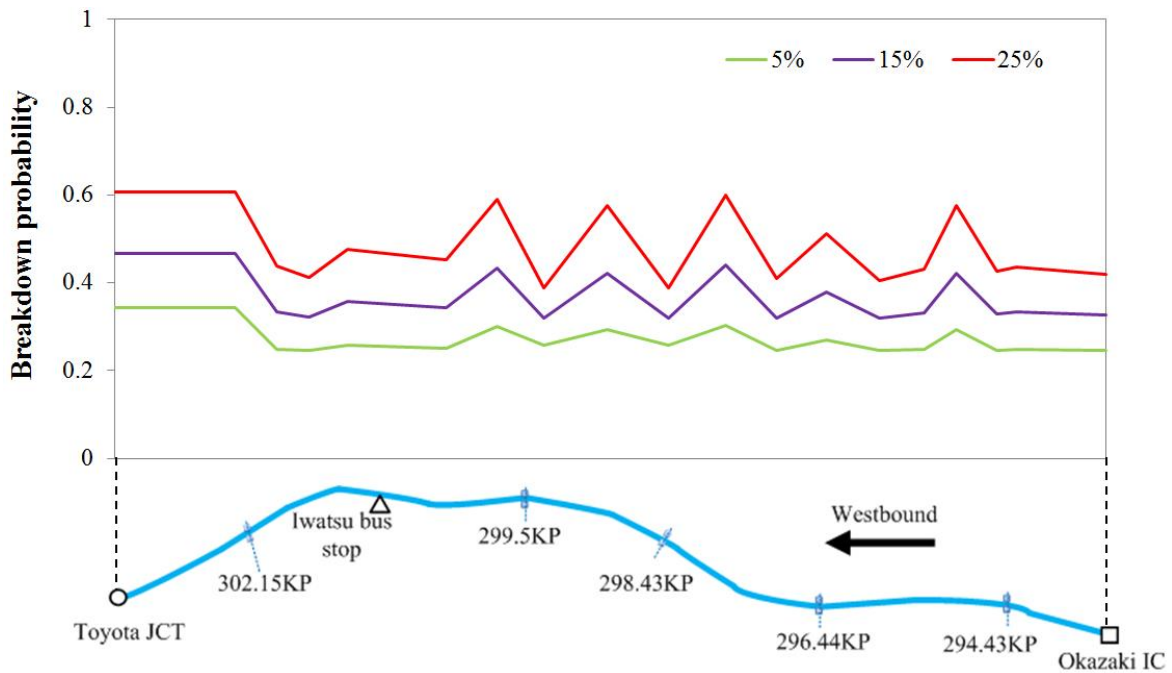


Figure 7.12 Breakdown probability distributions regarding heavy vehicle percentage (traffic demand=3700 veh/h)

Figures 7.11 and 7.12 present breakdown probability distributions regarding heavy vehicle percentage when traffic demands are set as 3300 veh/h and 3700 veh/h respectively. Similar tendencies can be found as discussed above.

7.4 Summary

This chapter has conducted the case study by applying the developed models. The selected test bed is located on Tomei Expressway of westbound direction from Okazaki IC to Toyota JCT.

As aforementioned, performance of intercity expressways is significantly affected by breakdown phenomena at bottleneck locations in the network. As for breakdown phenomena, they are impacted by traffic flow characteristics which are supposed to be changeable in future. Such changes are possibly related to change of expressway network, adjustment of charge schemes and etc.

For the test bed, with respect to traffic flow characteristics, they are supposed to change accompanying with change of expressway network. Changes may fall into several aspects

as follows. Firstly, traffic demand will possibly be impacted as drivers would prefer to the better driving perception on Shin-Tomei Expressway. Secondly, as for heavy vehicle, it is more influenced by the charging schemes on different expressways. As result, lane utilization rate will be impacted as descried in Chapter 2.

Therefore, case study will be performed by assuming change of traffic flow characteristics as described above. The distributions of breakdown probability along the test bed have been developed to evaluate impact on traffic demand and heavy vehicle percentage. Furthermore, proposal of breakdown relief schemes are discussed at the operational stage.

Chapter 8

CONCLUSIONS AND RECOMMENDATIONS

8.1 Conclusions

In practical application at both the operational and the planning stages, analyzing breakdown phenomena is a critical issue which quite depends on quantification of capacity of recurrent bottleneck.

Breakdown flow rate and discharge flow rate are known as two distinct aspects of recurrent bottleneck capacity which impact on breakdown occurrence and its duration respectively. They are characterized of stochastic natures which are influenced by traffic condition and geometric characteristics.

With respect to breakdown flow rate, breakdown probability model is a preferable measure to describe and quantify breakdown flow rate in light of its stochastic nature. However for discharge flow rate, stochastic modeling is also needed. Furthermore, the relationship between breakdown flow rate and discharge flow rate require taken into consideration when modeling.

In this study, both breakdown flow rate and discharge flow rate are modeled in a stochastic way considering traffic condition and geometric characteristics. Conclusions and results of the study are briefly described in the following sections.

8.1.1 Modeling lane utilization rate (*LUR*) by considering impacts of traffic condition and geometric characteristics

In this study, lane utilization rate (*LUR*) is used as a macroscopic variable to describe the lane-specific characteristics on the multilane expressway.

LUR has been modeled as a function of traffic flow and geometric characteristics for locations in the intercity expressway network of central Japan. The influencing factors on lane utilization rate are listed in Table 8.1 which have been taken into account when modeling.

Table 8.1 Influencing factor in *LUR* model

Items	Influencing factors
Traffic flow condition	Cross-section traffic flow rate
	Heavy vehicle percentage
	Distance to diverge section
Geometries	Distance from merge section
	Vertical slope
Traffic regulations	Speed limit

The developed *LUR* model enables quantification of traffic flow rate distribution on each lane for intercity expressway. This quantification can serve as base for analyzing breakdown phenomena from lane based viewpoint rather than the conventional cross-section based one. The improvement would be of significant meaning for investigating breakdown phenomena considering their occurrence.

8.1.2 Proposing lane based breakdown identification method

As for modeling breakdown probability and discharge flow rate on multilane intercity expressways, identification of breakdown occurrence is a decisive issue. To date, most of the existing identification methods have treated all lanes of mainline as one unit for a facility, and are conducted mainly through a check of the aggregated data of cross-section.

However, this cross-section based method oversimplifies breakdown occurrence for bottlenecks at the interrupted expressway facilities where lane usage preferences significantly differ like diverge and merge sections.

Table 8.2 Proposal of lane based method at diverge and merge bottlenecks

Items	Cross-section based method	Lane based method
The identified breakdown events	Improper identification for semi-congested cases and inappropriately determined timing of breakdown occurrence	Ability of overcome shortcomings of cross-based method
The extracted breakdown flow rate values	Underestimation	Improvement of the extracted breakdown flow rate values

Therefore, with respect to diverge and merge bottlenecks, a lane based method is proposed to identify breakdown on each lane as shown in Table 8.2. The proposed lane based method is applied to four diverge bottlenecks and three merge bottlenecks on intercity expressways in Japan. Superiorities of lane based method are highlighted as follows.

Firstly, it can identify and exclude semi-congested cases where some lanes are congested and others are not. At Toyota diverge bottleneck, 15 semi-congested cases are checked out through lane based method among 209 breakdown events which are identified by using cross-section based method.

Secondly, timing of breakdown occurrence can be appropriately determined by lane based method which applies to 34 cases for this diverge bottleneck. These superiorities significantly improve accuracy of extracting breakdown flow rates by 2.6% which are underestimated by the existing cross-section based method.

8.1.3 Breakdown probability modeling by considering traffic condition and geometric characteristics

This study has developed breakdown probability models by considering traffic condition and geometric characteristics as listed in Table 8.3. The developed models are based on

investigation at diverge, merge and sag bottlenecks in intercity expressway network of central Japan.

Table 8.3 Summary of breakdown probability models

Facility	Parameter ranges		Influencing factors	
	α	β	Traffic	Geometry
Diverge	12-13	4620-4836	<i>LUR, DR</i>	-
Merge	14-18	4198-4422	<i>LUR, MR</i>	-
Sag	8-19	3951-5859	<i>LUR</i>	Vertical slope values

For all bottleneck locations with respect to each facility type, parameters of breakdown probability models which are distributed in different ranges as listed in Table 8.3. These results enable the basic quantification of these recurrent bottleneck capacities.

The further contribution of this study is the consideration of traffic condition characteristics. At diverge and merge bottlenecks, besides lane utilization rate (*LUR*), diverge rate (*DR*) and merge rate (*MR*) are also found to have significant impacts on breakdown probability at diverge and merge bottlenecks respectively. Estimation accuracy can be improved by taking traffic condition characteristics into account. At Toyota diverge bottleneck, estimation accuracy can be improved by 20.5% when reproducing breakdown phenomena there.

Another contribution is development of general model by considering geometric characteristic. With respect to sag bottlenecks, the general breakdown probability model is established by considering impacts of site-specific geometries of negative and positive slopes. This contribution enables the estimation of potential bottleneck. Furthermore, it offers the necessary knowledge for improvement on geometric configurations to alleviate breakdown phenomena at the planning stage.

8.1.4 Modeling discharge flow rate in a stochastic way

This study has developed stochastic models of discharge flow rate as illustrated in Table 8.4.

Table 8.4 Summary of discharge flow rate models

Facility	Influencing factors		
	Traffic	Time	Geometry
Diverge			Deceleration lane length
Merge	Breakdown flow rate (<i>BDF</i>)	Elapsed time of breakdown duration	Acceleration lane length
Sag			Vertical slope values

As for modeling discharge flow rate, the contributions from this study can be highlighted as follows.

Firstly, the relationship between breakdown and discharge flow rate has been quantified which has not been answered by the existing researches before. This actually relates breakdown probability and discharge flow rate models. It enables the quantification of the transition from breakdown occurrence to its duration.

Secondly, a descending tendency of discharge flow rate is confirmed with increase of elapsed time of breakdown duration. Modeling the time-dependent characteristic of discharge flow rate enables the performance evaluation for breakdown duration in a stochastic way. This is quite significant knowledge for simulating breakdown event at the operational stage.

In addition, the general discharge flow rate models are established respectively for each bottleneck type. At diverge and merge bottlenecks, site-specific deceleration and acceleration lane lengths are taken into account when generalizing *DCF* model respectively. With respect to sag bottleneck, site-specific geometries of negative and positive slopes are considered. The knowledge is quite significant for improvement on geometric configurations to alleviate breakdown phenomena at the planning stage.

8.1.5 Simulating breakdown phenomena by applying the developed models

Simulation of breakdown phenomena has been achieved by using the developed breakdown probability and discharge flow rate models. Simulation is performed through Monte Carlo method in the way as follows: 1) breakdown flow rates are stochastically generated by using breakdown probability models, and then 2) discharge flow rate

distributions are reproduced based on input of breakdown flow rate values. The simulated number of breakdown occurrence, time-dependent frequency and breakdown duration are adopted as performance measure to evaluate simulation. This investigation verifies the effectiveness of the developed models for simulation in practice.

8.2 Recommendations for future work

The current research was accomplished based on empirical data on intercity expressway network of central Japan. Moreover, the scope of the research could be extended to achieve a more universal methodology. Some directions for future research are addressed in the following sections.

8.2.1 Application to three-lane sections

This study mainly focuses on recurrent bottlenecks located at two-lane sections on intercity expressways. As for insights of lane based analysis, there are possibly more different lane usage preferences towards each lane at three-lane sections. And for breakdown identification, the superiority of lane based method might be greater over the conventional cross-section based one there.

8.2.2 Estimation on change of geometric configuration

The impacts of geometric configurations on breakdown probability and discharge flow rate have been investigated in this study. For example, at diverge bottlenecks, influences of deceleration lane length have been modeled. When some configuration improvements regarding deceleration lane lengths are made, the resulted bottleneck performance can be estimated based on the developed models in this study. It would be significant to expressway authorities.

References

- 1) **Banks, J. H.** (1991) Two-capacity Phenomenon at Freeway Bottlenecks: a Basis for Ramp Metering?. Transportation Research Record 1320, pp. 83-90.
- 2) **Brilon, W., Geistefeldt, J. and Regler, M.** (2005). Reliability of Freeway Traffic Flow: a Stochastic Concept of Capacity. Proceedings of the 16th International Symposium on Transportation and Traffic Theory, pp.125-144.
- 3) **Brilon, W., Geistefeldt, J. and Regler, M.** (2006). Randomness of Capacity-Idea and Application. TRB 5th International Symposium on Highway Capacity and Quality of Service, Yokohama.
- 4) **Brilon, W., Geistefeldt, J. and Zurlinden, H.** (2007). Implementing the Concept of Reliability for Highway Capacity Analysis. Transportation Research Record, Vol. 2027, pp. 1-8.
- 5) **Cassidy, M. and R. Bertini.** (1999). Some Traffic Features at Freeway Bottlenecks. Transportation Research, Vol. B33, pp. 25-42.
- 6) **Daganzo, C. F., Cassidy, M. J. and Bertini, R.** (1999). Possible Explanations of Phase Transitions in Highway Traffic. Transportation Research Part A, 1999, pp.365-379.
- 7) **Dehman, A., and Drakopoulos, A.** (2008). New Insight into Urban Freeway Breakdown Phenomenon. Proceedings of the 2008 Mid-Continent Transportation Research Forum, Madison, Wisconsin.
- 8) **Dowling, R., Skabardonis, A. and Reinke, D.** (2008). Predicting Impacts of Intelligent Transportation Systems on Freeway Queue Discharge Flow Variability, Transportation Research Record, 2047, 49-56.
- 9) **Elefteriadou, L., and Lertworawanich. P.** (2003). Defining, Measuring and Estimating Freeway Capacity, Proceedings of TRB 82nd Annual Meeting, Washington, D.C.

- 10) **Elefteriadou, L., R.P. Roess, and W.R. McShane.** (1995). The Probabilistic Nature of Breakdown at Freeway-Merge Junctions. In *Transportation Research Record: Journal of the Transportation Research Board*, No. 1484, TRB, Transportation Research Board of the National Academies, Washington, D.C., pp. 80-89.
- 11) *Highway Capacity Manual*. TRB, National Research Council, Washington, D.C., 2010.
- 12) **Inano, A., Nakamura, H. and Utsumi, T.** (2008). An Analysis on the Stochastic Characteristics of Breakdown on Expressway Sections Including Several Bottlenecks. Expressways and Automobiles, Express Highway Research Foundation of Japan. (In Japanese).
- 13) **Lertworawanich P., and Elefteriadou, L.** (2001). Capacity Estimations for Type B Weaving Areas Based on Gap Acceptance. *Transportation Research Record: Journal of the Transportation Research Board*, No. 1776, TRB, Transportation Research Board of the National Academies, Washington, D.C., pp. 24-34.
- 14) **Lorenz, M. and L. Elefteriadou** (2000). A Probabilistic Approach to Defining Freeway Capacity and Breakdown. *Proceedings of the 4th International Symposium on Highway Capacity*, pp. 84-95. TRB-Circular E-C018, Transportation Research Board, Washington D.C.
- 15) **Japan Road Association** (1984). *Traffic Capacity of Roads*. (In Japanese).
- 16) **Jia, A., Williams, B. M. and Rouphail, N. M.** (2010). Identification and Calibration of Site-specific Stochastic Freeway Breakdown and Queue Discharge, *Proceedings TRB 89th Annual Meeting*, Washington, D.C.
- 17) **Kobayshi, M., Nakamura, H., Asano, M., and Yonekawa, H.** (2011). Analysis on Stochastic Characteristics of Capacities at Intercity Expressway Bottlenecks, *Annual Meeting of Society of Traffic Engineers*, pp. 133-138, CD-ROM. (In Japanese)
- 18) **Koshi, M., Kuwahara, M., and Akahane, H.** (1992). Capacity of Sags and Tunnels on Japanese Motorways. *ITE Journal*, pp. 17-22.
- 19) **Koshi, M.** (1986). Bottleneck Capacity of Expressways. *Journals of the Japan Society of Civil Engineers*, No. 371/IV-5. (In Japanese).

- 20) **Muñoz, J.C., and Daganzo, C.F.** (2002). The Bottleneck Mechanism of a Freeway Diverge. *Transportation Research Part A*, 2002, pp.483–505.
- 21) **Ma, D., Nakamura, H., Asano, M. and Wolfermann, A.** (2011). A Study on Expressway Breakdown Phenomenon Considering Flow Characteristics on Individual Lanes. *Proceeding of the 9th International Conference of the Eastern Asia Society for Transportation Studies (EASTS)*, 15 pages, CD-ROM, Jeju, Korea.
- 22) **Ma, D., Nakamura, H. and Asano, M.** (2011). Urban Expressway Capacity Characteristics of Lane Closure Sections due to Accidents. *Journal of the Eastern Asia Society for Transportation Studies*, Vol.9, pp.1286-1299.
- 23) **Ma, D., Nakamura, H. and Asano, M.** (2012). Effects of Heavy Vehicle Percentage and Diverge Flow Characteristics on Breakdown Phenomena at a Diverge Section, *Proceedings of the Annual Conference in Chubu Branch of JSCE*, 2 pages, CD-ROM.
- 24) **Ma, D., Nakamura, H. and Asano, M.** (2013). Stochastic Modeling on the Relationship between Breakdown and Discharge Flow Rates at Intercity Expressway Bottlenecks. *Proceedings of Infrastructure Planning*, No.47, 8 pages, CD-ROM.
- 25) **Ma, D., Nakamura, H. and Asano, M.** (2013). Identification Method at Diverge Sections for Modeling Breakdown Probability. *Journal of Transportation Research Record*, 20 pages. (In press).
- 26) **Muñoz, J. C., and Daganzo, C. F.** (2002). The Bottleneck Mechanism of a Freeway Diverge, *Transportation Research Part A*, pp.483–505.
- 27) **Mehran, B. and Nakamura, H.** (2009). Considering Travel Time Reliability and Safety for Evaluation of Congestion Relief Schemes on Expressway Segments, *International Association of Traffic and Safety Sciences (IATSS RESEARCH)*, Vol. 33.
- 28) **T. Oguchi** (2002). *The Nature of Occurrence of Queued Flow at Capacity Bottleneck of Ordinary Section*, *Traffic and Granular Flow '01*, Springer.
- 29) **Okamura, H., S. Watanabe and T. Watanabe.** (2000). An Empirical Study on the Capacity of Bottlenecks on the Basic Suburban Expressway Sections in Japan.

Proceedings of the 4th International Symposium on Highway Capacity, pp. 120-129.
TRB Circular E-C018, Transportation Research Board, Washington D.C.

- 30) **Okamura, H.** (2006). A Study on Highway Capacity based on the Breakdown Probability on Basic Intercity Motorway Sections, Proceedings of 5th International Symposium on Highway Capacity and Quality of Service.
- 31) **Saito, Y., Xing, J., Nonaka, Y., Ishida, T., and Uchiyama, H.** (2005). An Experimental Study on Mitigation of Expressway Traffic Congestion with LED Information Board. Proceedings of the Eastern Asia Society for Transportation Studies, Vol. 5, Bangkok, Thailand, pp. 919-928.
- 32) **Shawky, M. and Nakamura, H.** (2007). Characteristics of Breakdown Phenomenon in Merging Sections of Urban Expressways in Japan. Transportation Research Record 2012, pp.11-19.
- 33) **Wang, X., Asano, M., Chen, P. and Nakamura, H.** (2012). Modeling Lane Distribution on Two-lane Intercity Expressways, Proceedings of the Annual Conference in Chubu Branch of JSCE.
- 34) **Wang, X., Asano, Konda, H., Nakamura, H. and Asano, M.** (2013). Analysis on Characteristics of Lane Utilization Rate on Intercity Expressway, Annual Meeting of Society of Traffic Engineers. (In press, in Japanese)
- 35) **Zhang, L. and Levinson, D.** (2004). Some Properties of Flows at Freeway Bottlenecks, Transportation Research Record 1883, pp. 122-131.
- 36) **Zhang, L. and Levinson, D.** (2004). Ramp Metering and the Capacity of Active Freeway Bottlenecks. Transportation Research Part A: Policy and practice.